UNIVERSITÀ
DEGLI STUDI
DI PADOVA

University of Padova

Department of Developmental Psychology and Socialization

Ph.D. School in Psychological Science

XXXIV Series

Electrophysiological evidence of attentional control from working memory and long-term memory:

how conjunction features are represented during target repetition

Thesis written with the financial contribution of University of Padova and Guangzhou University

Coordinator: Prof. Giovanni Galfano

Supervisor: Prof. Roberto Dell'Acqua

Co-Supervisor: Prof. Shimin Fu

Ph.D. student: Yanzhang Chen

Table of contents

Abstract

Search efficiency can be mediated in a top-down fashion by representations of target's information, namely the attentional template. Template-guided search can be governed either by visual working memory (vWM) when searching for a varying target or by visual long-term memory (vLTM) when searching for a constant target. In some circumstances, target is defined by the conjunction of features (i.e., red square). It is not yet clear how conjunctive features are represented in vWM. This study aims exactly to fill this gap.

In three experimental chapters, we asked whether features of conjunctive stimuli are represented in a separated or integrated fashion in vWM. We measured several electrophysiological indices while participants were cued to search a constant target that was defined by color and shape conjunction in six consecutive trials. Based on the previous observation that attentional template would be off-loaded from vWM to an alternative mechanism during the same target learning, the underlying assumption of the present study is, if conjunctive features are represented in a separated fashion, their impact on task performance should be largely independent when attentional templates were off-loaded from vWM. We then manipulated the similarity between search targets and distractors in the last two trials. Specifically, all search distractors could match either target's shape or color, thereby blocking the role of shape and color during the target selection respectively. We also included a baseline condition to make the comparison, in which all search distractors have no target features overlap.

Experiment 1 & 2 first revealed that the mean amplitude of SPCN and LPC time-locked to the memory display systematically decreased as a function of target repetition,

suggesting the demands on vWM to maintain the attentional template was lessened. This phenomenon is likely due to an off-loading of the template from vWM to the vLTM. Results of the last two repetition trials provided fruitful information to evaluate the impact of color features and shape features on search performance. We found that, when all distractors matched the target shape, search efficiency was the same as the baseline condition (i.e., all distractors are heterogeneous) in the behavioral level, but the ERP results showed attentional guidance by search targets along with an attentional suppression by shape-matched distractors. Moreover, the target selection and distractor suppression appeared to be working in parallel when we further divided the data based on the vertical elevation in Experiment 2. Contrarily, search slope significantly dropped down relative to the baseline when all distractors matched the target color, but we did not observe the distractors suppression in the ERP level. Instead, targets elicited SPCN, presumably due to the guidance of attentional switched from feature-based to object-based manner. Further, we found the SPCN and FN400 time-locked to the cue increased in the memory phase when encountered color-matched distractors in the previous trial, suggesting a strategical resampling to enhance the search performance in the next trial.

Experiment 3 was designed to further examine whether objects are encoded in their entirety in the memory display. Participants implicitly learned which features of the to-be-remember object would direct to search target, targets could match either the color or shape of the memory cue in six consecutive trials. Again, in the last two repetitions, we then instructed participants to identify a full memory matched target (conjunction) instead of the previous single feature matched target. The successful identification revealed that participants did not discard the task-irrelevant feature regardless of search intentions required them to configure a color template or shape template. Besides, search efficiency was better when encountering the conjunction target in the remember

shape series than remember color series, suggesting the color feature acquire better learning even when the search task emphasized the role of shape features.

These findings indicated that the format and the structure of remembered information in vWM are better to be considered including both object-based and feature-based levels. That is, the initial object encoding follows an object-based manner, whereas conjunctive features are bound indirectly in a hierarchical structure.

Chapter 1 – General Introduction

The ability to identify one object among others is fundamental for humans. For doing so, a person may need to know the object-relative information to search for the most potential object that matches its knowledge (target), while rejecting others that do not (distractors). This cognitive process was assumed by most theories of attention, controlled by the mental representation named attentional template (Duncan & Humphreys, 1992; Wolfe, 2012) or attentional control sets (Folk, Remington, & Johnston, 1992). Once an attentional template is established, stimuli that match the template can outclass the others and attract attention (biased-competition model of visual selection; Desimone & Duncan, 1995). Although a growing number of studies have sought to test and complete the hypothesis of attentional template, how attention is driven by this mental representation, however, is far away from being understood.

1.1 The transient and sustained template

Depending on whether search target changes in a set of successive trials, some suggested that attentional template is stored in visual working memory (vWM) when the target is transient, varying from trial to trial (Beck, Hollingworth, & Luck, 2012; Soto, Heinke, Humphreys, & Blanco, 2005). But not when the target is sustained, constant across the entire experiment of a subset of sequential trials. There is a generally accepted viewpoint proposed that a sustained template was held in the vWM for a short period, as the target repeated, and attentional resources for template maintenance were freed up by this trial-by-trial basis. (Carlisle, Arita, Pardo, & Woodman, 2011; Giammarco, Paoletti, Guild, & Al-Aidroos, 2016). For example, Rossi et al. (2001; 2007; 2009) found that trained monkeys with impaired prefrontal regions were difficult

to complete search tasks when targets change at a high frequency but not when targets change at a low frequency. They proposed that attention templates of high-frequency targets are represented in vWM (see also Woodman, Luck, & Schall, 2007) and requires the prefrontal lobe, while templates of low-frequency targets would be gradually off-loaded from vWM into long-term memory (LTM), thereby reducing the participation of prefrontal lobe.

Studying visual attention and vWM in the lab using event-related potentials (ERPs) has substantially fostered our understanding of both these key aspects of human cognition, especially after the discovery that each of them is associated with a distinctive ERP signature. In different event-related potential (ERP) studies, the above off-loading process was observed in human participants via a sustained posterior contralateral negativity (SPCN) that indexed the vWM load, decreasing as a function of the target repetition (Carlisle et al., 2011; Grubert, Carlisle, & Eimer 2016). The SPCN was observed contralateral to an attended cue relative to an unattended one (alternatively named contralateral delay activity, or CDA, by Vogel & Machizawa, 2004; contralateral negative slow-wave, or CNSW, by Klaver, Talsma, Wijers, Heinze, & Mulder, 1999; contralateral search activity, or CSA, by Emrich, Al-Aidroos, Pratt, & Ferber, 2009), it presents when tasks require the retention of information in vWM, usually between about 300-400 ms after stimulus onset (Jolicœur, Brisson, Benoit, & Robitaille, 2008). The presentation of the target cue was lateralized in the visual field and a contrast stimulus was presented on the opposite side to balance the hemifield. Participants were instructed to attend the target cue. Then they had to compare this mnemonic cue with the one that appeared in the next search array. The mnemonic cue is thus consequential server as the attentional template. Among these, the decrease of SPCN was regarded as reducing the need for vWM to maintain the attentional template

(Grubert et al., 2016; Reinhart & Woodman, 2014). The accompanying improved search performance was interpreted based on the logic of learning theories (Logan, 1988), presumably, the attentional template is governed by LTM, guiding attention in the subsequent visual search (Carlisle et al., 2011; Woodman, Carlisle, & Reinhart, 2013 for review).

The way that how attentional templates guide our attention has long been interested in visual search. For example, the most commonly has focused on the point that template-guided search follows the principle of "features come first" (Desimone & Duncan, 1995; Treisman & Gelade, 1980; Wolfe, 2012). Kiss, Grubert & Eimer (2013) found that the N2pc component elicited by fully matching cue equaled the sum of the two N2pc components to color-matched and shape-matched cues. Subsequently, Eimer and Grubert (2014b) found that the later N2pc (250 ms after search) emerged by the conjunction target was larger than the sum of N2pc from the color-matching and shape-matching distractor. This superadditive role suggested that attention is controlled independently by guidance signals from different feature channels. Moreover, Berggren and Eimer (2018), instructed participants to search for two possible targets that were defined also by feature conjunctions. Their research also provides a perspective view in understanding how conjunctive features are represented by examining their effect in visual search. In their experiment 2, they manipulated a distractor that recombined from the two remembered objects (which they referred to as *incorrect conjunction*) to directly compete with targets in the visual search task. Based on the deduction that feature-based guidance cannot distinguish these objects from targets, any selective bias for targets will reflect object-based attentional control. The N2pc was greater for the target than for the incorrect conjunction object from 250 ms post-stimulus. While the SPCN activity in visual search, whose amplitude reflects the neural activity of attended objects

are retained in vWM (Jolicœur, Brisson, Benoit, & Robitaille, 2008; see Luria, Balaban, Awh, & Vogel, 2016, for review), was elicited when targets and incorrect conjunction objects appear in the same display, but not when incorrect conjunction objects appear alone, reflects only targets were encoded into vWM for the subsequent processing. This finding revealed the guidance of attention was controlled by different target features parallelly at the early perception (see also Eimer & Grubert, 2014a). The interpretation offered by Berggren and Eimer (2018) was only a single object-based target template is available to guide attention at any given moment while multiple feature-based templates are maintained concurrently.

While solid evidence has revealed the way of attentional template in the guidance of selection, what we lack, however, is a clear understanding of the architecture of attentional template. Specifically, how attentional templates are represented in vWM? Imagine a situation analogous to those typically designed to monitor template-guided search. When targets in the search task are defined by a specific feature (i.e., a particular color), attentional selections are undisputable feature-based. In this case, templates are established based on a single feature. Imagine however a target is defined by color-shape conjunction, guidance of attention can operate either by a color-based template, or a shape-based template, and even an object-based template under specific circumstances (Berggren & Eimer, 2018). However, little is known in which way the attentional template is configured in vWM. Because the establishment of attentional templates is strongly affected by target features of which higher ability in guiding attention than others. For example, previous research often found that participants were faster in detecting a color-defined target than a shape-defined target (Soto & Humphreys, 2009; Wolfe & Horowitz, 2004; Zhang et al., 2010). ERP research from Kiss et al., (2008) also implicitly suggested that the color dimension is more attractive

as compared to the shape dimension, as they observed the color singleton trigger a greater N2pc than the shape singleton. It is perhaps due to the shape information cannot provide as sufficient stimulus energy (Olivers, 2009) as the color information.

The current study aims to investigate how conjunctive features are represented in vWM when those features serve as attentional templates, and to provide insight in understanding the WM function more generally. As proposed in the review of Brady, Konkle, & Alvarez (2011), namely that "*one cannot fully understand memory systems or memory processes without also determining the nature of memory representations.*"

1.2 Integrated- versus separate-feature storage model

The human visual system is capable of receiving a large amount of perceptual input in a short period and classifying it into perceptual categories. Our attentional resources, on the other hand, are severely limited. To reconcile the vast amount of perceptual input and the limited quantity of information that is of interest, an effective mechanism, that is intimately linked by vWM and attention services to assist in information selection. Although the concept of WM depends on the theory embodied by its concept, there is a broad agreement that WM is referred to the mechanisms and processes of an individual to temporarily store and manipulate information for an ongoing cognitive task (Baddeley, 2010; Cowan, 2017; Oberauer, 2019). Information in the objective world is grouped into meaningful units called objects, over the past two decades, a substantial body of research has accumulated on how perceptual information is encoded into vWM (Hollingworth, 2007; Hollingworth & Rasmussen, 2010; Luria & Vogel, 2011; Markov et al., 2019; Saiki, 2016, 2019; Saiki & Miyatsuji, 2007; Wheeler & Treisman, 2002; Schneegans & Bays, 2019).

Since various research have generally shown evidence of the limited capacity of WM

(available to hold about four items at a time, Luck & Vogel, 1997; 2013; Xu & Chun, 2006; Zhang & Luck, 2008), a large amount of work has been sought to evaluate the storage units in WM. There is a long-running debate over whether object features are maintained independently or bound within the same unit. On the one end of the spectrum of theoretical positions are models assuming that all features of the mnemonic object are bound within an integer representation. For example, when researchers used conjunctive features objects (e.g., colored shapes) as stimuli, they observed that changing task-irrelevant features (i.e., shape) has an impact on probing task-relevant features (i.e., color). It was shown that, regardless of the observer's intentions, objects are encoded in their entirety. (Hollingworth & Matsukura, 2019; Luck & Vogel, 1997; Treisman & Zhang, 2006). On the other end of the theoretical spectrum are models of separate-feature storage, in which the encoding process is mediated by the top-down task set, observers can perfectly restrict their selection only to task-relevant features. The key assumption to evaluate the unit of representations is, if multiple features belonging to an attended object are bound together, one can expect a robust relationship of encoding/recalling multiple features of the same object. That is, features are more likely to be remembered or forgotten at the same rate. Nevertheless, several studies have found none or only weak correlations between the report of different feature values associated with the same remembered object (Bays, Wu, & Husain, 2011; Fougnie & Alvarez, 2011; Fougnie, Cormiea, & Alvarez, 2013; Woodman & Vogel, 2008).

To distinguish between integrated- versus separated-feature representations in vWM, a change detection paradigm, in which participants remembered multiple feature conjunctions (e.g., shape and color) that display opposite to each other on the screen. The efficiency of memory probes is compared between trials remembering a single feature and trials remembering multiple features (Chen et al., 2021; Schneegans & Bays,

2019; Olson & Jiang, 2002; Wheeler & Treisman, 2002). The underlying assumption is that if WM capacity is limited in terms of the number of features, then remembering multiple object features should have a cost. Initially work by Luck & Vogel (1997) found that participants' performance was identical whether in remembering single object feature or multiple object features, manifested the storage representations should be treated as object-based structures (see also Saiki & Miyatsuji, 2007; Wheeler & Treisman, 2002). In addition, there is considerable evidence revealed that significant advance when encoding multiple features from the same object relative to from different objects (Fougnie, Asplund, & Marois, 2010; Olson & Jiang, 2002; Quinlan & Cohen, 2011). For example, Saiki (2016) manipulated the memory location and probe features in the task. Results showed memory performance was faster and frontal N400 was larger when probe objects match both features of the mnemonic object as compared to single-feature match conditions. Furthermore, evidence of measuring SPCN compatible with this integrated assumption has been provided by Luria & Vogel (2011), who observed bicolor objects elicited smaller SPCN amplitude than the condition in which two colors were displayed separately. Because the SPCN is sensitive to the number of memorized objects instead of their spatial positions (Balaban & Luria, 2015), such a distinct SPCN pattern suggested that the representation of multi-feature objects can not be simply explained in terms of independent storage of those features per se, the representational unit of multiple feature object obeys the object-based account.

There is also empirical evidence against the purely object-based assumption. These researchers generally reported that participants do not encode the entered objects. For example, to evaluate the alternative account that equivalent performance in single feature and multiple features condition (Luck & Vogel, 1997) is due to participants are incapable of selectively encoding only one feature of an object, thereby multiple

features within an object are encoded obligatorily. Woodman & Vogel (2008), provided data demonstrating that learning rates varied as a function of which object feature values have to be remembered, with steeper slopes in learning object's color features than its shape and orientation. In other words, the encoding of perceptual input into vWM is under top-down control, participants can selectively encode task-relevant features (see also Bays et al., 2011; Fougnie & Alvarez, 2011). Furthermore, using the change detection task, Wheeler & Treisman (2002) found that WM capacity is determined not only by the number of objects that can be stored but also by the number of features from the same dimension (e.g., color). Their data suggested that the WM capacity is limited to a fixed number of three to four colors regardless of how those colors are artificially configured into bicolor objects.

Despite the burgeoning evidence of the positive outcomes of both object-based and feature-based representation, there is reason to believe the basic unit of representation in vWM may be more complex and varied than is depicted by previous research. One particular notion that has been discussed in previous literature, but remains empirically unexamined, is the top-down task setting induced by paradigms lead to an underestimation of the nature of representations. For instance, the change detection paradigm in some cases has been accused not sensitive to the alteration in representation's precision (Brady et al., 2011; Fougnie et al., 2010), leading to the null effect between single feature condition and multiple features condition — no cost for remembering multiple features of the same object. For example, memory performance in the change detection task was affected by featural context (or refer as ensemble statistics in Alvarez, 2011; Brady & Alvarez, 2011), say if the memory items are warm colors, and the detection items are warm colors as well, the precision of those memory items should accordingly higher than detection items are cool colors. Consequently, the

WM capacity measured in this way would probably not reach four items. This seems to imply that there is a trade-off between memory accuracy and memory capacity. The reduction in capacity may be the result of insufficient precision led to great interference during memory recognition, thereby decrease in the calculated capacity. Besides, it is ambiguous to attribute the error in performance is due to insufficient precision at the encoding stage, or capacity limited in the maintenance (Luria & Vogel, 2011). By contrast, Fougnie et al., (2010) found significant costs for encoding multiple features within an object in the continuous report paradigm, as remembering more features results in a significant impact on the memory precision of each feature representation (see also Fougnie & Marois, 2009; Wheeler & Treisman, 2002; Xu, 2002a, 2002b). These findings are strongly against those of Luck & Vogel (1997), with which multiple features can be encoded within an object unit without cost (Olson & Jiang, 2002;).

Other tasks that require explicit access to VWM, such as the recognition task (Saiki, 2016, 2019; insert), may neglect the additional role of spatial location. Specifically, memory retrieval and recognition are strongly modulated by remembered objects' locations (Hollingworth, 2007; Hollingworth & Rasmussen, 2010). For example, Thayer, Brett & Hollingworth (2021) accounted for the coactivation of features from previous literature was due to the explicit access on recognition task, of which the coactivation of features was promoted by a shared location. That is, such enhanced performance in the same object condition can be explained by the coactivated features that are either separately maintained or bound within a single unit in vWM. The only requirement for coactivation is both color and shape features were contributed to a common retrieval decision (i.e., memory probe task). Thayer at al. (2021), instead of reporting associated irrelevant feature, they probed the effects of features by visual search task, in which participants searched for a target letter among distractor letters

superimposed over color-shape conjunction items. Participants were instructed to maintain two conjunction objects, critically, one search item could occasionally matched either both the color and shape of one remembered object (same-object-match) or the color from one remembered object and the shape from the other (different-object-match). They found robust attentional guidance by search items that match the content of vWM. Interestingly, the magnitude of guidance effects has no significant different between same-object-match items and different-object-match items. Suggesting those conjunctive features were maintained in vWM independently.

Consider the case when you are typing a keyword in the search bar of your computer to locate a file, those outcome files should contain the one that matches your keywords, or the one that is associated with your keyword. For the memory probe task that requires explicit retrieval of the mnemonic object, it acts like you are typing a keyword to find the remembered object, the nature of those associated features from the same object in vWM may be overestimated. It seems practical to use the memory task combined with the visual search task to reconcile these contradictory findings and to answer the question of "how perceptual information is encoded into vWM". This secondary attention-demanding task, as we introduced in the previous section, visual search requires corresponding interaction from vWM and attention: our top-down control over search is rely on holding the mental representation of search intention in vWM – attentional template. Above all, the examination of features' representational fates does not require explicit retrieval of the mnemonic object and thus eliminates the influence of their previous locations.

In contrast to these above strong assumptions, a hierarchical feature assumption which has both object-level and feature-level has received growing research attention

over recent years. That is, the initial encoding process is object-based, but that the "unit" of vWM is a hierarchically structured feature bundle (Bays et al., 2011; Brady et al., 2011, for review; Fougnie & Alvarez, 2011; Fougnie et al., 2013; Markov, Tiurina & Utochkin, 2019; Thayer et al., 2021; Schneegans & Bays, 2017; Shen et al., 2013). We can consciously select which information is of interest in our real world, objectively speaking, the human visual system is efficient and economical when receiving those sensory inputs. If we can perfectly restrict our selection only for one feature dimension to enter the vWM (Woodman & Vogel, 2008), then we have to first decompose the perceptual object into its features when encoding a specific object. This is a resource- and time-consuming process that sounds counterintuitive. A more comprehensive inference is, object encoding follows an object-based manner, multi-feature representations may be decomposed into a hierarchical structure in which features are bound indirectly (via location-based manner or other task-setting) in vWM. This assumption can potentially explain those previous ambiguous findings in which perceptual objects appear to be encoded in their entirety, but the subsequent test of those features from the same object suggested they were maintained separately.

Chapter 2 – Experiment 1

To examine how conjunctive features are represented in vWM, we used conjunctive features defined stimuli that are unique for both color and shape. As we mentioned before when the target is defined by color-shape conjunction, in principle, the representational fates of color-based, shape-based, and object-based templates during the visual search may implicitly offer insight to pin down the template struct in vWM.

To this end, search stimuli were then configured into heterogeneous and homogeneous search arrays. Specifically, in the heterogeneous condition, the target and distractors differed in both colors and shapes, whereas two different types of homogeneous conditions were used to examine the assumption of a potential re-loaded of the attentional template. In the shape-matched condition, the target and distractors shared the same shape, but differed colors (i.e., targets are unique by its color); while in the color-matched condition, the target and the distractors shared the same color but differed shapes (i.e., targets is unique by its shape). Participants were instructed to search for the same target across six consecutive trials. The first four trials would be always heterogeneous conditions. Critically, to detect which memory status of target's color and shape attribute, 1/3 of trials 5 and 6 were the same preceded by either shape-matched or color-matched conditions, thus, the type of search condition was predictable between trials 5 and trials 6. The remaining 1/3 of trials 5 and 6 were heterogeneous conditions, severed as the baseline condition to observe how attentional template dynamic changes with the target repetition. For instance, in the shape-matched condition (4A+2B), when observers keep searching for a red square in the first four trials, they can selectively use either the color ("red") or shape attribute ("square") as a feature-based template (Guided Search 4.0; Wolfe, 2012). If the attentional template

was achieved based on the color attribute, the abrupt shape-matched condition on trials 5 should have virtually no impact on search performance when the target presents. Since a color template is sufficient to detect targets in search arrays when the target is surrounded either by heterogeneous distractors or shape-matched distractors. Whereas if encountered color-matched condition (4A+2C), to successfully identify the target among those color-matched distractors, the attentional template should obligatorily contain the shape information related to the target. In this circumstance, we were able to further detect the memory status of the target's shape attribute.

2.1 Method

2.1.1 Participants

Twenty-two healthy students from the University of Padova (4 males; mean age (± SD) = 20.52 ± 2.35 years) took part in the present experiment after providing written informed consent. Three participants were discarded from the analysis due to a mean search accuracy lower than 70%. Therefore, the final sample included 19 participants (2 males, mean age = 20.63 ± 2.54 years). All participants reported normal or corrected-to-normal vision and no history of neurological disorders. The experiment was approved by the local ethics committee (protocol n. 3486).

2.1.2 Stimuli, apparatus, and procedure

An example of the stimuli and a schematic illustration of the sequence of events on a trial are illustrated in Figure 1. Both cue and search arrays were composed of line-drawings shapes, each subtending a visual angle of 3.5° × 3.5°, randomly selected from a set of 10 shapes (see Figure 2-1). The cue array was composed of two stimuli, symmetrically located at 4.2° of visual angle on the left and right of fixation. One

stimulus represented the target, whereas the other one was a task-irrelevant white shape (either a white circle or a white triangle, which would never appear in the search array). The search arrays were composed of 6 stimuli, presented at equidistant (6° of visual angle) locations from fixation (either at 2, 4, 6, 8, 10, 12 or 1, 3, 5, 7, 9, 11 o'clock of an imaginary circle) displayed against a black background. Stimuli could either be of different colors or share the same color. Colors for the target in the cue array and the stimuli in the search array were same luminance (20 cd/m^2), randomly selected from seven possible values (i.e., CIE: 0.276/0.381; 0.214/0.254; 0.256/0.246; 0.355/0.231; 0.500/0.287; 0.526/0.388; 0.400/0.452; Zhang & Luck, 2008).

Participants could be exposed to three different search arrays (Figure 2-1): a) heterogeneous condition, in which the target and the distractors differed in both colors and shapes; b) shape-matched search condition, in which the target and the distractors shared the same shape, but differed in colors; c) color-matched search condition, in which the target and the distractors shared the same color, but differed in shapes. Participants were asked to report the presence or absence of the cued target by pressing one of the two response keys (i.e., "F" or "J", counterbalanced across participants). Each participant was exposed to the same cued target for six consecutive trials (a block). Critically, the first four trials were always heterogeneous conditions, whereas both the fifth and sixth trials could be either heterogeneous or shape-matched or color-matched conditions with equal probability (i.e., six consecutive heterogeneous search trials or four heterogeneous trials followed by two shape-/color-matched trials). The experiment consisted of 1080 trials (180 blocks), divided into two sessions, performed within a week.

Stimuli were presented on a 17-in cathode ray tube monitor with an 85 Hz refresh

rate controlled by a computer running E-prime 2.0 software. Participants were seated at a viewing distance of about 60 cm. Each trial began with the presentation of a fixation cross at the center of the screen (1200-1600 ms, randomly jittered), followed by a cue array, with the cued target either on the left or right of fixation, displayed for 100 ms. After a 1000 ms blank screen, a search array was displayed for 200 ms. Targets were presented on half of the trials with equiprobability in one of the positions of the imaginary circle, while in the other half of trials, targets were absent. The maximum time for responding was 1800 ms. Reaction times was recorded after the onset of search array. Participants were instructed to maintain their gaze on the fixation cross throughout the trial and to respond as fast and accurately as possible. To familiarize with the task, 18 practice trials (i.e., 3 repetitions) were performed at the beginning of each session.

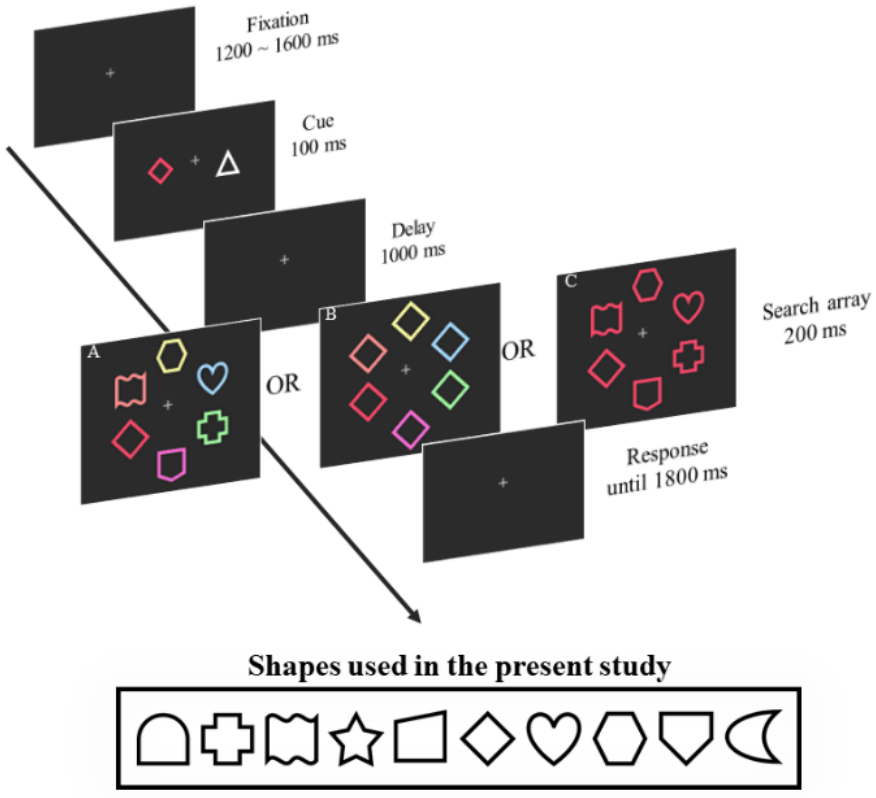

Figure 2-1 Schematic of the experimental paradigm. The experiment was divided into small blocks of 6 trials each. (A) heterogeneous condition; (B) shape-matched condition; (C) color-matched condition. From trial repetition 1 to 4, participants were always exposed to heterogeneous conditions, whereas, in trial repetitions 5 and 6, either of the three distractor types could occur.

2.1.3 Electrophysiological recording and data processing

EEG activity was recorded continuously from 64 Ag/Cl active electrodes placed on an elastic Acti-Cap (Brain Products, GmbH, Gilching, Germany). The EEG activity was band-pass filtered between 0.01 and 30 Hz, digitized at a sampling rate of 1000 Hz, referenced online to the left earlobe, and then re-referenced offline to the average of both earlobes. The electrooculogram (EOG) was recorded using bipolar electrodes placed 1 cm lateral to the outer canthi of both eyes to measure horizontal eye movements (HEOG) and bipolar electrodes above (Fp1) and beneath the left eye to measure vertical eye movements and blinks (VEOG). Individual trials were first rejected if a 200 ms window peak-to-peak analysis detected a threshold of 80 μV for HEOG or VEOG and 100 μV for all channels. This procedure led to three subjects being excluded due to more than 30% of trials being rejected. Continuous EEG was then segmented in epochs starting 200 ms either before the cue array onset, to investigate processes related to the memorization of the cued target, or before the visual search onset, to investigate processes related to the visual search task, and ending 1000 ms and 800 ms after respectively for the cue array and the visual search array. Epochs were baseline corrected using the average activity in the time interval between -200 ms and either cue or search array onset. After excluding trials associated with an incorrect response in the visual search task, independent component analysis (ICA) was then applied to correct EEG activity for residual eye blinks and eye movements (see Drisdelle, Aubin, & Jolicœur, 2017, for a detailed description of the method and

485 validation for use with lateralized ERP components).

486 EEG epochs were then averaged to obtain distinct ERPs for each search condition
487 and for each trial repetition within a block, both time-locked to the cue array and the
488 visual search array. In particular, for the ERPs time-locked to the visual search array,
489 we computed the contralateral and the ipsilateral portions of the N2pc (i.e., the average
490 between PO7 activity elicited by a right presented target and PO8 activity elicited by a
491 left presented target for the former, and vice versa for the latter), and the contralateral
492 and the ipsilateral portions of the SPCN (computed analogously as the N2pc). These
493 ERPs were obtained by averaging target-present trials only. The mean amplitude of the
494 N2pc and SPCN was computed as the subtraction of the ipsilateral activity from the
495 contralateral activity. N2pc amplitudes were estimated in a 220 and 320 ms interval
496 after search array onset whereas SPCN amplitudes in a 400 and 600 ms interval
497 (Berggren & Eimer, 2018). The mean latency of the subtracted N2pc was estimated
498 using the jackknife approach (Kiesel et al., 2008), correcting F, t, and p values
499 according to Miller, Patterson, & Ulrich (1998). Onset latency values were calculated
500 as the time point when individual jackknife waveforms reached the absolute threshold
501 of -0.8 μV, t vales, and F vales were corrected to compensate for the reduced variance
502 across jackknife averages using the equation $t_c = t / (n - 1)$ and $F_c = F / (n - 1)^2$
503 (Ulrich & Miller, 2001).

504 For the ERPs time-locked to the cue array, we computed the contralateral and the
505 ipsilateral portions of the SPCN using all available trials. The SPCN amplitude time-
506 locked to the cue was estimated in a 300-1000 ms interval after the cue array onset
507 (Carlisle et al., 2011). We also tracked the non-lateralized P3 component, a positive
508 sustained potential in the later posterior distribution, also known as the late positive

complex (LPC), is related to the effort of WM required in the current task (Gunseli et al., 2014; Polich, 2012; see review, Kok, 2001; Voss & Paller, 2008). The LPC can serve to index the episodic retrieval from LTM, as the accuracy of familiarity-based recognition was strongly correlated with the magnitude of LPC repetition effects (Voss & Paller, 2007). We chose three electrode sites suggested by previous studies to estimate the LPC waves (i.e., Fz, Cz, Pz). LPC was estimated in a 400-600 ms interval after the cue array onset.

All statistical analyses were performed with R (R Development Core Team, 2017), using the ezANOVA function of the 'ez' package (Lawrence, 2011) and anovaBF/ttestBF functions of the 'BayesFactor' package (Rouder & Morey, 2012), which implements the Jeffreys–Zellner–Siow (JZS) default prior on effect sizes (Rouder, Morey, Speckman, & Province, 2012). Greenhouse–Geisser adjustments were applied on *p*-values when appropriate (Jennings & Wood, 1976), and all the post-hoc comparisons were corrected using Bonferroni correction. The statistical parameters estimated using standard analyses of variance (ANOVAs) were complemented with Bayes factors (*BF*) in order to provide a complementary estimate of the probability that a given main effect or interaction was present (BF_{10}) relative to the alternative hypothesis of its absence ($BF_{01} = 1/BF_{10}$). For example, in case of non-significant factor effects in the ANOVA, the reported BF_{01} approximated the probability of the effective absence of such effects.

2.2 Results

2.2.1 Behavioral data

Figure 2-2 depicts the mean accuracy and reaction times (RTs), separately for target-present and target-absent trials, in each trial repetition and for the three types of search arrays. Only correct response trials were considered in the computation of the RTs. RTs exceeding three standard deviations above/below the mean for each participant and condition were considered outliers and excluded (1.09 %).

Participants were highly accurate in the first four trials, reaching a mean accuracy level of 97% ± 3%, whereas the accuracy level in trial repetition 5 and 6 was lower and depended on the distractors type (Figure2-2A). Given the low frequency of response errors in the first four trials, only mean accuracy in trials 5 and 6 were submitted to statistical analysis. Mean accuracy was submitted to a 2 × 3 × 2 repeated measures ANOVA with repetition (trials 5 vs. 6), distractors type (heterogeneous vs. shape-matched vs. color-matched), and target type (present vs. absent) as within-subject factors. Participants were generally more accurate in detecting the presence of a target rather than its absence (F (1, 18) = 29.45, p < .001, η_p^2 = .621, BF_{10} > 1000). The significant interaction between distractors type and target type (F (2, 36) = 53.03, p < .001, η_p^2 = .747, BF_{10} > 1000) further reflected that participants were less accurate in reporting the absence of the target, compared to the heterogeneous condition (99%), in both shape-matched condition (74%; p < .001, BF_{10} > 1000) and color-matched condition (90%; p < 0.001, BF_{10} > 1000). Participants were also less accurate to report the presence of the target in color-matched condition compared to heterogeneous condition (90% vs. 96%, respectively; p < .001, BF_{10} > 1000), whereas no differences were found between shape-matched and heterogeneous conditions for target-present

trials (97% vs. 96%; $p = .213$, $BF_{01} = 1.44$).

To investigate the effect of repetition in the heterogeneous condition, a 6 × 2 repeated measures ANOVA on RTs was performed, considering repetition (trials 1, 2, 3, 4, 5 vs. 6) and target type (present vs. absent) as within-subject factors. Participants were generally faster in detecting the presence of a target (374 ms) rather than its absence (387 ms) (F (1, 18) = 4.08, $p = .059$, $\eta_p^2 = .185$, $BF_{10} > 1000$). However, search performance did not show any modulation of the repetition, none of the interaction was statistically significant ($Fs < 1$; $ps > .1$).

RTs in trials repetition 5 and 6 were slower and depended on the distractors type (Figure2-2 B). Mean RTs were submitted to a 2 × 3 × 2 repeated measures ANOVA with the same factors described above. The significant interaction between distractors type and the target type (F (2, 36) = 60.10, $p < 0.001$, $\eta_p^2 = 0.770$, $BF_{10} > 1000$) indicated that participants were slower in detecting the absence of a target in both shape-matched (460 ms, $p < 0.001$, $BF_{10} > 1000$) and color-matched (555 ms, $p < 0.001$, $BF_{10} = 3.93$) than in heterogeneous (383 ms). Furthermore, participants were slower to detect the presence of a target in color-matched than in heterogeneous condition (429 ms vs. 366 ms, $p < 0.001$, $BF_{10} > 1000$). No significant different was found in both shape-matched and heterogeneous condition when target presented (377 ms vs. 366 ms, $p = 0.324$, $BF_{01} = 1.74$).

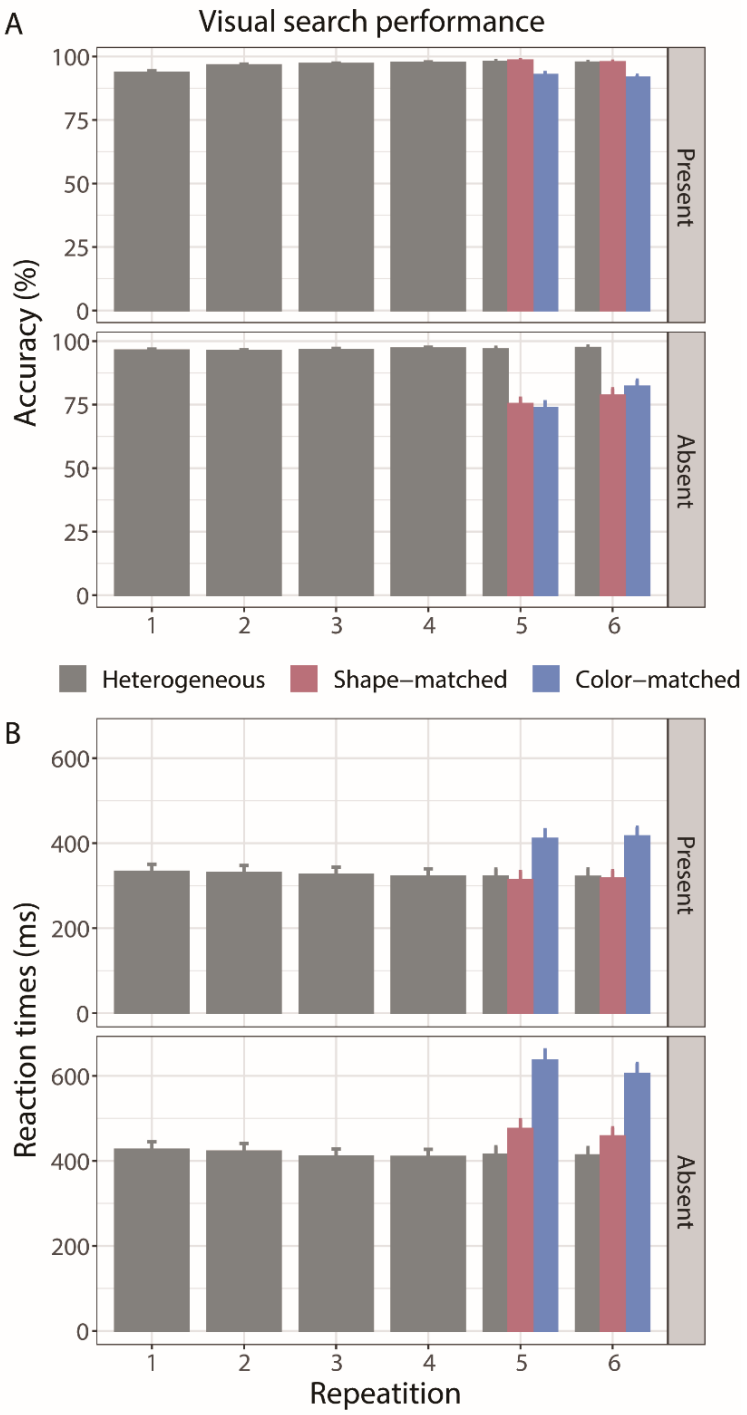

573

574 **Figure 2-2** Mean accuracy (A) and RTs (B) of the visual search task for each search
575 condition as a function of trial repetition. The error bars represent the standard errors.

576 **2.2.2 N2pc in the visual search task**

577 Figure 2-3 shows ERPs elicited at PO7/8 electrode sites in response to target-present

visual search arrays. ERPs are presented separately for repetition 1 to 4 (Figure 2-3A) and 5 to 6, further divided according to distractors type (Figure 2-3B & C).

To determine the effect of repetition on N2pc in the heterogeneous condition, N2pc amplitudes were submitted to a 6 × 2 repeated measures ANOVA, considering repetition (trials 1, 2, 3, 4, 5 vs. 6) and laterality (contralateral vs. ipsilateral) as within-subject factors. Results revealed a greater negativity at contralateral sites compared to ipsilateral sites in all trial repetitions (F (1, 18) = 70.47, p < .001, η_p^2 = .797, BF_{10} > 1000), suggesting that reliable N2pcs were present from trial repetition 1 to 6. The non-significant interaction between the two factors (F = .74, p = .596, BF_{01} = 40.78) further emphasized that the N2pc amplitude did not differ across trial repetitions (contralateral vs. ipsilateral: M diff = -1.82μV, -1.86 μV, -1.93 μV, -1.92 μV, -1.55 μV and -1.96 μV respectively). N2pc onset latencies were then submitted to a one-way repeated measures ANOVA, considering repetition (trials 1, 2, 3, 4, 5 vs. 6) as within-subject factors. This analysis revealed the N2pc onset difference did not significant from trial repetition 1 to 6 (F_c < 1, onset latency: 216 ms, 217 ms, 210 ms, 221 ms, 237 ms and 222 ms respectively). Hints to a possible cause of the lack of repetition effect on behavioral data.

To determine the impact of distractors type, N2pc amplitudes were submitted to a 2 × 3 × 2 repeated measures ANOVA, considering repetition (trials 5 vs. 6), distractors type (heterogeneous vs. shape-matched vs. color-matched), and laterality (contralateral vs. ipsilateral) as within-subject factors. Results revealed a greater negativity at contralateral compared to ipsilateral sites (F (1, 18) = 25.68, p <.001, η_p^2 =.588, BF_{10} > 1000), and a main effect of the search array (F (2, 36) = 46.80, p <.001, η_p^2 =.722, BF_{10} > 1000). These two effects combined non-linearly (F (2, 36) = 17.21, p <.001, η_p^2

=.489, BF_{10} > 1000), reflecting the presence of a reliable N2pc only in heterogeneous (contralateral vs. ipsilateral: *M diff* = -1.75 μV, p < .001) and color-matched (*M diff* = -.90 μV, p < .05), but not in shape-matched condition (*M diff* = -.11 μV, p = .546, BF_{01} = 4.50). There was a marginal significant of the three-way interaction (F (2, 36) = 2.84, p = .072, η_p^2 = .136, BF_{01} = 5.44). Further planned comparisons showed that N2pc amplitude did not differ in trials repetition 5 (heterogeneous vs. color-matched: -1.55 μV vs. -1.14 μV, p = .677, BF_{01} = 2.13), whereas in trials repetition 6, N2pc amplitude attenuated in color-matched as compared to heterogeneous condition (heterogeneous vs. color-matched: -1.95 μV vs. -.67 μV, p <.05, BF_{10} = 2.11).

Since the waveform of shape-match did not reach -0.75 μV at the given time range (as shown in Figure 2-3 B&C), the estimation of N2pc onset difference only concerned between heterogeneous and color-matched conditions. A 2 × 2 repeated measures ANOVA, considering repetition (trials 5 vs. 6), distractors type (heterogeneous vs. color-matched) as within-subject factors was conducted, this analysis revealed a main effect of distractors type (F_c (1, 18) = 9.32, p_c < 0.05, η_p^2 = 0.341), most importantly, the interaction between these two factors also significant (F_c (1, 18) = 38.10, p_c < 0.001, η_p^2 = 0.679). Further planned comparisons showed that in trial repetition 5, the N2pc onset difference did not significant between heterogeneous and color-matched condition (237 ms vs 226 ms, t_c (18) = -0.97, p = 0.347). Whereas in trial repetition 6, the N2pc onset delay about 50 ms between heterogeneous and color-matched condition (222 ms vs 278 ms, t_c (18) = 8.06, p < 0.001).

Visual inspection of Figure 2-3 B&C makes apparent — a contralateral positivity was elicited at 300-400 ms after visual search array onset in the shape-match condition (red line) and contralateral negativity followed by the presence of N2pc in the color-match

condition (blue line). These observations are corroborated by statistical analysis. The amplitude values recorded in the P_D and SPCN time window was separately submitted to a 2 × 3 × 2 repeated measures ANOVA, considering the same within-subject factors described above. In the 300-400 ms time window, the analysis detected a significant interaction between distractors type and laterality (F (2, 36) = 34.81, p < .001, η_p^2 = .659, BF_{10} > 1000). Pairwise comparisons confirmed that significant P_D was present for shape-match condition (contralateral vs. ipsilateral: *M diff* = 1.01 μV, p < .001, BF_{10} = 3.05). Whereas in 400-600 ms time window, results revealed the presence of a significant three-way interaction (F (2, 36) = 3.92, p < 0.05, η_p^2 = 0.179, BF_{01} = 1.53). Pairwise comparisons showed that sustained negativity in the SPCN time range emerged only for the shape search in trial repetition 5 (contralateral vs. ipsilateral: *M diff* = -0.87 μV, p < 0.05, BF_{10} = 2.96).

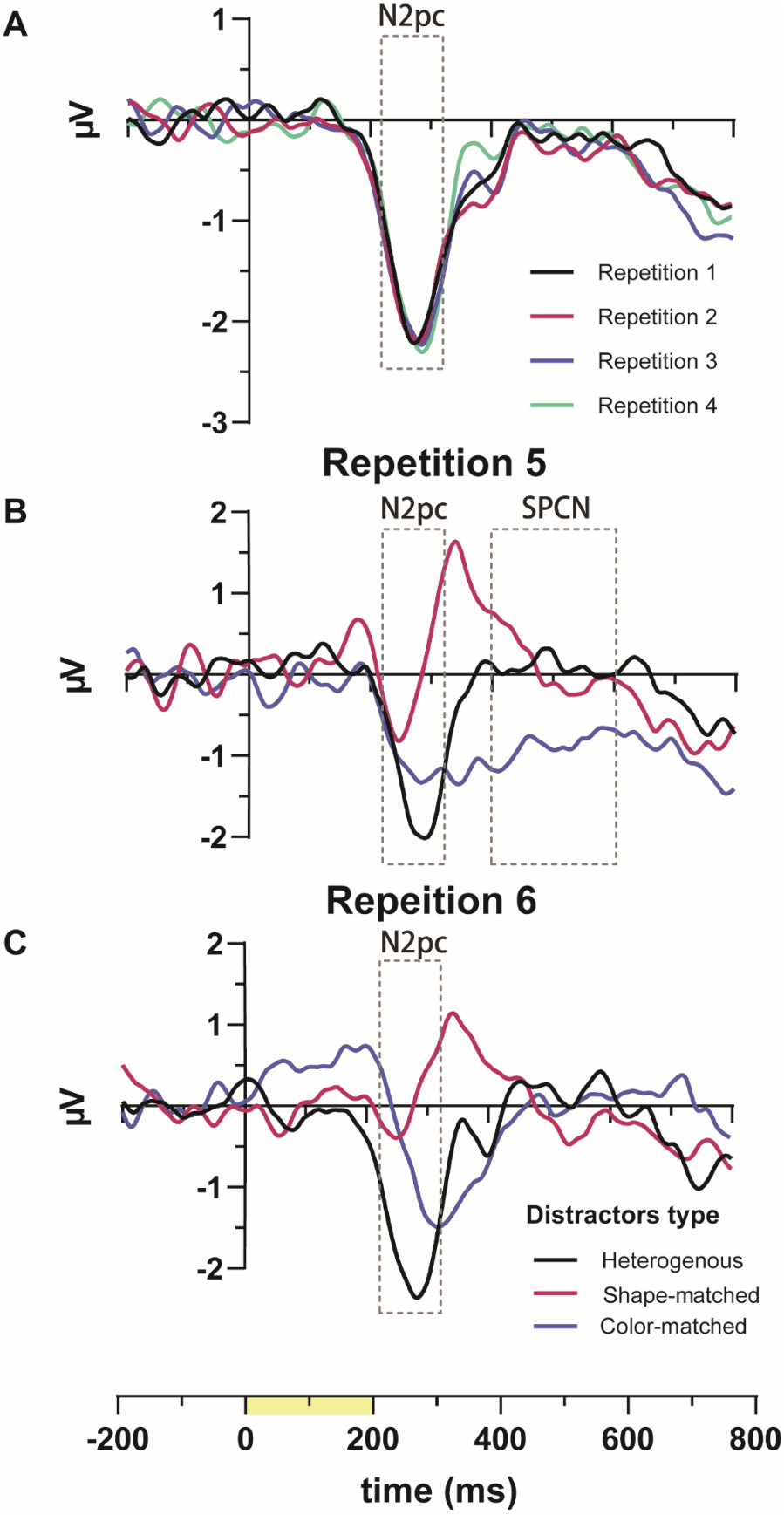
A
N2pc
μV
1
-1
-2
-3
Repetition 1
Repetition 2
Repetition 3
Repetition 4
Repetition 5
B
N2pc
SPCN
2
1
μV
-1
-2
Repeition 6
C
N2pc
2
1
μV
-1
-2
Distractors type
Heterogenous
Shape-matched
Color-matched
-200
0
200
400
600
800
time (ms)

638

Figure 2-3 Grand-averaged ERPs elicited at electrodes PO7/8 time-locked to the presentation of the search array for (A) the first four trial repetitions (heterogeneous condition) and for trial (B) repetition 5 and (C) 6, separately displayed for the distractors type (heterogeneous, shape-matched vs. color-matched). Color bars on the timeline indicate the exposure duration of the search array (yellow). The area indicated by the dashed-line rectangles in the graph represents the time window considered for ERP amplitude analyses. ERP functions were low-pass filtered at 15 Hz for visualization purposes.

2.2.3 SPCN in the cue array

Grand-average ERP waveforms time-locked to the presentation of the cue array elicited at posterior electrodes PO7/8 and separately displayed for repetition 1 to 5 (Figure 2-4 A) and 6, further divided according to distractors type (Figure 2-4 C).

To determine the effect of repetition, these amplitude values were then submitted to a 6 × 2 repeated measures ANOVA with repetition (trials 1, 2, 3, 4, 5 vs. 6) and laterality (contralateral vs. ipsilateral) as within-subject factors. Following the presentation of the cue, greater negativity was recorded at contralateral sites compared to ipsilateral ones (F (1, 18) = 48.68, $p < .001$, $\eta_p^2 = .730$, $BF_{10} > 1000$). There was also a significant interaction between repetition and laterality (F (5, 90) = 4.81, $p < .001$, $\eta_p^2 = .211$, $BF_{10} > 1000$). Pairwise comparisons confirmed that a reliable SPCN was present in all trial repetitions (contralateral vs. ipsilateral: M diff = -.94 μV, -.60 μV, -.57 μV, -.58 μV, -.51 μV, -.57 μV respectively). Further planned comparisons revealed that the SPCN amplitude was lower in trial repetition 6 than in trail repetition 1 (-.57 μV vs. -.94 μV, t (18) = -2.76, $p < 0.05$, $BF_{10} = 2.53$).

To investigate whether the SPCN amplitude increased after participants encountered different types of search array in repetition 6, an additional 3 × 2 repeated-measures ANOVA was conducted including distractors type (heterogeneous vs. color vs. shape search) and laterality (contralateral vs. ipsilateral) as within-subject factors. The

ANOVA revealed the difference significant main effect of laterality, F (1, 18) = 14.37, $p < .001$, $\eta_p^2 = .444$, $BF_{10} > 1000$, suggesting that the SPCN was present for all three types of search conditions. The lack of interaction ($F < 1$, $BF_{01} = 5.72$) further suggested that the SPCN amplitude did not differ between search conditions.

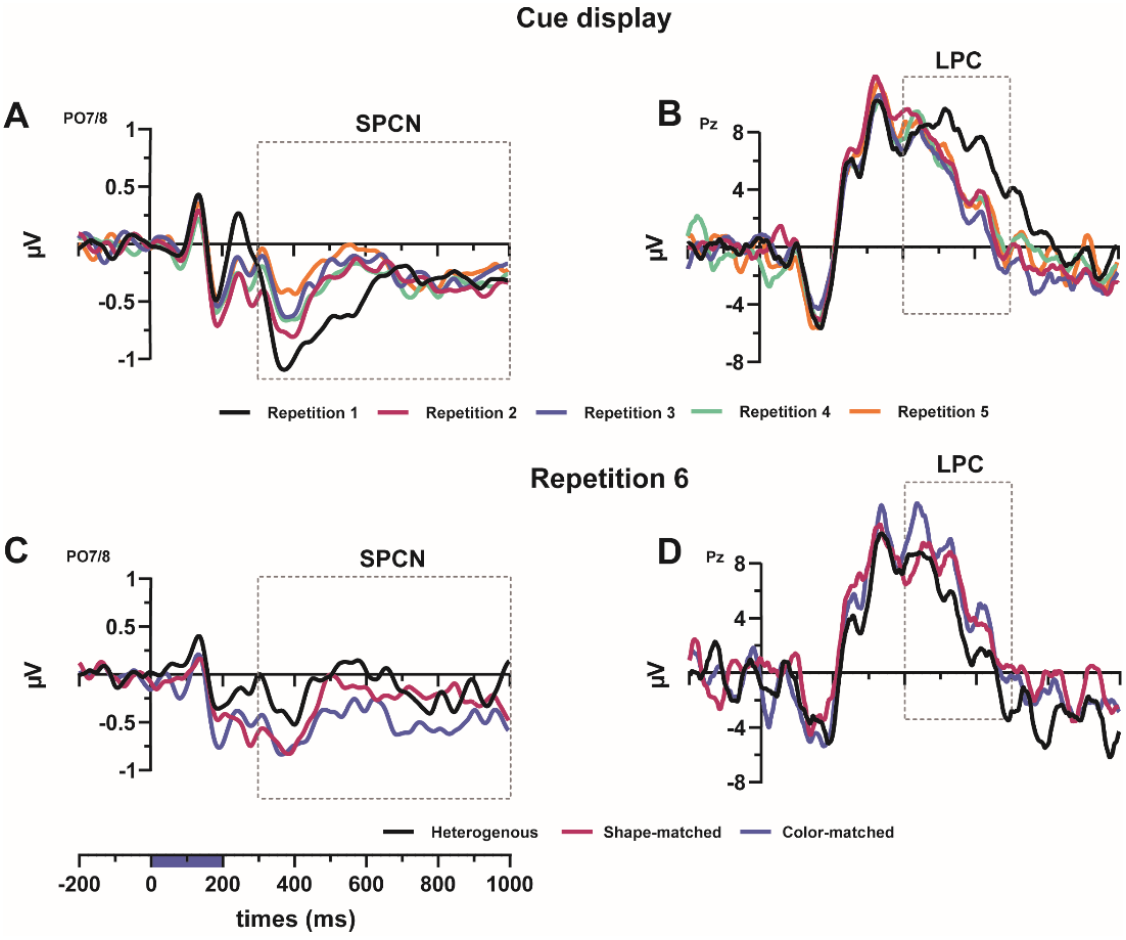

Figure 2-4 Grand-average ERP waveforms time-locked to the presentation of the cue. SPCN difference waves were computed from the contralateral minus ipsilateral waves elicited at electrodes PO7/8. LPC amplitude was estimated at electrodes Pz. There ERPs functions were separately displayed for (A/B) trial repetitions 1 to 5 and (C/D) repetition 6, separately displayed for the distractors type (heterogeneous, shape-matched vs. color-matched). Color bars on the timeline indicate the exposure duration of the cue display (blue). ERP functions were low-pass filtered at 15 Hz for visualization purposes.

2.2.4 LPC in the cue array

Figure 2-4 also shows the time window to estimate the LPC (gray bar). Mean LPC amplitudes in the heterogeneous search were submitted to a one-way repeated measures ANOVA with repetition (trials 1, 2, 3, 4, 5 vs. 6) as within-subject factors. This analysis revealed a significant main effect of repetition (F (5, 90) = 7.2, $p < 0.001$, $\eta_p^2 = 0.286$, $BF_{10} > 1000$), pairwise comparisons revealed that the amplitude of LPC was greater in trial 1 (3.68 μV), and then decreased in each repetition as compared to trial 1 (trial 2: 2.30 μV, $p < 0.05$, $BF_{10} = 17.32$; trial 3: 1.89 μV, $p < 0.05$; trial 4: 1.63 μV, $p < 0.05$; trial 5: 1.59 μV, $p < 0.001$; trial6: 1.90 μV, $p < 0.001$).

We then examined whether the LPC amplitude increased again in trial repetition 6 when a shape-match or color-match condition was presented in trial repetition 5. A repeated-measures ANOVA including distractors type (heterogeneous vs. shape-match vs. color-match) as within-subject factors showed no main effect of search array (F (2, 36) = 1.82, p = .176, BF_{01} = 1.99). Similar to the SPCN, the lack of the main effect provides critical support for the statistical equivalence of LPC on difference search conditions, suggesting there was no increase in WM effort after encountering the shape-match and color-match conditions.

2.3 Discussion of Experiment 1

Visual search with a known target can be guided by the attentional template which

699 was assumed to be maintained in vWM. However, after several consecutive trials of
700 learning, less demand was required on vWM of this top-down attentional guidance.
701 During the memory retention, the mean amplitude of SPCN and LPC time-locked to
702 the cue was systematically dropped down as a function of target repetition. In line with
703 previous studies, these findings revealed a reducing need for vWM while participants
704 were repeatedly searching for the constant target (Carlisle et al., 2011; Gunseli, Olivers,
705 & Meeter, 2014; Grubert, Carlisle, & Eimer, 2016; Reinhart & Woodman, 2014;
706 Woodman et al., 2013), which indicates the template that used to guide attention was
707 off-loaded to an alternative mechanism.

708 Experiment 1 provided a solution to further examine how conjunctive features related
709 to search target are represented in vWM, and most importantly, to have some insight
710 into how these conjunctive features were off-loaded. Using visual search task instead
711 of memory probe task, the guidance of attention requires no direct association between
712 feature values that are associated with the same object, such guidance would be
713 implemented in a manner of feature-based rather than object-based. This is supported
714 by the behavioral result that search performances are the same efficiency and accuracy
715 when distractors are heterogeneous or shared the same shape with targets, implying a
716 potential color-based guidance manner is predominantly. That is, participants were most
717 likely working in a color-detection mode, holding the color template would be sufficient
718 to identify the target. Such a color-detection mode has been proved in many
719 circumstances to be effective in the guidance of attention (Olivers, 2009; Soto et al.,
720 2005; Zhang et al., 2010), with higher salience than shape attribute (Wolfe & Horowitz,
721 2004). In our case, the target's color also contained the relevant information related to
722 the search intention. In terms of the Guide search model (Wolfe, 2012), the initial
723 attention deployment is controlled by the mediation of both bottom-up (i.e., most salient

724 feature) and top-down (i.e., attentional template) factors. The outcome of this mediation
725 is presumably to configure the color as attentional templates.

726 So far, the comparison between heterogeneous and shape-matched conditions is not
727 sufficient to make any surmises regarding the memory status of color or shape attribute.
728 For this reason, the color-matched condition was designed to investigate whether the
729 color feature has the same impact as the shape feature in visual search. We observed
730 different ERPs during two consecutive color-matched trials. In the first trial, the target
731 triggered an N2pc as well as an SPCN. This revealed the target was accessing to vWM
732 during search processes, presumably in order to make a choice response (Jolicœur et
733 al., 2008; Mazza, Turatto, Umiltà, & Eimer, 2007), or target were encoded into vWM
734 to compare with the current attentional template (Berggren & Eimer, 2018).

735 Says if a potential color-based guidance manner is predominantly existing in the
736 heterogeneous or shape-matched condition, this type of manner should be barely
737 available in our color-matched conditions, where targets were unique by their shape.
738 When collectively taking these results, early attentional deployment of object selection
739 may operate in a feature-based manner, guided by the target's color attribute, but the
740 shape attribute can be involved in the later recognition process. To serve this kind of
741 later recognition, in terms of the concentric model of WM (Oberauer, 2002), the target's
742 shape feature may likely be off-loaded to the region of direct access, in which holding
743 a limited subset of the activated representations, available to access and re-load back to
744 the focus of attention. Elements in the region of direct access are treated as selection
745 candidates. They linked with the focus of attention because of the task relevance. Since
746 participants were shown three types of search arrays before the formal experiment, they
747 might actively prepare both targets attributes available for the subsequent target

identification. As expected, the color attribute became the attentional template, the shape attribute, however, was prepared anytime to break into the focus. Therefore, interference in the shape-matched condition was observed due to the shape-matched distractors triggering the use of the target's shape attribute. As evidence shows that P_D appeared in the shape-matched condition.

However, ERPs from the shape-matched condition provided challenging findings. The N2pc was minimal and did not reach a significant level, in contrast, a contralateral positivity was elicited from 300 ms after search onset. This inverse N2pc pattern has been linked to distractor suppression (P_D component, Hickey, Di Lollo & McDonald, 2008), which may reflect shape-matched distractors interfered with the target selection. It is possible that attention was suppressed or withdrawn to shape-matched distractors before its arrival. Behavioral data in the target-absent trials provided preliminary evidence that participants generally took more time to quite the search. As they were less efficient in detecting the absence of a target in the shape-matched condition than in the heterogeneous condition (460 ms vs. 383 ms). However, one may interpret this finding as a serial scanning strategy, in which observes tend to scan lateral items prior to vertical items. This may be the case in the study by Kerzel & Burra (2020), who proposed that contralateral positivity is an inversed N2pc to the opposite side. This possibility would be further examined in Experiment 2.

The N2pc pattern in trials 6 suggested the guidance process is less efficient in the color-matched condition. As N2pc was significantly delayed compared to heterogeneous conditions (278 ms vs. 222 ms). Moreover, no SPCN time-locked to the target was observed, demonstrating that different attentional modulations have happened in the second shape search. One possible explanation is the focus of attention

772 was shifting from color- to shape-detection mode (Rhodes & Cowan, 2019), which was
773 also referred to as switching costs (Oberauer, 2002). In this scenario, a new template
774 was configured based on the shape instead of the color feature. Recent ERP studies
775 from Grubert & Eimer (2018; 2020) have shown evidence that attentional templates are
776 not continuously active, but are transiently activated before the arrival of the next search
777 display and deactivated after a response was made. The majority of heterogeneous trials
778 (77.8% of overall trials) somehow generate a familiarity signal that allows the color
779 feature to gain more attentional weight than the shape feature (Oberauer, 2006;
780 Oberauer, 2006; Oberauer, Awh, & Sutterer, 2016). After the first shape search, the
781 familiarity signal of the color feature had to be overridden by bringing the target's shape
782 feature back to the focus. The longer it takes to retrieve the target's shape feature, the
783 worse performance it will be in the shape search. As a result of this, the competition
784 between the target's shape and color feature impaired the search efficiency, leading to
785 the slower deployment of attention.

786 Noticed that after the reloading of the shape feature, some may argue the storage of
787 the target's conjunction features could be bound within an entire object-file (Kahneman
788 et al., 1992), thereby guiding attention in an object-based manner. This assumption was
789 testified by Berggren & Eimer (2018), who demonstrated that the object-based
790 attentional control is only involved when the feature-based guidance cannot distinguish
791 the target from target-like distractors. Convergent conclusions can be drawn also from
792 our color-matched condition. SPCN time-locked to the target emerged only in the first
793 color-matched trial whereas not in heterogeneous and shape-matched trials, suggesting
794 the selection of the potential object was different between search arrays. Attended
795 objects in heterogeneous and shape-matched can access vWM via feature-based
796 attentional control, whereas only objects that contained both color and shape features

797 could access vWM when surrounded by color-matched distractors. It is also notable
798 that the object-based manner seems to affect selection later than the feature-based
799 manner, in other ERP studies using conjunction target, in which a superadditive role of
800 N2pc which was assumed to reflect the object-based attentional biases. They found
801 N2pcs to target and target like distractors were initially equal in size, but that became
802 larger only for the target (Eimer & Grubert, 2014b; Berggren & Eimer, 2016, 2018).
803 Hence, the slower deployment of attention in the second shape search may imply that
804 object-based attentional control started to govern attentional selection.
805

Chapter 3 – Experiment 2

Experiment 2 aimed to further investigate the impact of the shape-matched condition by examining stimuli position in the vertical upper versus lower hemifield. Like others before us, studies regarding the contralateral polarities found larger negativity for N2pc when the target was in the lower hemifield compared to when it was in the upper hemifield (Bacigalupo & Luck, 2019; Doro et al., 2020; Luck et al., 1997; Monnier, Dell'Acqua, & Jolicœur, 2020; Perron et al., 2009). Whereas the modulation of vertical hemifield was the reversal in the contralateral positivity for distractor processing (P_D), larger P_D was recorded when the distractor was presented in the upper than in lower hemifield (Hickey et al., 2008). Thoughts provoked by these findings, the possibility to interpret the smaller N2pc in shape-matched condition — the attentional response was offset due to the average upper and lower hemifield contra-minus-ipsi waves — as averaged over upper and lower hemifield likely as averaged the N2pc with a temporal delay and polarity reversal P_D (i.e., the time point of the polarity reversal of N2pc and P_D). We then manipulated the vertical placement of the target (upper vs. lower hemifield) in Experiment 2 to evaluate this assumption.

As we mentioned in the discussion of Experiment 1, to reconcile whether the inverse N2pc pattern in shape-matched conditions was due to distractor suppression (P_D) or the tendency in which attentional response was directed from one lateral side to the opposite side, we produced a midline target trial in which target was displayed along the horizontal median. If participants have a bias to attend the lateral than vertical position, we would be able to expect a behavioral difference between the lateral versus vertical midline targets condition. Furthermore, the design of Experiment 2 allowed us to test whether the results of Doro et al. (2020) regarding the amplitude equivalence of

N2pc (lateral targets) and N2pcb (midline targets) could be replicated. According to their hypothesis, if a target is shown along the vertical midline, it is represented bilaterally in both posterior cerebral hemispheres, this target is intended to cause a bilateral N2pc (i.e., N2pcb), manifested as an attentional response to the target is projected over the posterior scalp. Nevertheless, each hemisphere would also receive input separately from contralateral distractors. In the midline target trials, if lateralized shape-matched distractors do interfere with the target selection, we may expect a bilateral inhibition overlapped with the N2pcb, resulting in attenuation or even elimination of this component (Doro et al., 2020). Furthermore, this type of distractor inhibition should have occurred primarily in the shape-matched condition, but not in the heterogeneous and color-matched condition. And if color-matched distractors trigger the use of object-based guidance manner, as evidence for the onset of SPCN follows the N2pc, we would also expect a bilateral SPCN (SPCNb) in the color-matched condition.

3.1 Method

3.1.1 Participants

Thirty-three students at the Guangzhou University (9 males; mean age = 20 years, SD = 1.3) took part in the present experiment after providing written informed consent. All participants had normal or corrected-to-normal visual acuity, and all reported normal color vision and no history of neurological disorders. The experiment was vetted by the local ethics committee.

3.1.2 Stimuli, apparatus, and procedure

The stimuli were displayed on the black background (CIE: 0.312/0.329, 1.0 cd/m2)

of a 17-inch CRT computer monitor with a refresh rate of 60 Hz, at a viewing distance of about 60 cm. The main procedure was identical to experiment 1, except that all stimuli in the visual search were presented at 2, 4, 6, 8, 10, 12 o'clock of an imaginary circle. As mentioned above, this manipulation allows us to separate ERPs when the target is displayed in the left, right, or midline locations, or whether in the upper or lower visual field. The experiment consisted of 1944 trials (324 blocks), divided into two sessions, performed within a week.

3.1.3 Electrophysiological recording and data processing

EEG activity was recorded continuously from 64 Ag/AgCl electrodes, positioned according to the 10–10 International system (Sharbrough, 1991), using a Neuroscan Curry 8 system (Compumedics USA, Charlotte, NC, USA) set in AC mode and using an electrode located between FPz and Fz as ground. The vertical electrooculogram (VEOG) was recorded from two electrodes positioned 1.5 cm above and below the left eye. The horizontal electrooculogram (HEOG) was recorded from two electrodes positioned on the outer canthi of both eyes. EEG, VEOG, and HOEG signals were band-pass filtered between 0.01 and 30 Hz and digitized at a sampling rate of 1000 Hz. EEG activity was referenced online to an electrode located approximately 1.5 cm posterior to Cz and re-referenced offline to the average value of the left and right mastoids.

Experiment 2 used the same criteria as Experiment 1, with the following exceptions. EEG epochs were then averaged to obtain three distinct ERPs for each distractors type, namely the contralateral and ipsilateral portions of the N2pc elicited by lateral targets, and crucially, a bilateral ERP (obtained by averaging the activity of PO7 and PO8) for midline targets. The mean amplitude of the N2pc and SPCN elicited by lateral targets was calculated by subtracting ipsilateral activity from contralateral activity in 200–300

ms and 400–600 ms intervals, respectively. The mean amplitude of the N2pcb and SPCNb elicited by midline targets was computed similarly to Doro et al. (2020) by subtracting the ipsilateral activity elicited by lateral targets from the bilateral activity elicited by midline targets at the same time windows as those considered for N2pc and SPCN amplitude estimation.

3.1.4 Scalp potentials and scalp current density

Using a spherical spline surface Laplacian (order of the splines = 4, regularization parameter = 1e-5, conductivity of the skin = 0.33 S/m), EEG data from the N2pc/N2pcb and SPCN/SPCNb time windows were translated into scalp current density (SCD) topographic maps (Perrin, Pernier, Bertrand, & Echallier, 1989). We chose SCD maps over spline-interpolated maps of voltage intensity because the SCD technique reduces the blurring effects of volume conduction on the scalp-recorded EEG voltage signal, resulting in a clearer topography (Pernier, Perrin, & Bertrand, 1988). SCD maps, in particular, allow reference-free mapping of scalp-recorded electrical activity, making ERP polarity clear. The SCD method of scalp topography requires no assumptions about neuroanatomy, number, direction, or independence of the underlying neuronal generators. The direction of the global radial currents underlying the EEG topography is directly reflected in the sign of these estimations, with positive values representing current flow from the brain towards the scalp and negative values showing current flow from the scalp into the brain.

3.2 Results

3.2.1 Behavioral data

RTs recorded on trials associated with an incorrect response and/or RTs exceeding

three standard deviations above/below individual mean RT (1.3%) were excluded from the analysis. Search performance was similar to what we found in Experiment 1. To make a comparison with the ERP result, we then investigated the possible accuracy and RT differences on target-present trials with targets at lateral versus midline positions. A summary of the target-present trial is illustrated in Figure 3-1, separately displayed for midline target and lateral target position.

Mean accuracy values in trial repetition 5 and 6 were submitted to a 2 × 3 × 2 repeated measures ANOVA with repetition (trials 5 vs. 6), distractors type (heterogeneous, shape-matched vs. color-matched), and target position (midline vs. lateral) as within-subject factors. The main effect of distractors type (F (2, 58) = 55.72, p < .001, η_p^2 = .658, BF_{10} > 1000) reflected that participants were less accurate to report the presence of the target in color-matched condition compared to heterogeneous condition (92.24% vs. 97.73%, respectively; p < .001), whereas no differences were found between shape-matched and heterogeneous conditions (98.10% vs. 97.73%, respectively; p = .854, BF_{01} = 5.35). The main effect of target position (F(1,29) = 1.04, p = .317, BF_{01} = 3.74) and interaction (F (2, 58) = 2.03, p = .160, BF_{01} = 1.29) were not significant.

An analogous 2 × 3 × 2 ANOVA was carried out for the Mean RTs. Results showed only a main effect of distractors type (F (2, 58) = 146.31, p < .001, η_p^2 = .835, BF_{10} > 1000), participants were slower to detect the presence of a target in color-matched than in heterogeneous condition (411 ms vs. 319 ms, p < .001). No significant different was found in both shape-match and heterogeneous condition (312 ms vs. 319 ms, p = .154). Although the effect of target position appeared to be confined (F (1, 29) = 3.92, p = .057, η_p^2 = .119, BF_{01} = 2.71), with slightly faster RTs in detecting the midline target than the lateral target (343 ms vs. 351 ms), the interaction between target position and distractors type was not significance (F (2, 58) = 1.91, p = .162, BF_{01} = 10.99).

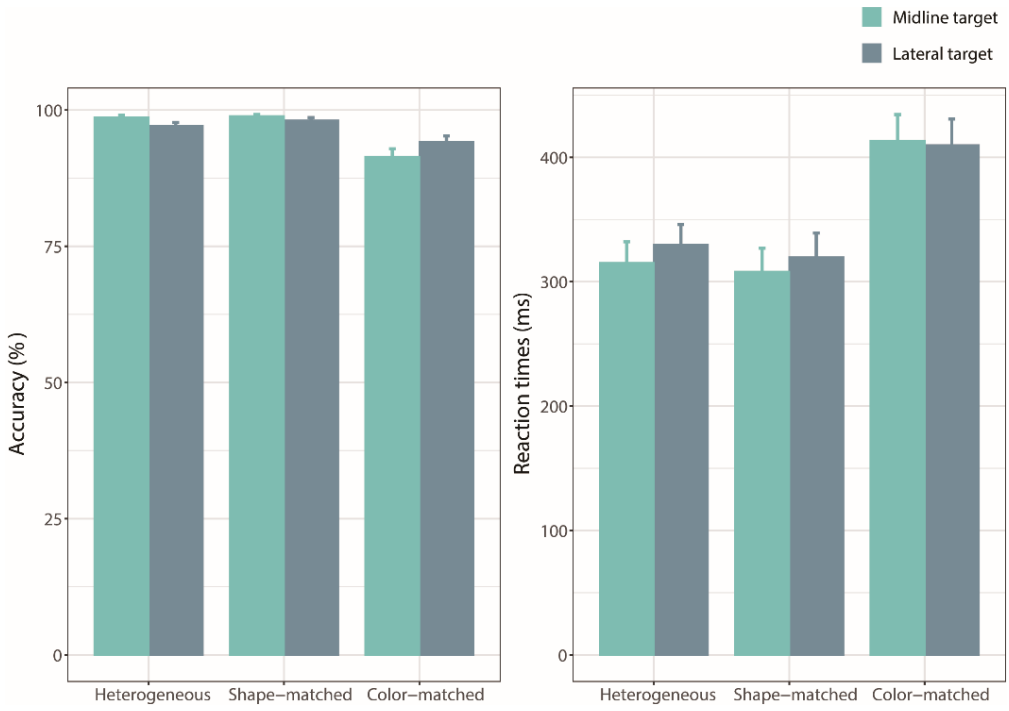

Figure 3-1 Mean percentage of correct responses (left panel) and mean RTs (right panel) in the visual search task, collapsed between trials 5 &6, plotted as a function of target position (midline vs. lateral) and distractors type (heterogeneous, shape-matched vs. color-matched). Error bars represent the standard error of the mean.

3.2.2 ERPs in the visual search task

As shown in Figure 3-2, both N2pc and N2pcb were strongly modulated by vertical elevation, as reported by Doro et al. (2020). This is more evident in Figure 3-3, where SCD topographies of difference ERPs are plotted. Recall that the amplitude of lateralized ERPs was calculated in the standard way by subtracting ipsilateral from contralateral ERP activity elicited by lateral targets. The amplitude of bilateral ERP was calculated by subtracting ipsilateral ERPs for lateral targets from the average of ERPs at PO7 and PO8 for midline targets.

These observations were corroborated by statistical analysis. The amplitude values recorded from trials repetition 1 to 4 in the N2pc/N2pcb time-window were first separately submitted to *t*-test to determine whether they differed from 0 μV. For target

displayed in the upper hemifield, N2pcs were significantly present in trials repetition 1 (-.50 μV, $t(29) = -2.62$, $p = .001$), 2 (-.59 μV, $t(29) = -3.57$, $p = .001$), 3(-.51 μV, $t(29) = -2.98$, $p = .005$), and 4 (-.53 μV, $t(29) = -2.84$, $p = .008$); but N2pcbs were basically absent (-.17 μV, -.30 μV, -.04 μV, -.25 μV, respectively; max $t = -1.84$, min $p = .076$). For target displayed in the lower hemifield, N2pcs and N2pcb were clearly larger in trials repetition 1 (N2pc: -1.80 μV, $t(29) = -7.56$, $p < .001$; N2pcb: -1.71 μV, $t(29) = -7.06$, $p < .001$), 2 (N2pc: -1.63 μV, $t(29) = -7.67$, $p < .001$; N2pcb: -1.44 μV, $t(29) = -6.42$, $p < .001$), 3 (N2pc: -1.62 μV, $t(29) = -8.22$, $p < .001$; N2pcb: -1.45 μV, $t(29) = -6.28$, $p < .001$), and 4 (N2pc: -1.65 μV, $t(29) = -7.06$, $p < .001$; N2pcb: -1.61 μV, $t(29) = -8.45$, $p < .001$). These amplitude values were then submitted to a 4 × 2 × 2repeated measures ANOVA, considering repetition (trial 1, 2, 3 vs. 4), component (N2pc vs. N2pcb) and visual hemifield (upper vs. lower) as within-subject factors. Results yielded the main effect of hemifield ($F(1, 29) = 69.42$, $p < .001$, $\eta_p^2 = .705$, $BF_{10} > 1000$) and of component ($F(1, 29) = 6.08$, $p = .020$, $\eta_p^2 = .173$, $BF_{10} = 3.61$). These two effects combined non-linearly ($F(1, 29) = 4.99$, $p = .033$, $\eta_p^2 = 0.147$, $BF_{10} = 2.52$), which was most likely driven by the smaller N2pcb in the upper hemifield. Further pairwise comparison showed that for targets displayed in the upper visual hemifield, the amplitude of N2pc was greater than that of N2pcb (-.54 μV vs. -.02 μV, $p = .004$), whereas no amplitude difference between N2pc and N2pcb for the lower hemifield target (- 1.68 μV vs. -1.55 μV, $p = .413$, $BF_{01} = 5.71$). Figure 7 suggests a substantial overlap of the current density peak of N2pc and N2pcb over the posterior scalp elicited by targets displayed in the lower visual hemifield.

For trials repetition 5, the amplitude values recorded in the N2pc/N2pcb time-window were first separately submitted to *t*-test to determine whether they differed from 0 μV. For target displayed in the upper hemifield, minimal N2pc and N2pcb

activity was observed in heterogeneous (N2pc: -.25 μV, $t(29) = -3.05$, $p = .005$; N2pcb: -.33 μV, $t(29) = -.68$, $p = .502$), shape-matched (N2pc: .25 μV, $t(29) = 1.06$, $p = .298$; N2pcb: -.33 μV, $t(29) = -.98$, $p = .337$) and color-matched condition (N2pc: - .47 μV, $t(29) = -2.32$, $p = .028$; N2pcb: -.88μV, $t(29) = -2.68$ $p = .012$). Whereas for targets displayed in the lower visual hemifield, N2pc and N2pcb amplitude was clearly larger in heterogeneous (N2pc: - 1.56 μV, $t(29) = -6.50$, $p < .001$; N2pcb: -1.31 μV, $t(29) = -5.55$, $p < .001$), shape-matched (N2pc: -.65 μV, $t(29) = -3.34$, $p = .002$; N2pcb: -.66 μV, $t(29) = -2.43$, $p = .021$) and color-matched condition (N2pc: - .55 μV, $t(29) = -3.38$, $p = .002$; N2pcb: -.74 μV, $t(29) = -2.54$, $p = .017$).

These amplitude values of N2pc and N2pcb were then submitted to a 3 × 2 × 2 repeated measures ANOVA, considering distractors type (heterogeneous vs. shape-matched vs. color-matched), component (N2pc vs. N2pcb), and visual hemifield (upper vs. lower) as within-subject factors. Results revealed a significant main effect of distractors type (F (2, 58) = 3.22, $p = .047$, $\eta_p^2 = .100$, $BF_{10} = 1.74$), and visual hemifield (F (1, 29) = 11.71, $p = .002$, $\eta_p^2 = .288$, $BF_{10} = 231.56$). More importantly, the interaction between distractors type and visual hemifield (F (2, 58) = 4.99, $p = .010$, $\eta_p^2 = .147$). Pairwise comparison showed that for upper-hemifield targets, N2pc and N2pcb did not show any modulation of the distractors type, while for targets displayed in the lower hemifield, larger N2pc and N2pcb for the heterogeneous condition than for color-matched and shape-matched condition. Given that the null effects of component and interaction between component and other factors were critical to support to examine whether the results of Doro et al. (2020) regarding the amplitude equivalence of N2pc (lateral targets) and N2pcb (midline targets) could be replicated. The BF_{01} was 8.93 for the effect of component, 4.54 for the interaction of component and visual hemifield, and more than 1000 for the interaction of component and distractors type.

These results provide critical support for the statistical equivalence of N2pc and N2pcb amplitudes.

In the shape-matched condition, we again observed a contralateral positivity when targets were displayed in the lateral position, this is more evident when we separated the ERPs based on their vertical position. As shown in Figure 3-4, such polarity reversal follows the onset of N2pc/N2pcb that is produced from lower hemifield. *T*-test revealed the P_D was significant when target was displayed in the upper hemifield (.57 μV, $t(29) = 3.19$, $p = .003$, $BF_{10} = 3.74$). In contrast, P_D did not differ from 0 μV for lower hemifield targets (.09 μV, $t(29) = -.37$, $p = .714$ $BF_{01} = 4.54$).

On the hypothesis of the same underlying mechanisms for N2pc and N2pcb — a midline displayed target would be represented bilaterally in both posterior cerebral hemispheres (Doro et al., 2020; Monnier et al., 2020). One may expect a bilateral P_D (P_Db), as well as SPCN (SPCNb), recorded over the posterior scalp, follows the N2pcb in our shape-matched and color-matched condition respectively. To test whether these components do exist, the amplitude values recorded in the P_Db time window for midline upper versus lower target were separately submitted to *t*-test to inspect whether each of these values differed from 0 μV. Result revealed the P_Db did not reach statistical significant for a upper hemifield target (.24 μV, $t(29) = 0.74$, $p = .464$), but was clear present for a lower hemifield target (.78 μV, $t(29) = 2.20$, $p = .004$). The ERP results illustrated in Figure 3-4 also suggests that both lateral and midline targets elicited a sustained negativity. The SCD map in Figure 3-5 also reveals that the density peak of SPCN and SPCNb has similar distribution. The amplitude values recorded in the SPCN/SPCNb time-window were first separately submitted to *t*-test to inspect whether each of these values differed from 0 μV. Both SPCN and SPCNb amplitude was

significantly different from 0 µV in upper (SPCN: SPCN: -.49 µV; $t(29) = -2.23$, $p = .033$; SPCNb: -.90 µV; $t(29) = -2.65$, $p = .012$) and lower hemifield (SPCN: -.65 µV; $t(29) = -4.49$, $p < .001$; SPCNb: -.80 µV; $t(29) = -2.39$, $p = .002$). These amplitude values were then submitted to a 2 × 2 ANOVA with component (SPCN vs. SPCNb) and visual hemifield (upper vs. lower) as within-subject factors. The analysis yielded a neither significant main effect of factors nor their interaction (max $F = 1.61$, min $p = .512$), suggesting a statistical equivalence of SPCN and SPCNb amplitudes in the color-matched condition.

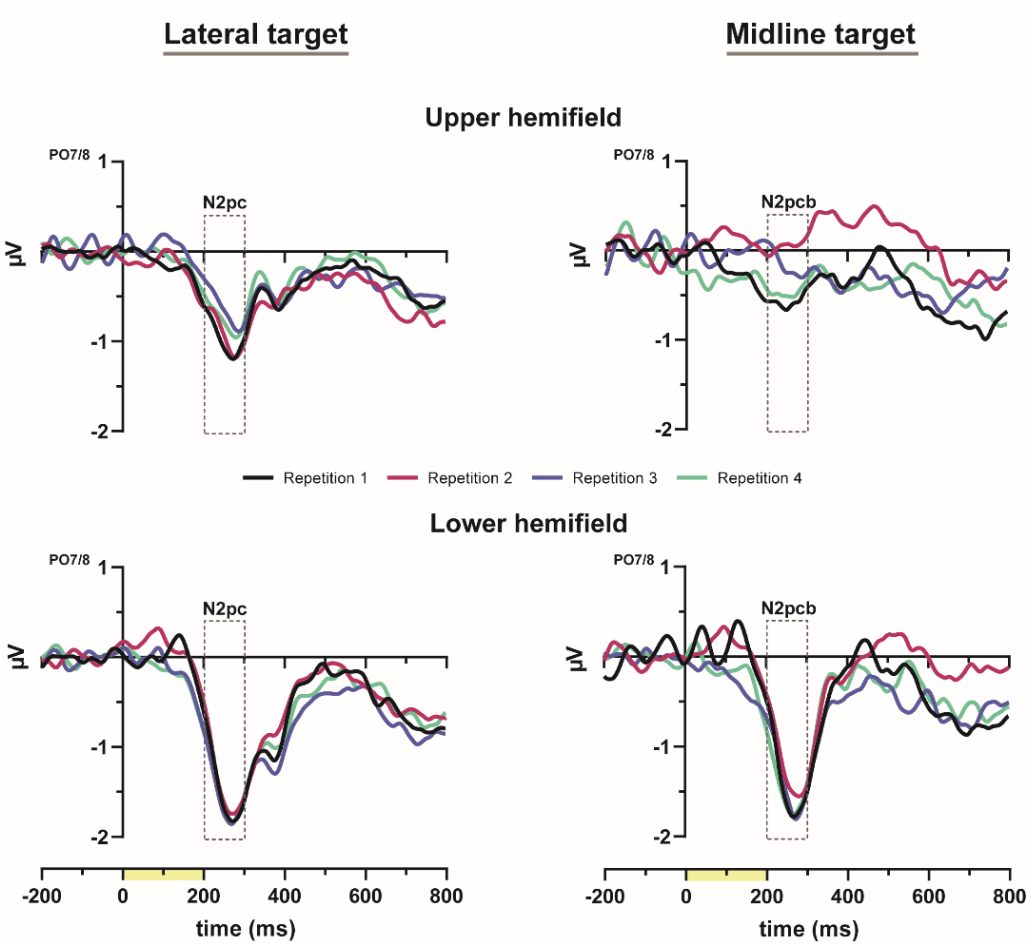

Figure 3-2 N2pc and N2pcb difference waveforms on the first four trial repetitions (heterogeneous condition), plotted as a function of target position (lateral vs. midline) and visual hemifield (upper vs. lower). Color bars on the timeline indicate the exposure duration of the search array (yellow). The area indicated by the dashed-line rectangles in the graph represents the time window considered for ERP amplitude analyses. ERP functions were low-pass filtered at 15 Hz for visualization purposes.

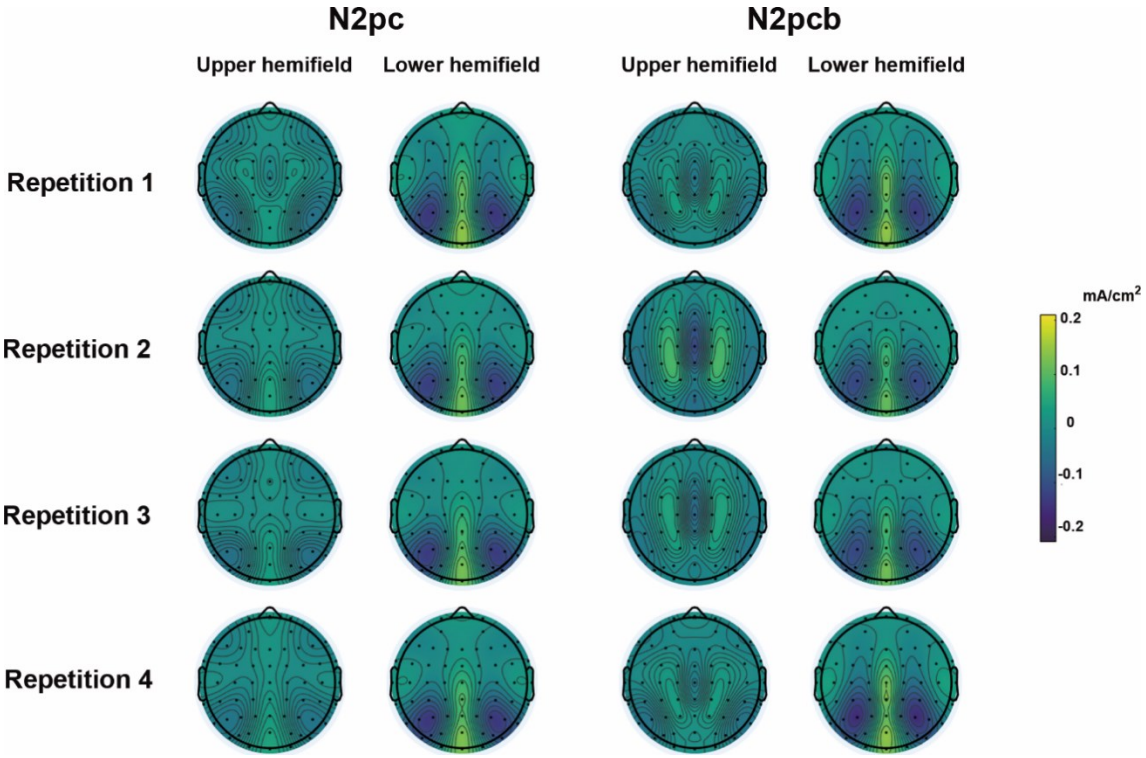

Figure 3-3 Scalp current density (SCD) maps of N2pc (left) and N2pcb (right) difference waveforms for lateral/midline targets presented in the upper and lower hemifields. The components are plotted mirrored in both the hemiscalps.

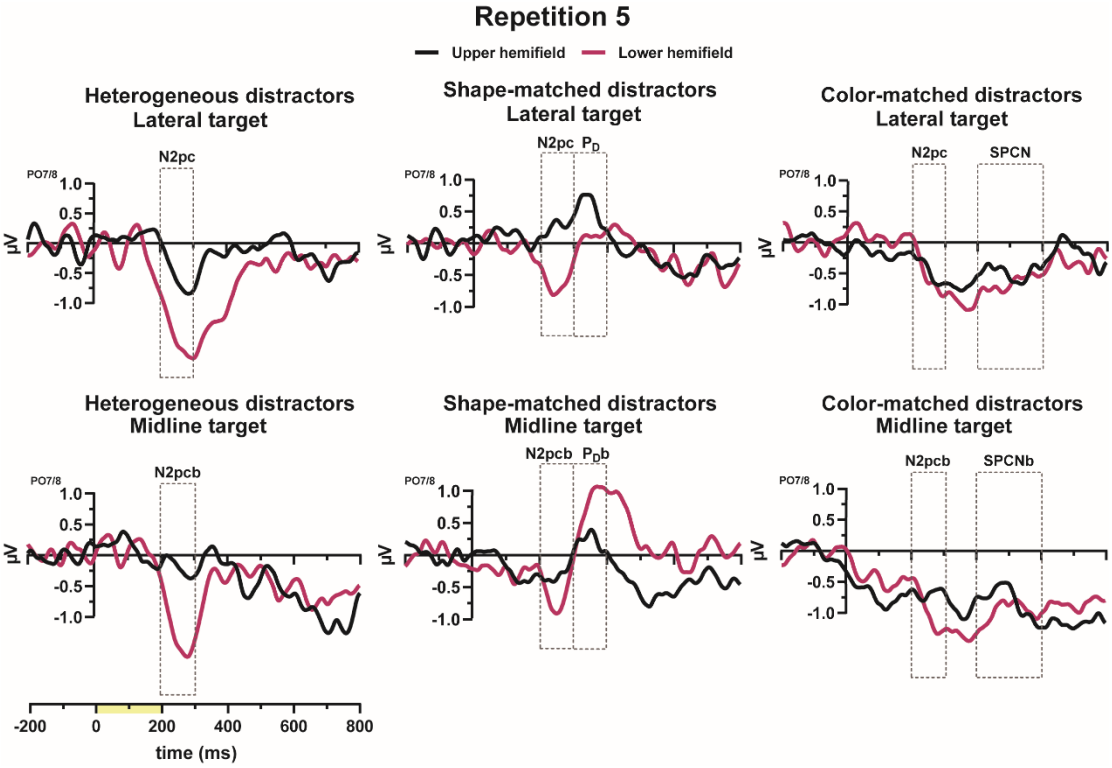

Figure 3-4 Grand-averaged ERPs elicited at electrodes PO7/8 time-locked to the presentation of the search array, separately displayed for the distractors type (heterogeneous, shape-matched vs. color-matched) and visual hemifield (upper vs. lower). The area indicated by the dashed-line rectangles in the graph represents the time window considered for ERP amplitude analyses. ERP functions were low-pass filtered at 15 Hz for visualization purposes.

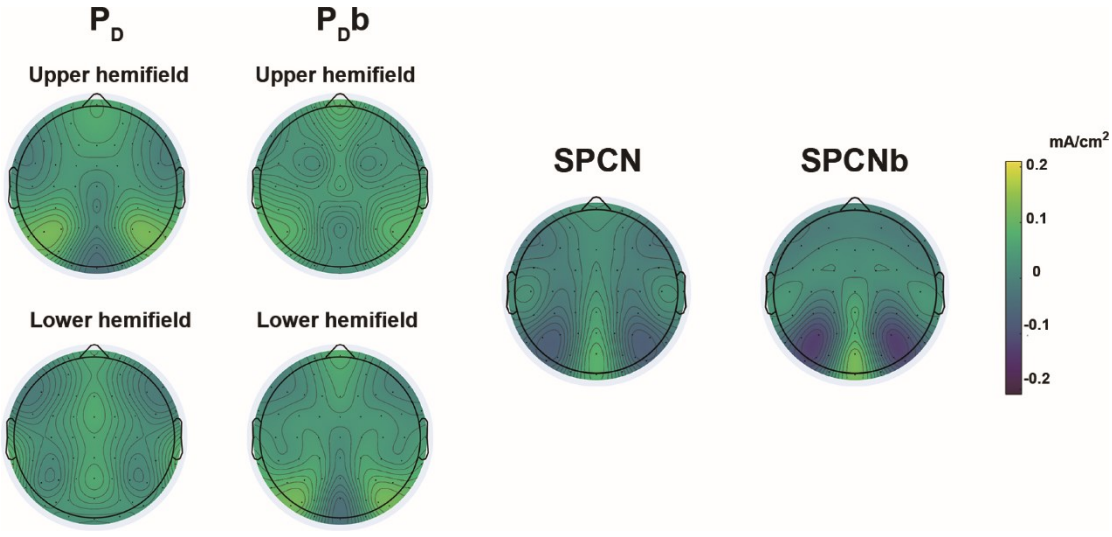

Figure 3-5 Scalp current density (SCD) maps of P_D and P_Db difference waveforms for lateral/midline targets presented in the upper and lower hemifields (left). SPCN and SPCNb difference waveforms for lateral/midline targets. The components are plotted mirrored in both the hemiscalps.

3.2.3 SPCN in the cue array

Visual inspection of Figure 3-6 makes apparent — the SPCN time-lock to the cue systematically decreased as the same-target runs. Figure 11 shows the corresponding scalp topographies. SPCN amplitude values in heterogeneous conditions were first submitted to *t*-test to determine whether they differed from 0 μV. SPCN amplitudes were significant for all trials (-.55 μV, -.31 μV, -.28 μV, -.33 μV, -.27 μV, -.21 μV, respectively, *ps* < .001). These amplitude values were then submitted to a one-way repeated measures ANOVA with repetition (trials 1, 2, 3, 4, 5 vs. 6) as within-subject factors. The main effect of repetition (F (5, 140) = 7.76, $p < .001$, $\eta_p^2 = .211$, $BF_{10} > 1000$) further confirmed the above visual inspection, as the amplitude of SPCN on trials repetition 6 was lower than that of SPCN on trial repetition 1 ($p < .001$).

Figure 3-7 shows SPCN in trials 6 when preceded by the heterogeneous vs. shape-matched vs. color-matched condition in trials 5. Figure 3-8 shows the corresponding scalp topographies. In line with Experiment 1, we then investigated whether the SPCN amplitude increased in trials repetition 6 after participants encountered different types of distractors. *T*-test first conformed that SPCN were clearly present in shape-matched (-.32 μV; $t(29) = -3.81$, $p < .001$), and color-matched condition (-.39 μV; $t(29) = -5.30$, $p < .001$). These amplitude values were then submitted to a one-way repeated measures ANOVA with distractors type (heterogeneous vs. shape-matched vs. color-matched) as within-subject factors. Results yielded a marginal significant of main effect (F (2, 58) = 2.62, $p = .081$, $\eta_p^2 = .083$, $BF_{10} = 1.67$), further planned comparison revealed that

the amplitude of SPCN in color-matched condition was larger than that of in heterogeneous ($t(29) = -2.63$, $p = .041$, $BF_{10} = 3.46$), whereas no amplitude difference between shape-matched and heterogeneous condition($t(29) = 1.40$, $p = .513$, $BF_{01} = 2.12$).

3.2.4 LPC in the cue array

Figure 3-6 also presents the ERPs elicited at Cz electrodes time-locked to the cue array for all trial repetitions and each search condition for trial repetition 6. Figure 3-8 shows the corresponding scalp topographies. The amplitude values recorded in the LPC time window were submitted to a one-way repeated measures ANOVA with repetition (trials 1, 2, 3, 4, 5 vs. 6) as within-subject factors. This analysis revealed a significant main effect of repetition for ($F(5, 145) = 15.83$, $p < .001$, $\eta_p^2 = .353$, $BF_{10} > 1000$). As can be seen in Figure 3-7 where scalp distributions were plotted (bottom panels), pairwise comparisons revealed that the LPC amplitude was significantly decreased in trials 6 as compared to trials 1 (.53 μV vs. 2.15 μV, $p < .001$, $BF_{10} > 1000$).

An analogous ANOVA as the SPCN with distractors type (heterogeneous vs. shape-matched vs. color-matched) as within-subject factors was considered to examine whether the LPC amplitude increased again in trial repetition 6 when a shape- or color-matched condition were preceded in trial repetition 5. As shown in Figure 3-6, this analysis revealed that LPC did not differ between distractors type ($F = .071$, $p = .494$).

3.2.5 FN400 in the cue array

Figure 3-7 also presents the ERPs elicited at Cz in trials 6 for each search condition. As the corresponding scalp topographies in Figure 3-8 suggest, a frontally distributed N400, sometimes called FN400 (300-500 ms) was larger after preceded a color-

matched condition. The amplitude values recorded in the FN400 time window were submitted to a one-way repeated measures ANOVA with distractors type (heterogeneous vs. shape-matched vs. color-matched) as within-subject factors. As suggested in Figure 3-7, where corresponding scalp topographies were plotted (middle panels). Results yielded the main effect of distractors type (F (2, 58) = 6.53, p = .003, η_p^2 = .184, BF_{10} > 1000), suggesting larger FN400 activity in trials 6 when preceded a color-matched condition (1.97 μV) than heterogeneous (1.27 μV, p = .016, BF_{10} = 43.53) and shape-matched condition (1.36 μV, p = .013, BF_{10} = 10.21).

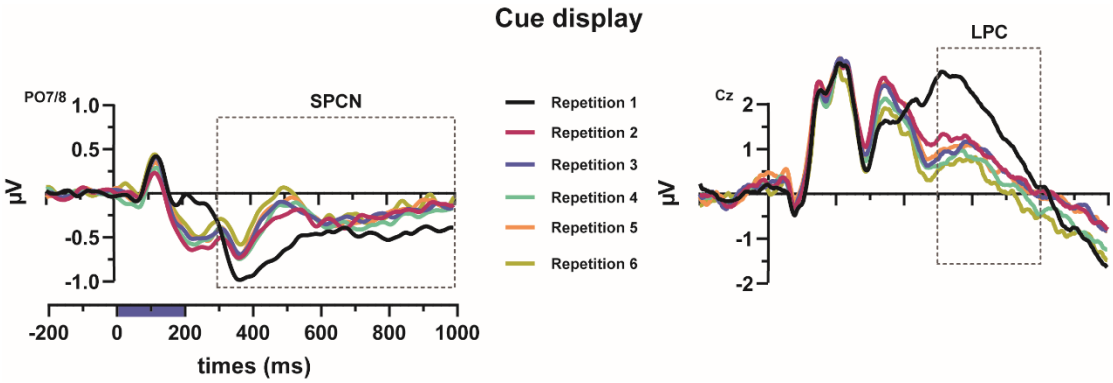

Figure 3-6 Grand-average ERP waveforms time-locked to the presentation of the cue. SPCN difference waveforms were computed from the contralateral minus ipsilateral waves elicited at electrodes PO7/8 (left panel), ERP functions were low-pass filtered at 15 Hz for visualization purposes. LPC amplitude was estimated at electrodes Cz (right panel). There ERPs functions were displayed for trial repetitions 1 to 6. Color bars on the timeline indicate the exposure duration of the cue display (blue).

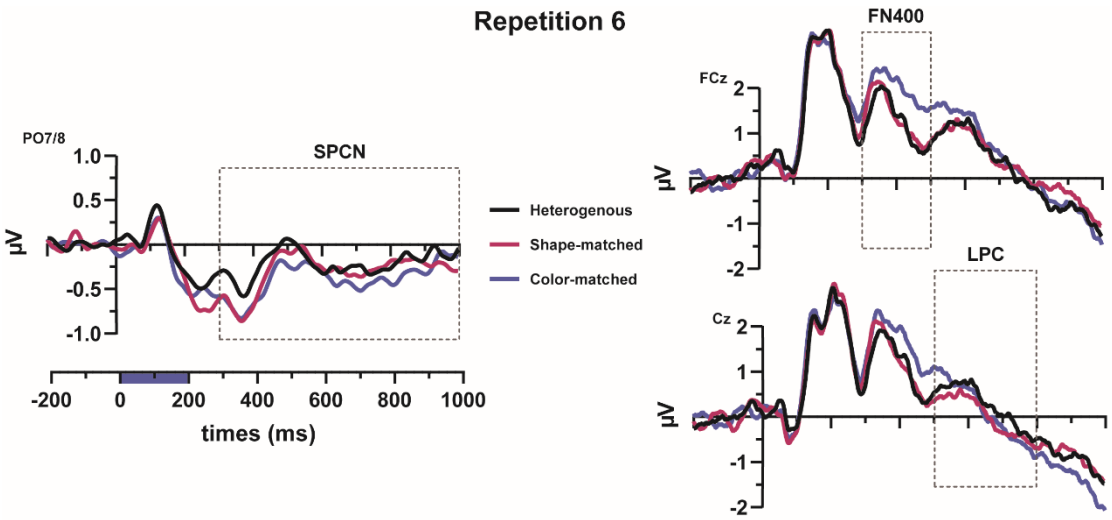

Figure 3-7 Grand-averaged ERPs at electrodes PO7/8, FCz, and Cz for trial repetitions 6, separately displayed for the distractors type (heterogeneous, shape-matched vs. color-matched). Color bars on the timeline indicate the exposure duration of the cue display (blue).

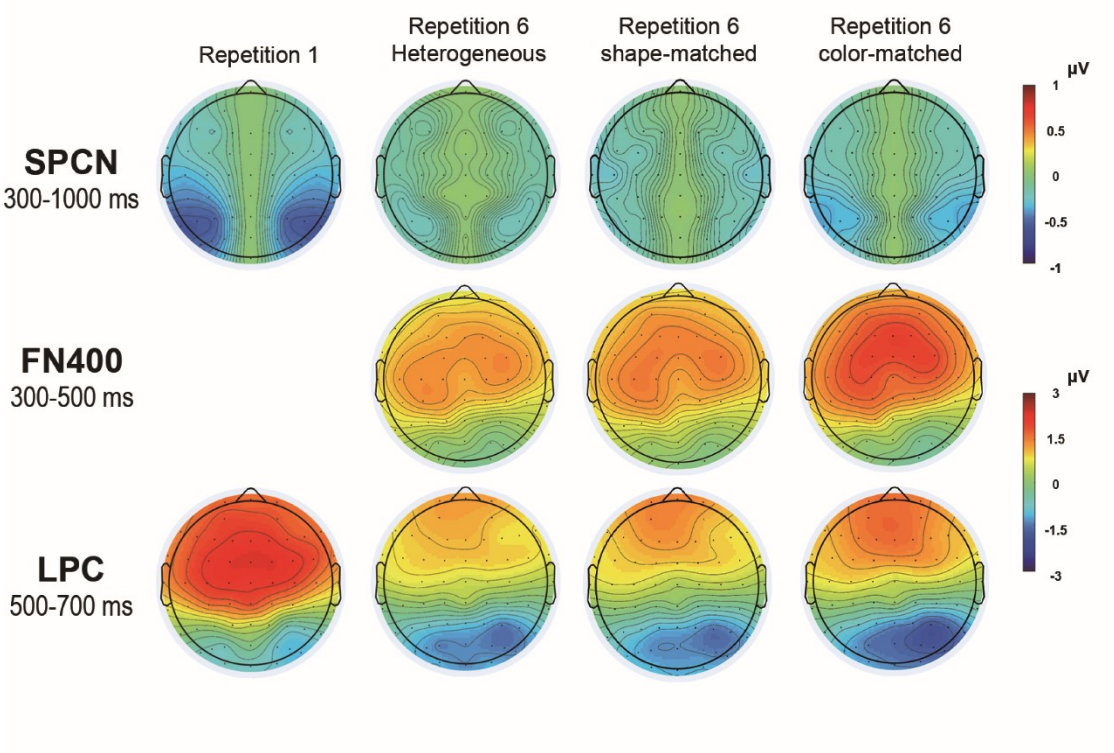

Figure 3-8 Scalp distributions of SPCN (top panels, 300-1000 ms), FN400 (middle panels, 300-500 ms) and LPC (bottom panels, 500-700 ms).

3.3 Discussion of Experiment 2

The result in Experiment 2 replicated those found in Experiment 1. We observed the SPCN and LPC time-loaded to the memory cue dropped down as a function of target repetition, suggesting the demands on vWM to maintain the attentional template were lessened. We again observed no behavioral differences when targets were surrounded either by heterogeneous or shape-matched distractors. As we proposed in the discussion of Experiment 1, a color-detection mode may involve in the visual search when targets were unique by their color. While increased RT and error when the target is accompanied by color-matched distractors, suggests additional processing may involve.

We first provided a comprehensive overview of studies supporting the assumption in Doro et al. (2020), that is, the N2pcb and the N2pc for lower hemifield stimuli are functionally equivalent ERP markers for the attentional selection of midline targets and lateral targets in the heterogeneous condition. This is important for what we further explore the challenging finding in shape-matched condition — a minimal N2pc followed by a contralateral positivity. This minimal N2pc was greater when we divided the data based on the vertical elevation, a dominant lower hemifield N2pc, and a dominant upper hemifield P_D. We then evaluated an alternative explanation, in which participants first examine the symmetric shape-matched distractors that presented in both left and right hemifield (Kerzel & Burra, 2020; Woodman & Luck, 2003). As we produced a midline target trial in Experiment 2, no selection bias between midline target and lateral target in the shape-matched conditions (308 ms vs. 316 ms). This is also important, in particular with what we accounted for this contralateral positivity as the P_D component. It appeared that in the present study, target selection and distractor suppression reacted in order of arrival — as the contralateral negativity peaked at 236 ms for the lower hemifield, approximately 100 ms after a contralateral positivity peaked for the upper hemifield. However, we felt less confident in treating the distractor suppression and target selection as serial processing. Work by Luck & Hillyard (1994) provided several crucial aspects of understanding the mechanism of N2pc. One of their findings was N2pc for target was eliminated when distractors present in the same field shared task-relevant features with the target. As they collectively took with other findings, their conclusions suggested in the discussion was "*N2pc component reflects a process whereby competing information from distractor items is suppressed*." This assumption was further discussed in the paper of Hickey et al. (2008), who decomposed the N2pc into two subcomponents, namely, the target negativity (N_T) and the distractor

positivity (P_D). As they fixed the target on the vertical midline, the amplitude of contralateral positivity was larger when the distractor presented in the upper hemifield than in the lower hemifield. They propose this contralateral positivity reflects the processing of the distractor rather than the processing of the target because the lateralized ERP can not be attributed to the central target. We also note that sometimes this contralateral positivity was observed following the typical N2pc. For example, Hilimire et al. (2011) measured a positive component they called Ptc (because more temporal), they found lateralized distractors first elicited the N2pc then followed by the Ptc, suggesting an attentional capture appear before a subsequent suppression to task-irrelevant information. Considering our results, search performance was barely different between the heterogeneous and shape-matched conditions, while attenuated N2pc was recorded when the target was surrounded by shape-matched distractors compared to when target was accompanied by heterogeneous distractors. It is unlikely due to the competition between all shape-matched items weaken the selection of target, because in this case the search slope should became larger in the shape-matched condition. The possible explanation would be the spatial filter of target and target-like distractors are working in parallel. As the attentional response to target-like distractors (P_D) overlapped with the attentional response to target (N2pc), thereby attenuating the N2pc. These processing was covered when we collapsed the data over upper versus lower hemifields, resulting in the elimination of N2pc (Experiment 1).

In the shape-matched condition where the target was displayed along the vertical midline, the target was accompanied by shape-matched distractors in the left and right visual field, premised on the assumption of Doro et al. (2020), we expected a bilateral inhibition may overlap with the N2pcb. On the observation of P_D was more pronounced for upper hemifield while a fully-fledged N2pc was found for lower hemifield, we

expected the P_Db to share with P_D the same pattern as a function of vertical elevation. Surprisingly, P_Db was significant when the midline target was displayed in the lower hemifield, but nearly absent in the upper hemifield. A possible interpretation could be the bilateral inhibition overlapped with the N2pcb — the attenuated N2pcb and the P_Db for upper hemifield — two polarities reversed components thereby neutralizing each other. However, as proposed by Monnier et al. (2020), the standard contra-minus-ipsi approach creates an inherent ambiguity when estimating lateralized readiness potentials, the change in those components, could be accounted for an attentional response in either contralateral or ipsilateral portion, or even both. As they subtracted both contralateral and ipsilateral activity from a control condition (contained only distractors), two phase lag positive components were observed in the contralateral and the ipsilateral activity respectively (ipsi following contra by about 55 ms). The standard approach to subtract the ipsilateral activity from the contralateral activity may wane the attentional response in the contralateral portion when processing stimuli are displayed in the upper hemifield. This could be the case when we subtracted the ipsilateral activity to upper lateral targets from bilaterally averaged activity to upper midline targets. Considering the present approach may provide an incomprehensive conclusion in understanding the bilateral inhibition (P_Db), given it was outside the scope of the present study, a better proposition for future study would be to use a control condition (a frame that contains only contrast items) like those of Monnier et al. (2020) to isolate the specific activity in the bilateral portion. As already argued in the discussion of Monnier et al. (2020), Experiment 2 provides further support for the necessity of separate stimuli presented for processing in the upper versus lower hemifield when monitoring these positive components, namely that as averaged upper and lower hemifield contra-minus-ipsi waves — as averaged the N2pc with a temporal delay P_D, thereby creates an inherent ambiguity

when estimating the time course of attentional response.

Compared to the result of shape-matched and color-matched conditions, their search pattern suggests manipulating the relationship between target and distractors did affect the identification of the target. Specifically, when the target was surrounded by color-matched distractors and thereby unique by its shape, both lateral and midline targets elicited sustained negativity instead of positivity in the visual search. The SPCN is commonly thought to reflect the sustained activation of vWM representations, especially in tasks where a further process of target features is required (Mazza et al., 2007). We interpret the absence of P_D in the color-matched condition as the target's color was off-loaded to the activated part of LTM, color information is now not part of the selected candidates. A gating mechanism between the focus and LTM was assumed to block any interference (Oberauer et al., 2016). As anticipated, only shape information can isolate the target in the color-matched condition. Certainly, the SPCN/SPCNb suggested after the initial selection in trials 5, the target was registered and encoded into vWM for further identification processes. When the shape information matched distractors in the shape-matched condition, the P_D/P_Db acted like a "stop signal" to quite the searching, whereas the SPCN/SPCNb in the color-matched condition indexed the processing of attended target to be continue. As we proposed in the discussion of Experiment 1, shape information related to target is more likely to be held in the region of direct access in this case.

In addition to what we have found in the visual search, we observed an increasing FN400 activity time-locked to the memory cue onset in trials 6, this frontal enhancement was present only after participants encountered color-matched distractors but not shape-matched distractors in trials 5. Previous research found a memory retrieval effect by using a recognition task when the probe object matched a previously

memory object. The familiarity signal educed by the probe object leads to a more positive FN400. Besides, larger SPCN during the memory cue display suggests attentional deployments were re-allocated to the cue during the memory retention in trials 6. As expected, only encountered the color-matched distractors triggered the return of SPCN. In line with our interpretation in visual search, the shape information is needed to isolate the target in color-matched conditions, so that participants re-loaded the shape attribute to create a shape template. As for no additional re-loading processed in the shape-matched condition, perhaps this was due to the color feature acquired better learning during each repetition, so that less attentional recourse was needed to re-load the color feature. These findings hint at a possible cause of the different memory status of the color and shape attributes. In Experiment 3, we would further examine this interpretation.

To sum up, in two Experiments, we asked whether conjunctive features are maintained independently or are bound within a single unit in vWM. To this end, we examined whether the guidance of attention is operated in a feature-based or object-based manner. Premised on the previous research that repeated the same target leading to the attentional template being off-loaded from vWM to an alternative mechanism. If the template is established based on the entire object, all features should be off-loaded together from vWM. Alternatively, if a single feature is achieved as a template based on the salient attribute, conjunctive features associated with the same remembered object should have different memory statuses during the target repetition. To further explore the memory status of these conjunctive features, in the fifth trial when participants were searching for the same target, all search distractors could occasionally share the target's shape, color attributes, or remain heterogeneous serving as a "baseline" condition. The results are in consist with previous studies, indicating that the guidance

of attention from VWM is largely feature-based. We proposed the concentric model of WM from Oberauer (2002) to interpret our results. That is, the target's color attribute was maintained in the focus of attention as the attentional template, guiding attention in the initial visual search. After a set of the same target trials, the color template was off-loaded to the activated part of LTM. As for the target's shape information, it is likely to be stored in the region of direct access as a selection candidate, prepared to be re-loaded back to the focus. We, therefore, interpret these findings as the maintenance of conjunctive features are separately rather than an integrated unit. If, however, color and shape features are bound within an integer representation, those feature values should be presumably off-loaded together, either in the activated part of LTM or the region of direct access. In this case, we would expect only the presence of either SPCN or P_D when encountering the color- or shape-matched conditions respectively, different merely in their magnitudes.

Chapter 4 – Experiment 3

Note however that the assumption of independent feature maintenance is not necessarily in opposition to the hypothesis that object encoding follows an object-based manner. As we mentioned in the Introduction, it is counterintuitive that one can restrict his/her selection only for one feature dimension to enter the vWM, it is also illogical that one would decompose the perceptual object into its features when encoding a specific object. Albeit our findings support a separate-feature storage model, mechanisms for retaining perceptual feature values over time and mechanisms for encoding objects deserve to be treated as fundamental distinctions. Experiment 3 was designed to further examine the assumption that whether all features from the same encoded object come together into vWM.

We assumed better learning for color attributes than shape attributes so that the memory retrieval effect was absent for the color feature. In the same design as we apply in previous experiments, imagine a situation when the to-be-remember object always points to targets that match only one of its feature dimensions in the six consecutive trials (e.g., shape), it is safe to say participants initiatively configure one feature as task-relevant templates. But this raises the issue of whether the task-irrelevant feature (e.g., color) is discarded or is blocked from further learning during the same target repetitions. If all features from this encoded object are bound within the same representation initially in vWM, features that do not provide target information should accordingly still in vWM, and then implicitly off-loaded from vWM during the trial-by-trial repetition. As such, when we strategically produce a condition to recall the use of this task-irrelevant feature in trials 5, the subsequence trials 6 should show a large familiarity effect when we monitor the ERP time-locked to the cue display. To test

whether such object-based encoding exists, Experiment 3 again used conjunctive stimuli defined by color and shape. Participants were asked to remember and to search for the same target across six consecutive trials. The memory cue would predict only the color or shape feature of the search target, thus marking one feature of the memory cue as the search template while the other as task-irrelevant information. Crucially, we then again manipulate the search array in trials 5, in which they have to identify a full memory matched target while ignoring the other partial memory matched distractors. By comparing the search performance and ERP patterns in trials 5 when searching for partial memory matched targets (single feature) and fully memory matched targets (conjunction). We would be able to test whether task-irrelevant features associated with memory cues are discarded or off-loaded.

Method

4.1 Method

4.1.1 Participants

Twenty-five students at the Guangzhou University (8 males; mean age = 21 years, SD = 2.2) took part in the present experiment after providing written informed consent. All participants had normal or corrected-to-normal visual acuity, and all reported normal color vision and no history of neurological disorders. The experiment was vetted by the local ethics committee.

4.1.2 Stimuli, apparatus, and procedure

A schematic illustration is illustrated in Figure 4-1. Both cue and search arrays were composed of line-drawings shapes, each subtending a visual angle of 3.5° × 3.5°, randomly selected from a set of 10 shapes (see Figure 2-1). The cue array was composed

of two stimuli, symmetrically located at 4.2° of visual angle on the left and right of fixation. One stimulus represented the target, whereas the other one was a task-irrelevant white shape (either a white circle or a white triangle, which would never appear in the search array). The search arrays were composed of 6 search items, presented at equidistant (6° of visual angle) locations from fixation (at 2, 4, 6, 8, 10, 12 o'clock of an imaginary circle) displayed against a black background (CIE: 0.312/0.329, 1.0 cd/m2). Each search items contain either a plus sign or a multiplication sign. Participants were instructed to identify the sign within targets by pressing one of the two response keys (i.e., "F" or "J", counterbalanced across participants). The memory cue could indicate either the shape or color of targets. Specifically, in the color-target series, search targets always share the same mnemonic color but differ in shapes across six consecutive trials, or vice versa in the shape-target series. Critically, participants were always exposed either to color- or shape-target conditions in the first four trials, whereas in the fifth and sixth trials, 33% of all trials were arranged equally to color-target conditions and shape-target conditions, respectively. For the rest 34% of trials, the search array would occasionally contain a fully memory-matched target (conjunction target), accompanied by a color-matched distractor and a shape-matched distractor. The experiment consisted of 1728 trials (288 blocks), divided into two sessions, performed within a week.

4.1.3 Electrophysiological recording and data processing

All recording and analysis procedures were the same as in Experiment 2. The artifact rejection procedure led to four subjects being excluded due to more than 30% of trials being rejected.

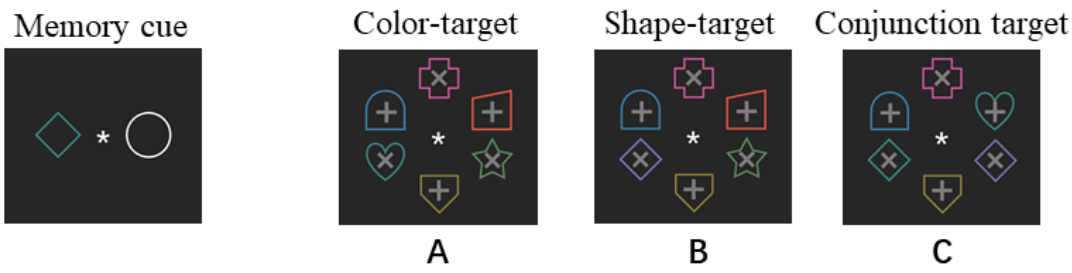

Figure 4-1 Schematic of the experimental paradigm. The experiment was divided into small blocks of 6 trials each. Following the presentation of the color-shape cue in the memory task, participants were randomly assigned to one of two search conditions. (A) Participants were encouraged to search for a color-matched target in 6 consecutive trials and to identify the symbol inside the target (i.e., "×" or "+"). Whereas in the (B) shape-target condition, search targets were always indicated by the memory shape. (C)The search task would occasionally contain a fully memory-matched target (conjunction target), accompanied by a color-matched distractor and a shape-matched distractor in trials repetition 5 and 6 of both search conditions. In this condition, participants were instructed to identify the symbol inside the conjunction target.

4.2 Results

4.2.1 Behavioral data

Figure 4-2 depicts the mean accuracy and reaction times (RTs), separately for color-targets, shape-targets trials, and conjunction targets in each trial repetition. Only correct response trials were considered in the computation of the RTs. RTs exceeding three standard deviations above/below the mean for each participant and condition were considered outliers and excluded (.85 %).

Mean accuracy was first submitted to a 4 × 2 repeated measures ANOVA with repetition (trials 1, 2, 3 vs. 4), target type (color- vs. shape-target) as within-subject factors. Results revealed that participants were generally more accurate in detecting color-targets than shape-targets (92.99% vs. 89.74%; $F(1, 20) = 65.69$, $p < .001$, $\eta_p^2 = .767$) and a main effect of repetition ($F(3, 60) = 44.84$, $p < .001$, $\eta_p^2 = .692$, $BF_{10} > 1000$). These two effects combined non-linearly ($F(3, 60) = 3.22$, $p = .045$, $\eta_p^2 = 0.139$,

BF_{10} = 1.20), further pairwise comparison reflected that search accuracy has no differences between color-target and shape-target in the first trials (87.03% vs. 85.65%, p = .126, BF_{01} = 2.73, respectively). After 4 trials repetition, accuracy was found significantly increase in the color-target (87.03% vs. 96.19%, p < .001, BF_{10} > 1000) and shape-target trials (85.65% vs. 91.98%, p < .001, BF_{10} > 1000). Nevertheless, the improvement of accuracy was higher when targets were defined by color rather than shape (96.19 % vs. 91.83, p < .001, BF_{10} = 453.77).

The analogous 4 × 2 ANOVA was carried out for mean RTs, this analysis yielded both main effects of repetition (F (3, 60) = 124.43, p < .001 η_p^2 = 0.862, BF_{10} > 1000) and target type (F (1, 20) =305.80, p < .001, η_p^2 = 0.939, BF_{10} > 1000) and, more importantly, a significant interaction between repetition and the target type (F (3, 60) = 30.73, p < .001, η_p^2 = .606, BF_{10} > 1000). Further pairwise comparison showed that participants were faster in detecting the target after 4 trials repetition (trials 4 vs. trials 1: 955 ms vs. 1095 ms, p < .001). While participants were slower in detecting shape-targets (trials 1: 1173 ms; trials 2: 1077 ms; trials 3: 1089 ms; trials 4: 1082 ms) than color-targets (trials 1: 1017ms; trials 2: 839 ms; trials 3: 840 ms; trials 4: 829 ms) across the repetition (ps < 0.001).

Notice that two types of conjunction targets should be evaluated separately; one appeared after the color-target and one after the shape-target. To investigate the impact of encountering the conjunction target in trials 5 and 6, a 2 × 2 × 2 repeated-measures ANOVA was performed sparely for mean accuracy and RTs, considering repetition (trials 5 vs. 6), memory type (remember color vs. remember shape) and target type (single-feature vs. conjunction) as within-subject factors. There analyses detected significant three-way interaction (accuracy: F(1, 20) = 8.69, p = .008, η_p^2 = .303 , BF_{10} >

1000; RTs: $F(1, 20) = 11.17$, $p = .003$, $\eta_p^2 = .358$, $BF_{10} > 1000$). For analysis of accuracy, result revealed that when first encounter the conjunction target, participants made more error relative to color targets (conjunction vs. color: 87.30% vs. 95.55%, $p < .001$, $BF_{10} > 1000$), but this pattern fell short of significant when compared to shape targets (conjunction vs. shape: 89.95% vs. 92.10%, $p = .061$, $BF_{10} = 1.17$). However, no significant different was found when they again encountered the conjunction target in trial 6 (conjunction vs. color: 95.50% vs. 95.63%, $p = .919$, $BF_{01} = 4.96$; conjunction vs. shape: 93.03% vs. 92.57%, $p = .757$, $BF_{01} = 3.84$, respectively). For analysis of RTs, the pairwise comparison revealed that participants were slower in detecting conjunction targets in trials 5 relative to color targets (conjunction vs. color: 1064 ms vs. 827 ms, $p < .001$, $BF_{10} > 1000$); but were faster when the conjunction target appeared in the remember shape series (conjunction vs. shape: 980 ms vs. 1081 ms, $p < .001$, $BF_{10} > 1000$). This pattern was sustained to trial 6, in which they would expect to encounter the conjunction target secondly (conjunction vs. color: 952 ms vs. 831 ms, $p < .001$, $BF_{10} > 1000$; conjunction vs. shape: 926 ms vs. 1090 ms, $p < .001$, $BF_{10} > 1000$ respectively).

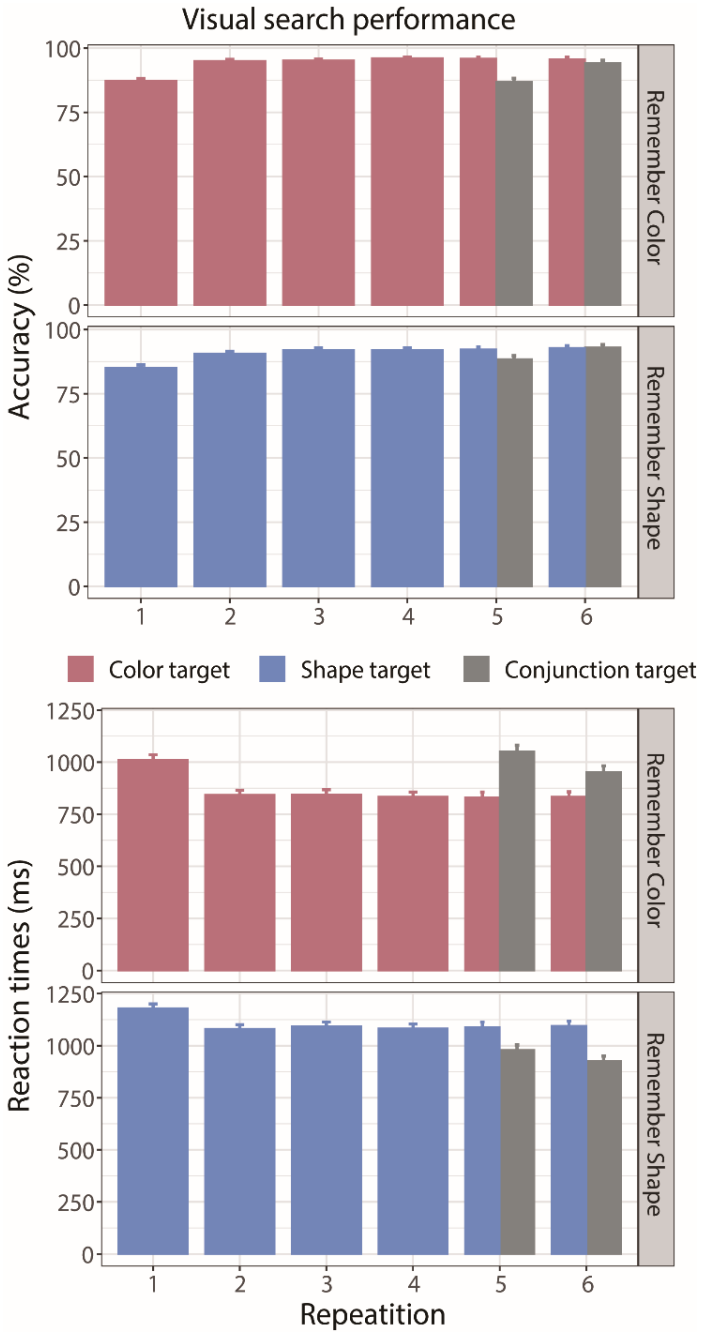

Figure 4-2 Mean accuracy (top) and RTs (down) of the visual search task for each search condition as a function of trial repetition. The error bars represent the standard errors.

4.2.2 N2pc in the visual search task

Figure 4-3 shows difference ERPs at PO7/8 electrode sites in response to visual search arrays (difference waves were calculated by subtracting ipsilateral from contralateral ERP activity elicited by lateral target). ERPs are presented separately for

repetition 1 to 4, further divided according to the target type.

To determine the effect of repetition on N2pc in the color- and shape-target trials, the amplitude values recorded in the N2pc time-window were first submitted to *t*-test to determine whether they differed from 0 μV. N2pc was significant for both color-target trials and shape-target trials in trial 1 (color: -1.28 μV, $t(20) = -6.25$, $p < .001$; shape: -.40 μV, $t(20) = -2.98$, $p = .007$), 2 (color: -1.53 μV, $t(20) = -6.09$, $p < .001$; shape: -.66 μV, $t(20) = -6.34$, $p < .001$), 3 (color: -1.68 μV, $t(20) = -8.81$, $p < .001$; shape: -.51 μV, $t(20) = -4.89$, $p < .001$), and 4 (color: -1.50 μV, $t(20) = -5.22$, $p < .001$; shape: -.42 μV, $t(20) = -4.61$, $p < .001$). These amplitude values were then submitted to a 4 × 2 repeated measures ANOVA, considering repetition (trials 1, 2, 3 vs. 4) and target type (color- vs. shape-target) as within-subject factors. Results revealed main effect of target type ($F(1, 20) = 32.10$, $p < .001$, $\eta_p^2 = .616$, $BF_{10} > 1000$). Further planned comparisons showed that the amplitude of N2pc was greater on color-target trials than on shape-target trials (-1.50 μV vs. -.52 μV). However, N2pc did not show any modulation of the repetition ($BF_{01} = 5.89$), no interaction was statistically significant ($BF_{01} = 12.26$).

An analogous 4 × 2 ANOVA was carried out for the onset latencies of N2pc, as determined by jackknife-based procedures (see Methods for details). There was a significant main effect of target type ($F_c(1, 20) = 3.43$, $p_c = .040$, $\eta_p^2 = .055$), reflecting the fact that N2pc was triggered earlier in color-target trials compared to shape-target trials (211 ms vs. 259 ms). Besides, no other factor effects (max $F_c = .10$; min $p_c = .957$), suggesting the N2pc onset difference between color- and shape-target was equally present from trial repetition 1 to 4.

As it can be appreciated in Figure 4-3, both color-targets and shape-targets elicited an N2pc as well as an SPCN. To determine the effect of repetition and target type on

SPCN, the amplitude values recorded in the SPCN time window were submitted to an analogous 4 × 2 ANOVA. This analysis detected only a main effect of target type ($F(1, 20) = 5.52$, $p = .029$, $\eta_p^2 = .216$, $BF_{10} = 3.51$). Further planned comparisons showed that color-targets elicited larger SPCN than shape-targets (-.97 µV vs. -.76 µV).

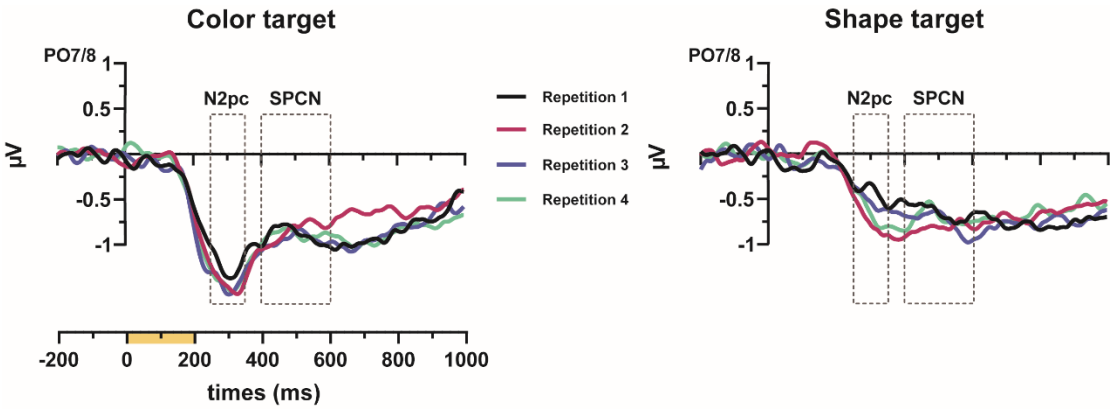

Figure 4-3 N2pc difference waveforms on the first four trial repetitions, plotted as a function of target type (color target vs. shape target). Color bars on the timeline indicate the exposure duration of the search array (yellow). The areas delimited by the dashed-line rectangles in the graph indicate the time windows considered for ERP amplitudes estimation. ERP functions were low-pass filtered at 15 Hz for visualization purposes.

In line with the RTs, the ERP results illustrated in Figure 4-4 suggest that N2pc for the conjunction target was strongly modulated in trial 5 and 6 depending on search series. The amplitude values of N2pc were first separately submitted to *t*-test to inspect whether each of these values differed from 0 µV. N2pc was clearly present in both trial 5 and 6 for color-target (trial 5: -1.46 µV, $t(20) = -7.71$, $p < .001$; trial 6: -1.39 µV, $t(20) = -5.02$, $p < .001$) , shape-target (trial 5: -.69 µV, $t(20) = -5.19$, $p < .001$; trial 6: -.50 µV, $t(20) = -3.04$, $p = .006$), conjunction target in remember color series (trial 5: -.95 µV, $t(20) = -3.78$, $p = .001$; trial 6: -1.32 µV, $t(20) = -3.95$, $p < .001$), and conjunction target in remember shape series (trial 5: -1.18 µV, $t(20) = -5.46$, $p < .001$; trial 6: -1.02 µV, $t(20) = -5.60$, $p < .001$).

To determine the impact of encountering the conjunction target in search color series,

N2pc and SPCN amplitudes were then separately submitted to a 2 × 2 repeated measures ANOVA, considering repetition (trials 5 vs. 6), target type (color target vs. conjunction target) as within-subject factors. For N2pc estimation, the interaction between repetition and target type fell just short of significance (F (1, 20) = 2.90, p = .083, η_p^2 = .142, BF_{01} = 2.03). Further planned comparison showed that when first encountered the conjunction target in the search color series, the amplitude of N2pc attenuated as compared to a color-target (-.91 μV vs. -1.42 μV; p = .010), whereas no amplitude difference was found in trial 6 (-1.32 μV vs. -1.37 μV; p = .813). Whereas for SPCN in the search color series, neither the main effect nor their interaction was significant (max F = 1.03, min p = .323), suggesting the statistical equivalence of SPCN for color-targets and conjunction targets.

For the impact of conjunction targets in search shape series, N2pc and SPCN amplitudes were then separately submitted to a 2 × 2 repeated measures ANOVA, considering repetition (trials 5 vs. 6), target type (shape vs. conjunction target) as within-subject factors. In the N2pc time window, the analysis detected only a main effect of target type (F (1, 20) = 16.71, p < .001, η_p^2 = .455, BF_{10} > 1000), which was most likely driven by the smaller N2pc in shape-target trials. Further planned comparisons confirmed that the amplitude of N2pc was greater on conjunction target trials than on shape-target trials (-1.22 μV vs. -.64 μV; p < .001). As for the SPCN, neither main effect nor their interaction was significant (max F = 2.79, min p = .110).

To estimate the N2pc onset latency in trials 5 and 6, a 2 × 2 × 2 repeated measures ANOVA, considering repetition (trials 5 vs. 6), memory type (remember color vs. remember shape), and target type (single-feature vs. conjunction) as within-subject factors was conducted, this analysis revealed no main effect nor interaction was

significant (max F_c = 1.07; min p_c = .311).

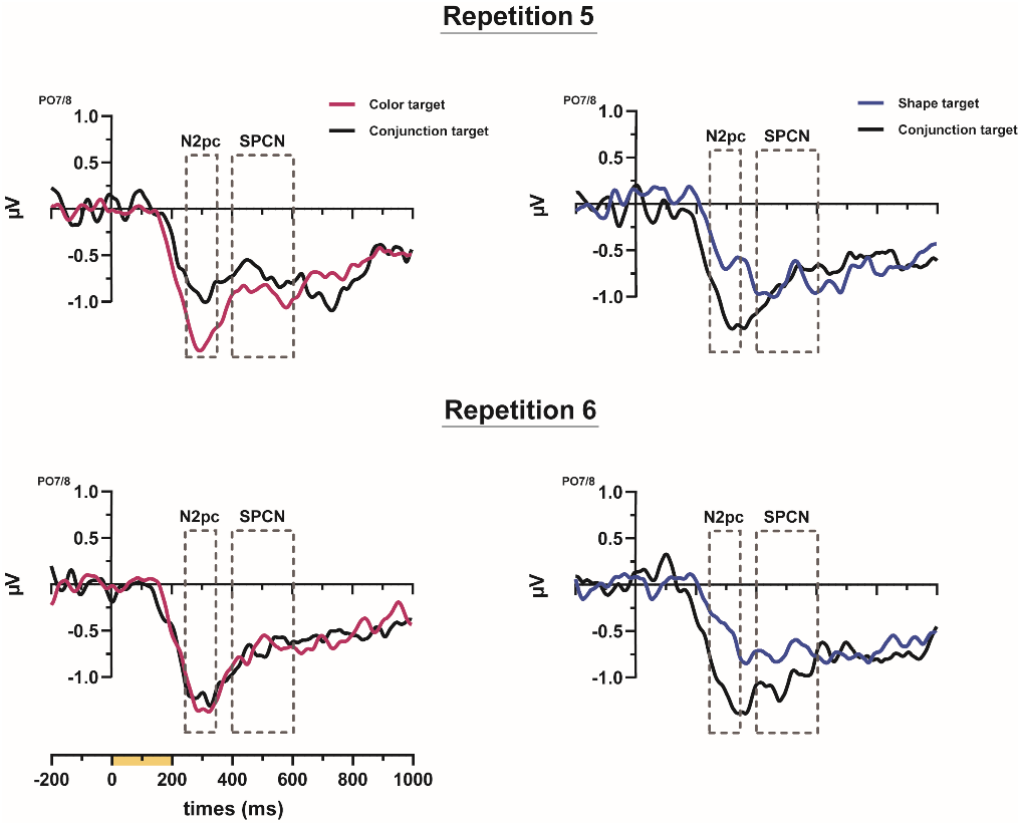

Figure 4-4 Grand-averaged ERPs elicited at electrodes PO7/8 time-locked to the presentation of the search array, separately displayed for repetition (trials 5 vs. 6), memory type (remember color vs. remember shape), and target type (single-feature vs. conjunction). The area indicated by the dashed-line rectangles in the graph represents the time window considered for ERP amplitude analyses. ERP functions were low-pass filtered at 15 Hz for visualization purposes.

4.2.3 SPCN in the cue array

Grand-average ERP waveforms time-locked to the presentation of the cue array, elicited at posterior electrodes PO7/8 and separately displayed for repetition 1 to 2 (Figure 4-5 A) and 3 to5, further divided to color-target (Figure 4-5 B) and shape-target (Figure 4-5 C). SPCN amplitude values in each memory type were first submitted to *t*-test to determine whether they differed from 0 μV. SPCN amplitudes were significant in trials 1 (-.75 μV, $t(20) = 6.91$, $p < .001$), and trials 2 to 6 in remember color series

(-.60 μV, -.43 μV, -.43 μV, -.35 μV, -.48 μV, respectively, *ps* < .001) and remember shape series (-.38 μV, -.55 μV, -.51 μV, -.39 μV, -.42 μV, respectively, *ps* < .001).

To determine the effect of repetition, these amplitude values recorded in the SPCN time-window were then submitted to a 6 × 2 repeated measures ANOVA, considering repetition (trials 1, 2, 3, 4, 5 vs. 6) and memory type (remember color vs. remember shape) as within-subject factors. Results revealed the SPCN amplitude elicited by the memory cue systematically decreased ($F(5, 100) = 3.04$, $p < .013$, $\eta_p^2 = .132$, $BF_{10} = 40.23$). Further planned comparisons showed that SPCN amplitude was lower in trials 6 than in trails 1 (-.75 μV vs. -.45 μV, $p = .032$). The analysis detected no other factor effects (max $F = 1.52$; min $p = 0.189$). The null effects of memory type and their interaction further emphasized the statistical equivalence of SPCN in remembering color and shape.

To estimate whether the modulation in trial repetition 5 when preceded by a conjunction target in visual search, we then examine whether SPCN increased in trials 6. The amplitude values recorded in the SPCN time window for trials 6 were submitted to a 2 × 2 repeated measures ANOVA, considering memory type (remember color vs. remember shape) and target type (single-feature vs. conjunction) as within-subject factors. Neither main effect nor their interaction was significant (max $F = .16$, min $p = .690$), suggesting that the SPCN amplitude did not increase in trials 6 when preceded by a conjunction target in trials 5.

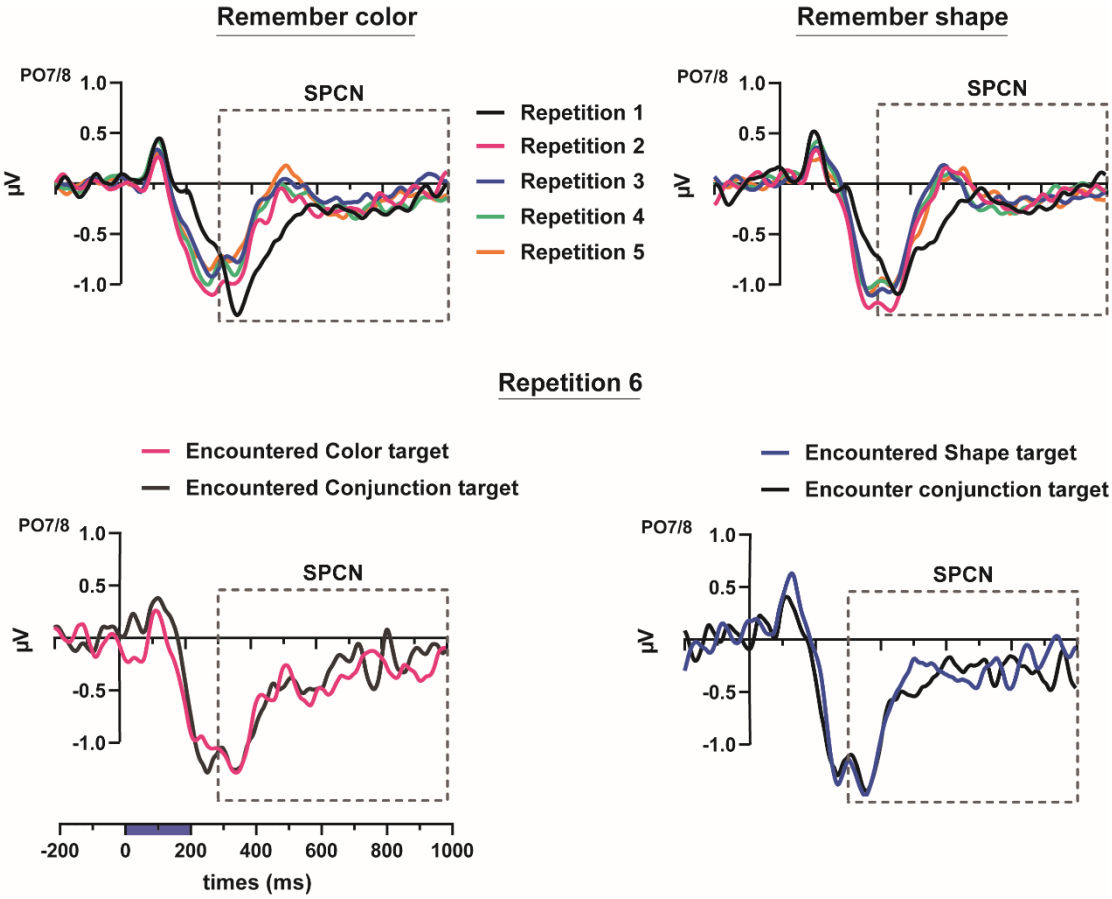

Figure 4-5 Grand-average ERP waveforms time-locked to the presentation of the cue. SPCN difference waves were computed from the contralateral minus ipsilateral waves elicited at electrodes PO7/8. There ERPs functions were separately displayed for trial repetitions 1 to 5 and (top panels) repetition 6 (bottom panels), separately displayed for the memory type (remember color vs. remember shape) and target type (single feature vs. conjunction). Color bars on the timeline indicate the exposure duration of the cue display (blue). ERP functions were low-pass filtered at 15 Hz for visualization purposes.

4.2.4 P170/LPC/FN400 in the cue array

A collapsed localizers approach (Luck & Gaspelin, 2017) was used to determine the analysis electrodes for the estimation of P170, FN400, and LPC. Specifically, data were first averaged across all conditions, and then the electrode sites showing the largest activity were used to measure the repetition effect in each condition. The same one-way ANOVA consider electrode (Fz, FCz, Cz, CPz, Pz) as within-subject factor was performed separately for P170, FN400, and LPC. Result revealed larger P170 was recorded at electrode FCz (3.29 μV; $F(4, 80) = 24.82$, $p < .001$, $\eta_p^2 = .554$). While

FN400 and LPC was observed to maximum at CPz (3.17 μV; $F(4, 80) = 15.29$, $p < .001$, $\eta_p^2 = .433$; 1.06 μV; $F(4, 80) = 6.92$, $p < .001$, $\eta_p^2 = .257$).

To determine the effect of repetition, the amplitude values recorded in the P170 time-window were then first submitted to a 6 × 2 repeated measures ANOVA, considering repetition (trials 1, 2, 3, 4, 5 vs. 6) and memory type (remember color vs. remember shape) as within-subject factors. In line with the visual impression on Figure 4-6, and Figure 4-7, where corresponding scalp topographies were plotted. The anterior repetition effects was confirm by the significant main effect of repetition ($F(5, 100) = 15.13$, $p < .001$, $\eta_p^2 = .431$, $BF_{10} > 1000$). Further planned comparison revealed that P170 amplitude was greater in trials 1 (4.81 μV), and then decreased in trials 2 (3.31 μV, $p = .011$). No amplitude difference between trials 2 to 6 ($ps = 1$). The non-significant interaction between the two factors ($BF_{01} = 22.41$) further emphasized that the P170 amplitude did not differ across memory types.

An analogous 6 × 2 repeated measures ANOVA was carried out for the amplitude of LPC. Results showed a similar pattern as the P170. As there is only a main effect of repetition ($F(5, 100) = 24.64$, $p < .001$, $\eta_p^2 = .552$, $BF_{10} > 1000$) and no other factor effects (max $F = 0.76$; min $p = 0.552$). Further planned comparison revealed that LPC amplitude was greater in trials 1 (3.09 μV), and then decreased in trials 2 (.88 μV, $p < .001$). No amplitude difference between trials 2 to 6 ($ps = 1$). Similarly, LPC did not modulated by memory type ($BF_{01} = 6.79$).

While clear evidence shows that P170 and LPC systematically decreased as the same target repeated, the effect of repetition to FN400 fell just short of significance ($F(5, 100) = 2.68$, $p = .067$, $\eta_p^2 = .118$, $BF_{01} = 2.73$). As same as the analysis of SPCN in trials 6, to estimate whether the modulation in trial repetition 5 when preceded by a conjunction

target in visual search, we then examine whether familiarity effect occurred in trials 6. The amplitude values recorded in the FN400 time window for trials 6 were submitted to a 2 × 2 repeated measures ANOVA, considering memory type (remember color vs. remember shape) and target type (single-feature vs. conjunction) as within-subject factors. As shown in Figure 4-6, increased FN400 activity when participants preceded by the conjunction target. This can be inferred from the topographical maps reported in Figure 4-7. These observations were corroborated by statistical analysis, in which larger FN400 in trials 6 when participants encountered the conjunction target rather than the single feature target in trials 5 (3.64 μV vs. 2.84 μV, $F(1, 20) = 5.15$, $p = .034$, $\eta_p^2 = .205$, $BF_{10} = 4.47$). The null effect of memory type ($BF_{01} = 4.01$) and their interaction ($BF_{01} = 3.38$) further emphasized that FN400 did not differ across memory type.

Two additional tests were performed to explore whether the amplitude of P170 and LPC in trial 6 varied as a function of target type in trial repetition 5. For the anterior repetition effects indexed by the P170, results showed no main effect as well as the interaction (max $F = 1.43$, $p = .245$). This was the case also for the LPC (max $F = 2.92$, min $p = .103$).

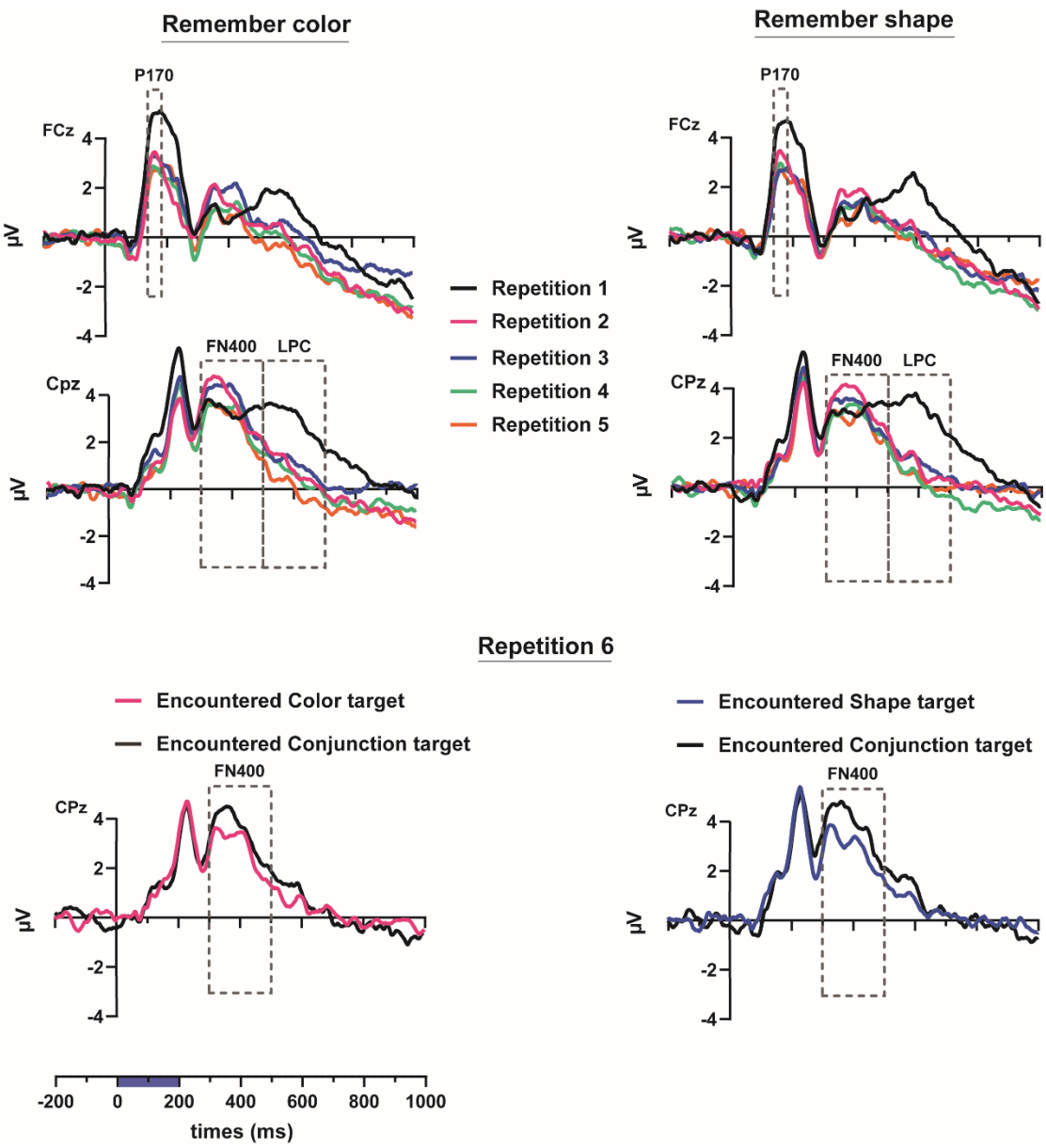
Remember color
Remember shape
P170
FCz
FN400
LPC
Cpz
CPz
μV
Repetition 1
Repetition 2
Repetition 3
Repetition 4
Repetition 5
Repetition 6
Encountered Color target
Encountered Conjunction target
Encountered Shape target
Encountered Conjunction target
-200
0
200
400
600
800
1000
times (ms)

1564

Figure 4-6 Grand-averaged ERPs at electrodes FCz, and CPz time-locked to the presentation of the cue. There ERPs functions were separately displayed for trial repetitions 1 to 5 and (top panels) repetition 6 (bottom panels), separately displayed for the memory type (remember color vs. remember shape) and target type (single feature vs. conjunction). Color bars on the timeline indicate the exposure duration of the cue display (blue).

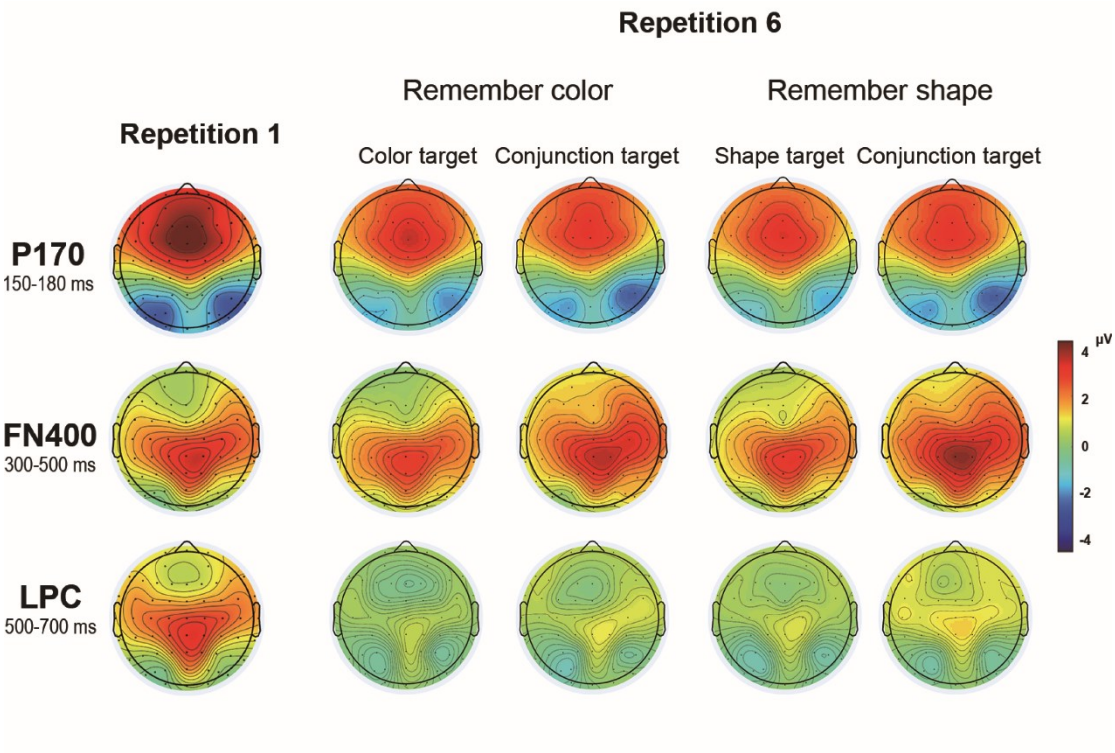

Figure 4-7 Scalp distributions of P170 (top panels, 150-180 ms), FN400 (middle panels, 300-500 ms), and LPC (bottom panels, 500-700 ms) for trial repetitions 1 and repetition 6, separately displayed for the memory type (remember color vs. remember shape) and target type (single feature vs. conjunction).

4.3 Discussion of Experiment 3

The results in Experiment 3 first observed that repeatedly viewing the same target cue can engender a familiarity effect as indexed by the P170, LPC, and SPCN. We observed the P170 negatively increased, followed by systematic drop-down inactivity of LPC and SPCN, reflecting the neural response to the memory cues was reduced across repetitions. This pattern was interpreted as the pathway for information to be off-loaded from vWM to LTM (Carlisle et al., 2011; Reinhart & Woodman, 2014;

Woodman et al., 2013). Across the same target runs, the behavior data found significant improvement in search performance. Furthermore, targets that shared the same memory color were processed more efficiently than targets that shared the same memory shape. In addition to faster RTs in detecting color targets than shape targets, the N2pc and SPCN elicited by color targets were greater than that of shape targets. These findings are in line with our previous experiments that color feature is more efficient in guiding attention than shape feature. This is as we expected that participants were reducing the need upon vWM when targets were constant.

One issue deserves a comment regarding the present ERP findings in Experiment 3. That is, we failed to find a similar P170 effect in Experiments 1 & 2. Search task in Experiments 1 & 2 required identifying the presence of targets, whereas Experiment 3 calls for deeper processing, in which participants were required to identify the symbol among the targets. It must be stressed that the memory cue can hint at either a color target or a shape target when it was given in trials 1. Participants have no clues in which features could be the potential target for the upcoming search task, they have to selectively refresh both color- and shape-template to locate the correct target in the first trials. This additional process may consume more resources at the beginning and then release after trial-by-trial learning, thereby eliciting a pronounced P170 effect. Our findings implicated that task demanding plays a role in sharpening ERP patterns that index the LTM accumulation. It is also worthy of mention the interpretation by Gunseli et al. (2014), who proposed a "rapidly saturation" assumption that P170 was not pronounced due to participants can faster consolidate target features throughout the experiment when there were few potential targets.

The main purpose of Experiment 3 is to examine whether task-irrelevant features

were discarded from the above off-loading processing. To do so, we manipulated 34% of trials 5 & 6 in which participants have to identify the symbol among a fully matched target in visual search (i.e., conjunction target), instead of the previous color-matched or shape-matched target. To ensure they have to recall the use of task-irrelevant features and to restrict the selection must be focused on the conjunction target. The search array also includes a color-matched distractor and a shape-matched distractor. We then compared the search performance and ERP patterns in trials 5 when searching for single-feature targets and conjunction targets. On the observation of better learning in the color feature than shape feature in Experiment 2, one would expect the recall of color information to be effortless when compared with the recall of shape. As expected, at the behavioral level, clear advance when encountered the conjunction target in the remember-shape series, as participants were faster in detecting conjunction targets than shape targets. Corresponding ERPs results indicated the enhanced attentional guidance that conjunction targets appear to draw attention to their location more efficiently, as it elicited larger N2pc than shape targets. Whereas in the remember-color series, we observed significant RT slowing and sharply reduced N2pc when subjects maintain the intention to find targets conjunction targets. In this case, attentional guidance appears to be less efficient when holding a color template instead of a shape template. Analysis of RTs reveals that participants were slower in detecting conjunction targets in remember-color than remember-shape series (1058 ms vs. 978 ms). Since the efficiency of color in guiding attention is clear-cut in the present study, presumably, holding a shape template then retrieving color information can promote the selection of conjunction targets. While opposite effect happened when holding a color template then recalling the shape information. One possible account is that holding the color template brought out more distractor interference with the target selection. Unlike the color-

matched condition in Experiment 2, in which all search items shared the same color with the target, in Experiment 3, the conjunction target was always accompanied by a color-matched distractor and shape-matched distractor. According to previous findings that are based on the biased-competition model (Desimone & Duncan, 1995), perceptual inputs matching vWM contents are more robust than those of mismatching stimuli (Beck & Hollingworth, 2015; Han & Kim, 2009; Olivers, 2009; Soto et al., 2005). active maintenance of the template provides a competitive advantage for matching stimuli in the visual scene. Such competition should have occurred primarily in the remember-color series, where holding the color template results in the coactivation of conjunction target and color-matched distractor. This conflict caused by direct competition was resolved by the retrieval of shape information — attentional was directed to the conjunction target. While no such competition when holding the shape template, perhaps due to the inefficient shape-based guidance, and less saliency than colors. As the color information of the memory cue was retrieved, rapid guidance of attention was deployed to the conjunction target.

It sounds tempted when assuming task-irrelevant features are thrown out from vWM as soon as participants voluntarily pick up the task-relevant features of the remembered objects. Surprisingly, while the FN400 time-locked to the memory cue did not show clear modulation of repetition, its amplitude became more positive in trials 6 after the conjunction target was presented in trials 5, hints to a potential familiarity-based recognition. At the same time, the P170, LPC, and SPCN that are deemed to show familiarity effect, were practically blind to observe similar modulations. Unlike Experiment 2 where we found the enhanced FN400 only when visual search required a potential re-loading of the shape information, the enhanced FN400 activity was observed in both color target and shape target series. This suggests our task demand

that required participants to selectively remember one of the other features did not affect the object-based encoding, as the task-irrelevant features were off-loaded during target repetition. Therefore, we propose that object-based fashion typically occurs during encoding, but that features from the same object are maintained independently.

Chapter 5 – General discussion

The format and the structure of remembered information in vWM have been a focal research topic in recent research on visual memory (Hollingworth, 2007; Hollingworth & Rasmussen, 2010; Luria & Vogel, 2011; Markov et al., 2019; Saiki, 2016, 2019; Saiki & Miyatsuji, 2007; Wheeler & Treisman, 2002; Schneegans & Bays, 2019). In three experiments, we asked whether features of conjunctive stimuli are represented as separated or integrated fashion in vWM. The design of repeatedly encountering the same target provided new insight into understanding how conjunctive features are represented in vWM. Based on the previous observation that attentional template would be off-loaded from vWM to an alternative mechanism during the same target learning, the underlying assumption of the present study is, if conjunctive features are represented in a separated fashion, their impact on task performance should be largely independent when the attentional template was off-loaded from vWM. To avoid associating conjunctive features via the probe location, we then manipulated the similarity between search targets and distractors in visual search tasks. Each search task was presented after a memory cue display, in six consecutive trials, participants were cued to search for the same target.

It's also informative to compare our findings with those using visual search tasks to determine what is being represented and to generalize across processes. To our knowledge, there are two studies attempt to address this question. One considerable piece of evidence from Soto and his colleagues (2009), who asked participants to remember only the shape feature of the presented object, while search distractors that matched either the color or shape feature with the remembered object impaired search performance, suggesting participants encode all object's feature during the memory

task. But their results and discussion do not give further information concerning their findings can also be accounted for the coactivation of both color and shape features (Bays et al., 2011; Fougnie & Alvarez, 2011; Shen et al., 2013; Thayer et al., 2021). Other evidence was those from Thayer et al. (2021), who found robust attentional guidance by searching items that match the content of vWM, but the magnitude of guidance effects has no significant difference between same-object-match items and different-object-match items. Our findings are potentially consistent with their interpretations, in which conjunctive features were maintained independently but associated indirectly.

Experiments 1 & 2 first revealed that when all distractors matched the target shape, search efficiency was the same as the baseline condition (i.e., all distractors are heterogeneous) at the behavioral level, but the ERP results showed attentional guidance by search targets along with an attentional suppression by shape-matched distractors. Moreover, the target selection and distractor suppression appeared to be working in parallel when we further divided the data based on the vertical elevation in Experiment 2. Contrarily, the search slope significantly dropped down relative to the baseline when all distractors matched the target color, but we did not observe the distractors suppression in the ERP level. Instead, targets elicited SPCN, presumably due to the guidance of attentional switched from feature-based to object-based manner (Berggren & Eimer, 2018). Further, we found the SPCN and FN400 time-locked to the cue increased in the memory phase when encountered color-matched distractors in the previous trial, suggesting a strategical resampling to enhance the search performance in the next trial (Reinhart & Woodman, 2014). Experiment 3 provides further evidence that memory cues were encoded in their entirety regardless of search intentions. Further, across three experiments, we observed better learning for color attributes than shape

attributes (see also Woodman & Vogel, 2008, for similar findings).

In our opinion, simple conjunctive features are represented as an integrated proto object (Wolfe & Bennett, 1997) at the perceptual stage, of which the human visual system can effortlessly extract information. Inspired by the proposal of Brady et al. (2011; see also Ullman, 2007 for similar assumption), we propose the format and the structure of remembered information in vWM is better to be considered including both object-based and feature-based levels. That is, the initial object encoding follows an object-based manner, whereas conjunctive features are bound indirectly in a hierarchical structure, as their impact on search performance were largely independent. To serve this kind of hierarchically structured, in terms of the concentric model of WM (Oberauer, 2002), the target's color was off-loaded to the activated part of LTM, shape information related to target is more likely to be held in the region of direct access in our case. It is also notable that elements held in the region of direct access can interfere with the ongoing process, slowing down the attentional selection as we observed P_D elicited by shape-matched distractors in Experiments 1 & 2. For example, in a memory-updating task reported by Oberauer (2002), participants had to memorize six digits presented in two rows. Arithmetic operations (e.g., "+ 3" or "- 6") were required either for both rows or only one row of digits. The focus of attention serves to operate the updating for each digit at one time. Digits to be updated, required both the "storage" and "working" function of WM, were assumed to hold in the region of direct access as an active set. While digits only to be remembered was declared as a passive set in the activated part of LTM. Results showed the set size of a passive set did not impact the latencies for the arithmetic operation. In contrast, object switch cost was observed as a function of the numbers of the active set, slowing down the RTs to complete the updating. Following the logic of the concentric model, if the target's shape feature is

off-loaded to the activated part of LTM, interference is not expected.

In sum, our interpretation for a hierarchical structure of memory representations can potentially resolve previous ambiguous findings, in which perceptual objects appear to be encoded in their entirety, but the subsequent test of those features from the same object suggested they were maintained independently.

References

Alvarez, G. A. (2011). Representing multiple objects as an ensemble enhances visual cognition. *Trends in Cognitive Sciences*, *15*(3), 122–131.

Bacigalupo, F., & Luck, S. J. (2019). Lateralized suppression of alpha-band EEG activity as a mechanism of target processing. *Journal of Neuroscience*, *39*(5), 900–917. https://doi.org/10.1523/JNEUROSCI.0183-18.2018

Baddeley, A. (2010). Working memory. *Current Biology*, *20*(4), R136–R140.

Balaban, H., & Luria, R. (2015). The number of objects determines visual working memory capacity allocation for complex items. *NeuroImage*, *119*, 54–62. https://doi.org/10.1016/j.neuroimage.2015.06.051

Bays, P. M., Wu, E. Y., & Husain, M. (2011). Storage and binding of object features in visual working memory. *Neuropsychologia*, *49*(6), 1622–1631. https://doi.org/10.1016/j.neuropsychologia.2010.12.023

Beck, V. M., & Hollingworth, A. (2015). Evidence for negative feature guidance in visual search is explained by spatial recoding. *Journal of Experimental Psychology: Human Perception and Performance*, *41*(5), 1190–1196. https://doi.org/10.1037/xhp0000109

Beck, V. M., Hollingworth, A., & Luck, S. J. (2012). Simultaneous Control of Attention by Multiple Working Memory Representations. *Psychological Science*, *23*(8), 887–898. https://doi.org/10.1177/0956797612439068

Berggren, N., & Eimer, M. (2016). The control of attentional target selection in a colour/colour conjunction task. *Attention, Perception, and Psychophysics*, *78*(8), 2383–2396. https://doi.org/10.3758/s13414-016-1168-6

Berggren, N., & Eimer, M. (2018a). Electrophysiological correlates of active

suppression and attentional selection in preview visual search. *Neuropsychologia*, *120*(August), 75–85. https://doi.org/10.1016/j.neuropsychologia.2018.10.016

Berggren, N., & Eimer, M. (2018b). Object-based target templates guide attention during visual search. *Journal of Experimental Psychology: Human Perception and Performance*, *44*(9), 1368–1382. https://doi.org/10.1037/xhp0000541

Brady, T. F., & Alvarez, G. A. (2011). Hierarchical encoding in visual working memory: Ensemble statistics bias memory for individual items. *Psychological Science*, *22*(3), 384–392. https://doi.org/10.1177/0956797610397956

Brady, T. F., Konkle, T., & Alvarez, G. A. (2011). A review of visual memory capacity: Beyond individual items and toward structured representations. *Journal of Vision*, *11*(5), 1–34. https://doi.org/10.1167/11.5.1

Brown, G., Kasem, I., Bays, P. M., & Schneegans, S. (2021). Mechanisms of feature binding in visual working memory are stable over long delays. *Journal of Vision*, *21*(12), 7. https://doi.org/10.1167/jov.21.12.7

Carlisle, N. B., Arita, J. T., Pardo, D., & Woodman, G. F. (2011). Attentional templates in visual working memory. *Journal of Neuroscience*, *31*(25), 9315–9322. https://doi.org/10.1523/JNEUROSCI.1097-11.2011

Chen, S., Kocsis, A., Liesefeld, H. R., Müller, H. J., & Conci, M. (2021). Object-based grouping benefits without integrated feature representations in visual working memory. *Attention, Perception, and Psychophysics*, *83*(3), 1357–1374. https://doi.org/10.3758/s13414-020-02153-5

Cowan, N. (2017). The many faces of working memory and short-term storage. *Psychonomic Bulletin and Review*, *24*(4), 1158–1170. https://doi.org/10.3758/s13423-016-1191-6

Desimone, R., & Duncan, J. (1995). Neural Mechanisms of Selective Visual Attention. *Annual Review of Neuroscience*, *18*(1), 193–222. https://doi.org/10.1146/annurev.ne.18.030195.001205

Doro, M., Bellini, F., Brigadoi, S., Eimer, M., & Dell'Acqua, R. (2020). A bilateral N2pc (N2pcb) component is elicited by search targets displayed on the vertical midline. *Psychophysiology*, *57*(3), 1–12. https://doi.org/10.1111/psyp.13512

Drisdelle, B. L., Aubin, S., & Jolicoeur, P. (2017). Dealing with ocular artifacts on lateralized ERPs in studies of visual-spatial attention and memory: ICA correction versus epoch rejection. *Psychophysiology*, *54*(1), 83–99.

Duncan, J., & Humphreys, G. (1992). Beyond the Search Surface: Visual Search and Attentional Engagement. *Journal of Experimental Psychology. Human Perception and Performance*, *18*, 578–588; discussion 589. https://doi.org/10.1037//0096-1523.18.2.578

Eimer, M., & Grubert, A. (2014a). Spatial attention can be allocated rapidly and in parallel to new visual objects. *Current Biology*, *24*(2), 193–198. https://doi.org/10.1016/j.cub.2013.12.001

Eimer, M., & Grubert, A. (2014b). The gradual emergence of spatially selective target processing in visual search: From feature-specific to object-based attentional control. *Journal of Experimental Psychology: Human Perception and Performance*, *40*(5), 1819–1831. https://doi.org/10.1037/a0037387

Emrich, S. M., Al-Aidroos, N., Pratt, J., & Ferber, S. (2009). Visual search elicits the electrophysiological marker of visual working memory. *PloS One*, *4*(11), e8042.

Folk, C., Remington, R., & Johnston, J. (1992). Involuntary Covert Orienting Is Contingent on Attentional Control Settings. *Journal of Experimental Psychology. Human Perception and Performance*, *18*, 1030–1044.

https://doi.org/10.1037//0096-1523.18.4.1030

Fougnie, D., & Alvarez, G. A. (2011). Object features fail independently in visual working memory: Evidence for a probabilistic feature-store model. *Journal of Vision*, *11*(12), 3.

Fougnie, D., Asplund, C. L., & Marois, R. (2010). What are the units of storage in visual working memory? *Journal of Vision*, *10*(12), 27.

Fougnie, D., Cormiea, S. M., & Alvarez, G. A. (2013). Object-based benefits without object-based representations. *Journal of Experimental Psychology: General*, *142*(3), 621.

Fougnie, D., & Marois, R. (2009). Attentive tracking disrupts feature binding in visual working memory. *Visual Cognition*, *17*(1–2), 48–66.

Giammarco, M., Paoletti, A., Guild, E., & Al-Aidroos, N. (2016). Attentional capture by items that match episodic long-term memory representations. *Visual Cognition*, 1–24. https://doi.org/10.1080/13506285.2016.1195470

Grubert, A., Carlisle, N. B., & Eimer, M. (2016). The control of single-color and multiple-color visual search by attentional templates in working memory and in long-term memory. *Journal of Cognitive Neuroscience*, *28*(12), 1947–1963. https://doi.org/10.1162/jocn_a_01020

Grubert, A., Carlisle, N. B., & Martin Eimer. (2016). The control of single-colour and multiple-colour visual search by attentional templates in working memory and in long-term memory. *Behavioral and Brain Sciences*, *33*(6), 458–459.

Grubert, A., & Eimer, M. (2018). The time course of target template activation processes during preparation for visual search. *Journal of Neuroscience*, *38*(44), 9527–9538. https://doi.org/10.1523/JNEUROSCI.0409-18.2018

Grubert, A., & Eimer, M. (2020). *Preparatory Template Activation during Search for*

Alternating Targets. 1–11.

Gunseli, E., Olivers, C. N. L., & Meeter, M. (2014). Effects of Search Difficulty on the Selection, Maintenance, and Learning of Attentional Templates. *Journal of Cognitive Neuroscience*, *26*(9), 2042–2054. https://doi.org/10.1162/jocn_a_00600

Han, S. W., & Kim, M. S. (2009). Do the Contents of Working Memory Capture Attention? Yes, But Cognitive Control Matters. *Journal of Experimental Psychology: Human Perception and Performance*, *35*(5), 1292–1302. https://doi.org/10.1037/a0016452

Hickey, C., Di Lollo, V., & McDonald, J. J. (2008). Electrophysiological Indices of Target and Distractor Processing in Visual Search. *Journal of Cognitive Neuroscience*, *21*(4), 760–775. https://doi.org/10.1162/jocn.2009.21039

Hilimire, M. R., Mounts, J. R. W., Parks, N. A., & Corballis, P. M. (2011). Dynamics of target and distractor processing in visual search: Evidence from event-related brain potentials. *Neuroscience Letters*, *495*(3), 196–200. https://doi.org/10.1016/j.neulet.2011.03.064

Hollingworth, A. (2007). Object-position binding in visual memory for natural scenes and object arrays. *Journal of Experimental Psychology: Human Perception and Performance*, *33*(1), 31.

Hollingworth, A., & Matsukura, M. (2019). Feature-based guidance of attention during post-saccadic selection. *Attention, Perception, & Psychophysics*, *81*(6), 1822–1835.

Hollingworth, A., & Rasmussen, I. P. (2010). Binding objects to locations: The relationship between object files and visual working memory. *Journal of Experimental Psychology: Human Perception and Performance*, *36*(3), 543.

Hu, Y., Xu, Z., & Hitch, G. J. (2011). Strategic and automatic effects of visual working memory on attention in visual search. *Visual Cognition*, *19*(6), 799–816. https://doi.org/10.1080/13506285.2011.590461

Jennings, J., & Wood, C. (1976). The ?Adjustment Procedure for Repeated-Measures Analyses of Variance. *Psychophysiology*, *13*, 277–278. https://doi.org/10.1111/j.1469-8986.1976.tb00116.x

Jolicœur, P., Brisson, B., & Robitaille, N. (2008). Dissociation of the N2pc and sustained posterior contralateral negativity in a choice response task. *Brain Research*, *1215*, 160–172. https://doi.org/10.1016/j.brainres.2008.03.059

Kerzel, D., & Burra, N. (2020). Capture by context elements, not attentional suppression of distractors, explains the PD with small search displays. *Journal of Cognitive Neuroscience*, *32*(6), 1170–1183.

Kiesel, A., Miller, J., Jolicœur, P., & Brisson, B. (2008). Measurement of ERP latency differences: A comparison of single-participant and jackknife-based scoring methods. *Psychophysiology*, *45*(2), 250–274. https://doi.org/10.1111/j.1469-8986.2007.00618.x

Kiss, M., Jolicœur, P., Dell'Acqua, R., & Eimer, M. (2008). Attentional capture by visual singletons is mediated by top-down task set: New evidence from the N2pc component. *Psychophysiology*, *45*(6), 1013–1024. https://doi.org/10.1111/j.1469-8986.2008.00700.x

Klaver, P., Talsma, D., Wijers, A. A., Heinze, H.-J., & Mulder, G. (1999). An event-related brain potential correlate of visual short-term memory. *NeuroReport*, *10*(10), 2001–2005.

Kok, A. (2001). On the utility of P3 amplitude as a measure of processing capacity. *Psychophysiology*, *38*(3), 557–577. https://doi.org/10.1017/S0048577201990559

Lawrence, M. (2011). ez: Easy Analysis and Visualization of Factorial Experiments. *Computer Software Manual](R Package Version 3.0-0)*.

Logan, G. D. (1988). Toward an Instance Theory of Automatization. *Psychological Review*, *95*(4), 492–527. https://doi.org/10.1037/0033-295X.95.4.492

Luck, S., & Hillyard, S. (1994). Spatial Filtering During Visual Search: Evidence From Human Electrophysiology. *Journal of Experimental Psychology. Human Perception and Performance*, *20*, 1000–1014. https://doi.org/10.1037/0096-1523.20.5.1000

Luck, S. J., & Gaspelin, N. (2017). How to get statistically significant effects in any ERP experiment (and why you shouldn't). *Psychophysiology*, *54*(1), 146–157. https://doi.org/10.1111/psyp.12639

Luck, S. J., Girelli, M., McDermott, M. T., & Ford, M. A. (1997). Bridging the gap between monkey neurophysiology and human perception: An ambiguity resolution theory of visual selective attention. *Cognitive Psychology*, *33*(1), 64–87.

Luck, S. J., & Vogel, E. K. (1997). The capacity of visual working memory for features and conjunctions. *Nature*, *390*(6657), 279–281.

Luck, S. J., & Vogel, E. K. (2013). Visual working memory capacity: from psychophysics and neurobiology to individual differences. *Trends in Cognitive Sciences*, *17*(8), 391–400.

Luria, R., Balaban, H., Awh, E., & Vogel, E. K. (2016). The contralateral delay activity as a neural measure of visual working memory. *Neuroscience and Biobehavioral Reviews*, *62*, 100–108. https://doi.org/10.1016/j.neubiorev.2016.01.003

Luria, R., & Vogel, E. K. (2011). Shape and color conjunction stimuli are represented

as bound objects in visual working memory. *Neuropsychologia*, *49*(6), 1632–1639. https://doi.org/10.1016/j.neuropsychologia.2010.11.031

Markov, Y. A., Tiurina, N. A., & Utochkin, I. S. (2019a). Different features are stored independently in visual working memory but mediated by object-based representations. *Acta Psychologica*, *197*(April), 52–63. https://doi.org/10.1016/j.actpsy.2019.05.003

Markov, Y. A., Tiurina, N. A., & Utochkin, I. S. (2019b). Different features are stored independently in visual working memory but mediated by object-based representations. *Acta Psychologica*, *197*(October), 52–63. https://doi.org/10.1016/j.actpsy.2019.05.003

Mazza, V., Turatto, M., Umiltà, C., & Eimer, M. (2007). Attentional selection and identification of visual objects are reflected by distinct electrophysiological responses. *Experimental Brain Research*, *181*(3), 531–536.

Miller, J., Patterson, T., & Ulrich, R. (1998). Jackknife-based method for measuring LRP onset latency differences. *Psychophysiology*, *35*(1), 99–115. https://doi.org/10.1017/S0048577298000857

Monnier, A., Dell'Acqua, R., & Jolicoeur, P. (2020). Distilling the distinct contralateral and ipsilateral attentional responses to lateral stimuli and the bilateral response to midline stimuli for upper and lower visual hemifield locations. *Psychophysiology*, *57*(11), 1–18. https://doi.org/10.1111/psyp.13651

Mowei, S., Ning, T., Fan, W., Rende, S., & Zaifeng, G. (2013). Robust object-based encoding in visual working memory Mowei. *Assistance to Victims of Aviation Accidents and Their Families: Proceedings*, *13*, 1–11. https://doi.org/10.1167/13.2.1.doi

Oberauer, K. (2002). Access to Information in Working Memory: Exploring the

Focus of Attention. *Journal of Experimental Psychology: Learning Memory and Cognition*, *28*(3), 411–421. https://doi.org/10.1037/0278-7393.28.3.411

Oberauer, K. (2006). Is the focus of attention in working memory expanded through practice? *Journal of Experimental Psychology: Learning Memory and Cognition*, *32*(2), 197–214. https://doi.org/10.1037/0278-7393.32.2.197

Oberauer, K. (2019). Working Memory and Attention – A Conceptual Analysis and Review. *Journal of Cognition*, *2*(1), 1–23. https://doi.org/10.5334/joc.58

Oberauer, K., Awh, E., & Sutterer, D. W. (2016). *Proactive Facilitation but No Proactive Interference The Role of Long-Term Memory in a Test of Visual Working Memory :* https://doi.org/10.1037/xlm0000302

Olivers, C. N. L. (2009). What Drives Memory-Driven Attentional Capture? The Effects of Memory Type, Display Type, and Search Type. *Journal of Experimental Psychology: Human Perception and Performance*, *35*(5), 1275–1291. https://doi.org/10.1037/a0013896

Olson, I. R., & Jiang, Y. (2002). Is visual short-term memory object based? Rejection of the “strong-object” hypothesis. *Perception and Psychophysics*, *64*(7), 1055–1067. https://doi.org/10.3758/BF03194756

Pernier, J., Perrin, F., & Bertrand, O. (1988). Scalp current density fields: concept and properties. *Electroencephalography and Clinical Neurophysiology*, *69*(4), 385–389.

Perrin, F., Pernier, J., Bertrand, O., & Echallier, J. F. (1989). Spherical splines for scalp potential and current density mapping. *Electroencephalography and Clinical Neurophysiology*, *72*(2), 184–187.

Perron, R., Lefebvre, C., Robitaille, N., Brisson, B., Gosselin, F., Arguin, M., & Jolicœur, P. (2009). Attentional and anatomical considerations for the

representation of simple stimuli in visual short-term memory: evidence from human electrophysiology. *Psychological Research*, *73*(2), 222–232.

Polich, J. (2012). Neuropsychology of P300. In *The Oxford Handbook of Event-Related Potential Components*. Oxford University Press. https://doi.org/10.1093/oxfordhb/9780195374148.013.0089

Quinlan, P. T., & Cohen, D. J. (2011). Object-based representations govern both the storage of information in visual short-term memory and the retrieval of information from it. *Psychonomic Bulletin & Review*, *18*(2), 316–323.

R Development Core Team. (2017). R: A language and environment for statistical computing. In *Vienna, Austria* (p. 1). https://doi.org/R Foundation for Statistical Computing, Vienna, Austria. ISBN 3-900051-07-0, URL http://www.R-project.org.

Reinhart, R. M. G., & Woodman, G. F. (2014). High stakes trigger the use of multiple memories to enhance the control of attention. *Cerebral Cortex*, *24*(8), 2022–2035. https://doi.org/10.1093/cercor/bht057

Rhodes, S., & Cowan, N. (2019). Flexible representations in visual working memory and interactions with long-term learning: Commentary on the special issue. *British Journal of Psychology*, *110*(2), 449–460. https://doi.org/10.1111/bjop.12380

Rossi, A F, Bichot, N. P., Desimone, R., & Ungerleider, L. G. (2001). Top-down, but not bottom-up: deficits in target selection in monkeys with prefrontal lesions. *Journal of Vision*, *1*(3), 18.

Rossi, Andrew F., Bichot, N. P., Desimone, R., & Ungerleider, L. G. (2007). Top-down attentional deficits in Macaques with lesions of lateral prefrontal cortex. *Journal of Neuroscience*, *27*(42), 11306–11314.

https://doi.org/10.1523/JNEUROSCI.2939-07.2007

Rossi, Andrew F., Pessoa, L., Desimone, R., & Ungerleider, L. G. (2009). The prefrontal cortex and the executive control of attention. *Experimental Brain Research*, *192*(3), 489–497. https://doi.org/10.1007/s00221-008-1642-z

Rouder, J. N., & Morey, R. D. (2012). Default Bayes Factors for Model Selection in Regression. *Multivariate Behavioral Research*, *47*(6), 877–903. https://doi.org/10.1080/00273171.2012.734737

Rouder, J. N., Morey, R. D., Speckman, P. L., & Province, J. M. (2012). Default Bayes factors for ANOVA designs. *Journal of Mathematical Psychology*, *56*(5), 356–374. https://doi.org/10.1016/j.jmp.2012.08.001

Saiki, J. (2016). Location-Unbound Color-Shape Binding Representations in Visual Working Memory. *Psychological Science*, *27*(2), 178–190. https://doi.org/10.1177/0956797615616797

Saiki, J. (2019). Robust color-shape binding representations for multiple objects in visual working memory. *Journal of Experimental Psychology: General*, *148*(5), 905.

Saiki, J., & Miyatsuji, H. (2007). Binding deficit in visual short-term memory reflects maintenance, not retrieval. *Journal of Vision*, *7*(9), 853.

Schneegans, S., & Bays, P. M. (2017). Neural architecture for feature binding in visual working memory. *Journal of Neuroscience*, *37*(14), 3913–3925. https://doi.org/10.1523/JNEUROSCI.3493-16.2017

Schneegans, S., & Bays, P. M. (2019). New perspectives on binding in visual working memory. *British Journal of Psychology*, *110*(2), 207–244. https://doi.org/10.1111/bjop.12345

Sharbrough, F. (1991). American Electroencephalographic Society guidelines for

standard electrode position nomenclature. *J Clin Neurophysiol*, *8*, 200–202.

Soto, D., Heinke, D., Humphreys, G. W., & Blanco, M. J. (2005). Early, involuntary top-down guidance of attention from working memory. *Journal of Experimental Psychology: Human Perception and Performance*, *31*(2), 248–261. https://doi.org/10.1037/0096-1523.31.2.248

Soto, D., & Humphreys, G. W. (2009). Automatic selection of irrelevant object features through working memory evidence for top-down attentional capture. *Experimental Psychology*, *56*(3), 165–172. https://doi.org/10.1027/1618-3169.56.3.165

Thayer, D. D., Bahle, B., & Hollingworth, A. (2021). Guidance of attention from visual working memory is feature-based, not object-based: Implications for models of feature binding. *Journal of Experimental Psychology: General*, *November*. https://doi.org/10.1037/xge0001116

Treisman, A. M., & Gelade, G. (1980). A feature-integration theory of attention. *Cognitive Psychology*, *12*(1), 97–136. https://doi.org/10.1016/0010-0285(80)90005-5

Treisman, A., & Zhang, W. (2006). Location and binding in visual working memory. *Memory & Cognition*, *34*(8), 1704–1719.

Ullman, S. (2007). Object recognition and segmentation by a fragment-based hierarchy. *Trends in Cognitive Sciences*, *11*(2), 58–64.

Ulrich, R., & Miller, J. (2001). Using the jackknife-based scoring method for measuring LRP onset effects in factorial designs. *Psychophysiology*, *38*(5), 816–827. https://doi.org/10.1017/S0048577201000610

Vogel, E. K., & Machizawa, M. G. (2004). Neural activity predicts individual differences in visual working memory capacity. *Nature*, *428*(6984), 748–751.

https://doi.org/10.1038/nature02447

Voss, J L, & Paller, K. (2008). Neural substrates of remembering: Electroencephalographic studies. *Learning and Memory: A Comprehensive Reference*, *3*, 79–97.

Voss, Joel L., & Paller, K. A. (2007). Neural correlates of conceptual implicit memory and their contamination of putative neural correlates of explicit memory. *Learning and Memory*, *14*(4), 259–267. https://doi.org/10.1101/lm.529807

Wheeler, M. E., & Treisman, A. M. (2002). Binding in short-term visual memory. *Journal of Experimental Psychology: General*, *131*(1), 48–64. https://doi.org/10.1037/0096-3445.131.1.48

Wolfe, J. M. (2012). Guided Search 4.0: Current Progress with a Model of Visual Search. In *Integrated Models of Cognitive Systems*. Oxford University Press. https://doi.org/10.1093/acprof:oso/9780195189193.003.0008

Wolfe, J. M., & Bennett, S. C. (1997). Preattentive object files: Shapeless bundles of basic features. *Vision Research*, *37*(1), 25–43.

Wolfe, J. M., & Horowitz, T. S. (2004). What attributes guide the deployment of visual attention and how do they do it? In *Nature Reviews Neuroscience* (Vol. 5, Issue 6, pp. 495–501). Nature Publishing Group. https://doi.org/10.1038/nrn1411

Woodman, G. F., Carlisle, N. B., & Reinhart, R. M. G. (2013). Where do we store the memory representations that guide attention? *Journal of Vision*, *13*(3). https://doi.org/10.1167/13.3.1

Woodman, G. F., & Luck, S. J. (2003). Serial Deployment of Attention During Visual Search. *Journal of Experimental Psychology: Human Perception and Performance*, *29*(1), 121–138. https://doi.org/10.1037/0096-1523.29.1.121

Woodman, G. F., Luck, S. J., & Schall, J. D. (2007). The role of working memory representations in the control of attention. *Cerebral Cortex*, *17*(SUPPL. 1). https://doi.org/10.1093/cercor/bhm065

Woodman, G. F., & Vogel, E. K. (2008). Selective storage and maintenance of an object's features in visual working memory. *Psychonomic Bulletin and Review*, *15*(1), 223–229. https://doi.org/10.3758/PBR.15.1.223

Xu, Y. (2002a). Encoding color and shape from different parts of an object in visual short-term memory. *Perception & Psychophysics*, *64*(8), 1260–1280.

Xu, Y. (2002b). Limitations of object-based feature encoding in visual short-term memory. *Journal of Experimental Psychology: Human Perception and Performance*, *28*(2), 458.

Xu, Y., & Chun, M. M. (2006). Dissociable neural mechanisms supporting visual short-term memory for objects. *Nature*, *440*(7080), 91–95.

Zhang, B., Zhang, J. X., Kong, L., Huang, S., Yue, Z., & Wang, S. (2010). Guidance of visual attention from working memory contents depends on stimulus attributes. *Neuroscience Letters*, *486*(3), 202–206. https://doi.org/10.1016/j.neulet.2010.09.052

Zhang, W., & Luck, S. J. (2008). Discrete fixed-resolution representations in visual working memory. *Nature*, *453*(7192), 233–235. https://doi.org/10.1038/nature06860

Appendix – Supplementary of SPCNb

We recently showed that deploying attention to target stimuli displayed along the vertical meridian elicits a bilateral N2pc, that we labelled N2pcb (Doro et al., 2020, Psychophysiology). Here we investigated whether a different component, the sustained posterior contralateral negativity (SPCN), shows the same property when a varying number of visual stimuli are displayed either laterally or on the vertical meridian. We displayed one or two cues that designated candidate targets to be detected in a search array that was displayed after a retention interval. The cues were either on the horizontal meridian or on the vertical meridian. When the cues were on the horizontal meridian, we observed an N2pc followed by an SPCN in their classic form, as negativity increments contralateral to the cues. As expected, SPCN amplitude was greater when two cues had to be memorized than when only one cue had to be memorized. When the cues were on the vertically meridian, we observed an N2pcb followed by a bilateral SPCN (or SPCNb). Critically, like SPCN, SPCNb amplitude was greater when two cues had to be memorized than when only one cue had to be memorized. A series of additional parametrical and topographical comparisons between N2pcb and SPCNb revealed similarities but also some important differences between these two components that we interpreted as evidence for their distinct neural sources.

6.1 Introduction

In order to identify visual stimuli of interest, we are required to scan our complex environment. In most cases, finding such objects does not seem to pose any insurmountable obstacle to our daily living. At the neural level, however, visual search involves a complex set of processes required to maintain a stable representation of the

visual environment in spite of the massive changes of the retinal images caused by head and/or eye movements (e.g., Henderson, 2008; Hollingworth, Richard, & Luck, 2008). Visuo-spatial attention and visual working memory are said to play a crucial role in these processes, with visuo-spatial attention often described as a filter set to individuate target stimuli, and visual working memory as a system optimized to maintain target information in a representational state amenable to further, higher-level processing.

Studying visual attention and visual working memory in the lab using event-related potentials (ERPs) has advanced our understanding of both these key aspects of human cognition, especially after the discovery that each of them is associated with a distinctive ERP signature. The ERP signature of the deployment of visuo-spatial attention to candidate targets is the N2pc component (Eimer, 1996; Luck & Hillyard, 1994). N2pc is often studied in the context of visual search tasks. When a target is displayed laterally relative to fixation, N2pc manifests itself as a transient negativity enhancement usually unfolding in a 200–300 ms time-window at parieto-occipital sites (i.e., PO7/PO8) contralateral to the visual hemifield in which the target is displayed. The ERP signature of the active maintenance of a representation in visual working memory for a laterally-displayed stimulus is the sustained posterior contralateral negativity component (SPCN; Jolicœur, Brisson, & Robitaille, 2008; alternatively named contralateral delay activity, or CDA, by Vogel & Machizawa, 2004; contralateral negative slow wave, or CNSW, by Klaver, Talsma, Wijers, Heinze, & Mulder, 1999; contralateral search activity, or CSA, by Emrich, Al-Aidroos, Pratt, & Ferber, 2009). SPCN was initially explored using cued change detection tasks, in which subjects are cued to memorize objects displayed in either visual hemifield for later comparison with objects that can unpredictably remain the same or one of which can be changed. SPCN is often detected at the same recording sites as those used to observe N2pc (i.e.,

PO7/PO8) and, similarly to N2pc, manifests itself as a larger negativity contralateral to the visual hemifield in which target information is displayed. This surface similarity aside, SPCN onsets later (at about 400 ms) and lasts substantially longer than N2pc, namely, as long as objects are retained in visual working memory (see Luria, Balaban, Awh, & Vogel, 2016, for a comprehensive review). Furthermore, unlike N2pc, a distinctive feature of SPCN is that its amplitude increases as the number of objects to be retained in memory is increased, as long as this number does not exceed an individual's visual working memory capacity (Vogel & Machizawa, 2004), which averages to about 3 objects across individuals (Balaban, Fukuda, & Luria, 2019; Cowan, 2001).

Source localization analyses of MEG recordings have localized the neural generators of the N2pc in the extra-striate visual cortex, in the infero-temporal cortex, with a possible early parietal contribution (Hopf et al., 2000, 2002, 2006; Jolicœur et al., 2011). MEG and fMRI recordings concur that the neural generators of SPCN are located in the parietal cortex, in the intra-parietal sulcus in particular, and in more lateral/ventral regions also involved in the generation of N2pc activity (Becke, Müller, Vellage, Schoenfeld, & Hopf, 2015; Brigadoi et al., 2017; Duma et al., 2019; Jolicœur et al., 2011; Naughtin, Mattingley, & Dux, 2016; Robitaille, Marois, Todd, Grimault, Cheyne, & Jolicœur, 2010; Todd & Marois, 2004; Xu & Chun, 2006). Although some uncertainty remains as to whether N2pc and SPCN have exactly the same or slightly different neural sources, it is important for the present purposes to note that the receptive fields of neurons located in the aforementioned regions and receiving inputs from foveal retinal receptors extend into the ipsilateral hemifield, a subset of them for as much as 2° of visual angle (Hubel & Wiesel, 1967; Nakamura, Chaumon, Klijn, & Innocenti, 2007; Papaioannou & Luck, 2020; Wandell, Dumoulin, & Brewer, 2007;

Zeki, 1993). As a result, visual input displayed along (or close to) the vertical meridian activates homologous neurons located in posterior regions of both hemispheres, and is therefore bilaterally represented in the posterior cortex.

We have recently explored whether N2pc reflects this neuroanatomical organization of the receptive fields of neurons underpinning the selection and encoding phases of target information. Using a visual search task in which singleton or feature targets could be displayed laterally or aligned to the vertical meridian, we observed N2pc activity in its classical form, namely, as a larger negativity for contralateral relative to ipsilateral PO7/PO8 recording sites when targets were displayed laterally relative to the vertical meridian. Targets displayed along the vertical meridian elicited a bilateral negativity, that we quantified as the average activity detected at PO7 and PO8, that was undistinguishable from the contralateral negativity elicited by lateral targets. This pattern suggests that 'midline' targets elicited a bilateral N2pc (or N2pcb; Doro, Bellini, Brigadoi, Eimer, & Dell'Acqua, 2020; Monnier, Dell'Acqua, & Jolicœur, 2020). The comparison between the ERP results observed in the singleton and feature search conditions was critical in corroborating this conclusion. As others before us (e.g., Feldmann-Wüstefeld & Schubö, 2015; Mazza, Turatto, & Caramazza, 2009), we observed that the N2pc elicited by lateral targets emerged earlier in singleton search than in feature search. An identical result was observed for N2pcb elicited by midline targets, thus strengthening considerably our hypothesis of the close similarity between N2pc and N2pcb activity (Doro et al., 2020). Further support for the supposed similarity between N2pc and N2pcb has been reported by Monnier, Dell'Acqua, and Jolicœur (2020), who showed that N2pc and N2pcb share an additional property. It is now well established that the amplitude of N2pc is substantially reduced, sometimes even reversed in polarity, for lateral targets displayed above the horizontal meridian, that is,

in the upper visual hemifield, compared to those displayed below the horizontal meridian, that is, in the lower visual hemifield (e.g., Bacigalupo & Luck, 2019; Luck, Girelli, McDermott, & Ford, 1997). A likely explanation of this N2pc asymmetry refers to the neuroanatomical organization of the retinotopic topography in the posterior cortex. Stimuli in the lower visual field project to more dorsal regions of the posterior cortex, whereas stimuli in the upper visual field project to more ventral regions of the posterior cortex. Relative to ventral regions, dorsal regions are closer to the scalp, and this explains why N2pc can be more easily detected for stimuli in the lower visual field compared to stimuli in the upper visual field. Using a singleton search design, Monnier et al. (2020) observed a fully-fledged N2pc for lateral targets in the lower visual hemifield, and a N2pc polarity reversal for lateral targets in the upper visual hemifield (i.e., a contralateral positivity). Critically, an identical pattern was observed for N2pcb for midline targets when these targets were presented above versus below fixation, a result that was interpreted as suggesting a similarity of the neural sources of N2pc and N2pcb.

The issue at stake in the present context is the lack of a test for SPCN conceptually analogous to those provided by Doro et al. (2020) and Monnier et al (2020) for N2pc. Would a midline stimulus that must be retained in visual working memory elicit a bilateral SPCN (or SPCNb) of equal amplitude compared to the contralateral portion of the SPCN elicited by a lateral stimulus? Moreover, would SPCNb share with SPCN the peculiar property to scale in amplitude with the number of midline visual stimuli? Of course, given the overlap, or close proximity, of the neural generators of N2pc and SPCN activity, the expected answers to both these questions are in the positive. Perhaps, an issue that warrants close inspection in relation to the possible distinction of the neural sources of N2pc and SPCN would be to observe a different modulation of

N2pc and SPCN as far as the vertical elevation of the visual stimuli is concerned. Would the amplitude of SPCN/SPCNb — similarly to the amplitude of N2pc/N2pcb — be reduced to nil, or even reversed in polarity, for stimuli displayed in the upper visual hemifield compared to SPCN/SPCNb elicited by stimuli displayed in the lower visual hemifield? To answer all these questions, we employed a cued visual search task akin to that of Carlisle, Arita, Pardo, and Woodman (2011), that is illustrated in Figure 6-1.

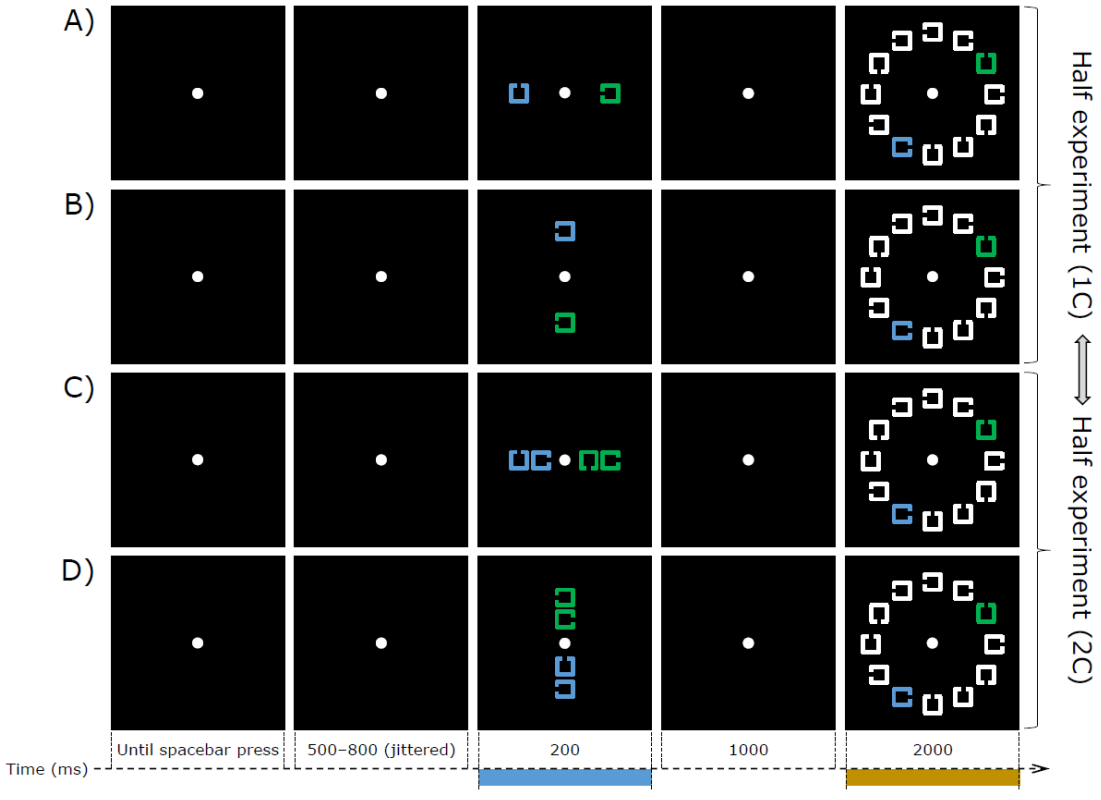

Figure 6-1 Sequence of events on four types of trials (A to D) in the experiment showing the orthogonal combination of the number of items in the cue array (labelled here as 1C and 2C, as in trials A and B and in trials C and D, respectively) and the spatial arrangement of the cues, horizontal (as in trials A and C) or vertical (as in trials B and D). The stimuli in this figure are just approximately to scale with the stimuli displayed on the computer monitor. See section '2. Method' for further details.

One or two colored squares (cues) with a gap on one side were displayed either on the horizontal meridian (left or right of fixation) or on the vertical meridian (above or below fixation) at the beginning of each trial. The cues of given color (e.g., green)

indicated the candidate target(s), and subjects were instructed to memorize the position of the gap(s) for later search in an array composed of uniformly white distractor gapped squares, accompanied by a differently colored (blue) distractor in the opposite hemifield so as to avoid sensory imbalance. The task required first to select the candidate target(s) based on color, to keep the information about the gap position(s) in memory for a short interval (1 s), and finally to inspect a square of the same color as the cue(s) for a correspondence in gap position. The information needed to answer all the above questions were extracted from ERP activity time-locked to the cue array onset. We expected to find clear SPCN components during the retention of lateral cues that should be larger for two cues than for one cue, as reported by Carlisle et al. (2011). The new question asked here was whether we would find SPCNb activity of similar amplitude when the cues were presented aligned to the vertical midline. As argued in the foregoing introduction, this is what we expected, and in fact what we found.

6.2 Method

6.2.1 Participants

Twenty-one students at the Guangzhou University (4 males; mean age = 23 years, SD = 2.4) took part in the present experiment after providing written informed consent. All participants had normal or corrected-to-normal visual acuity, and all reported normal color vision and no history of neurological disorders. The experiment was vetted by the local ethics committee.

6.2.2 Stimuli and procedure

An example of the stimuli and an illustration of the sequence of events on four trials in the experiment are shown in Figure 6-1. The stimuli were displayed on the black

background (CIE: 0.312/0.329, 1.0 cd/m2) of a 17" CRT computer monitor with a refresh rate of 60 Hz, at a viewing distance of about 60 cm. The stimuli in the cue array (marked by the cyan bar on the timeline in Figure 1) were 2 or 4 equiluminant outlined squares (1.2° × 1.2°, 0.2° line thickness), colored in green (CIE: 0.278/0.393, 20 cd/m2) or in blue (CIE: 0.213/0.272, 20 cd/m2) with a gap (0.3°) on the left, right, top, or bottom side. When the cue array was composed of 2 gapped squares, each gapped square was displayed 3.5° to the left/right or above/below the center of the monitor. When the cue array was composed of 4 gapped squares, the 2 more eccentric gapped squares were presented 3.5° to the left/right or above/below the center of the monitor and the 2 less eccentric gapped squares were presented 1.8° to the left/right or above/below the center of the monitor. The stimuli in the search array (marked by the orange bar on the timeline in Figure 6-1) were 12 gapped squares identical in dimension to those composing the cue array, 10 of which were displayed in white (CIE: 0.313/0.329, 90 cd/m2), with the addition of two gapped squares, one blue and one green (same colors as the cues) always displayed laterally (i.e., left/right) on opposite sides relative to the center of the monitor. The stimuli in the search array were arranged along a notional circle of 5.8° in diameter and positioned in correspondence to the number locations on a clock face. With the exception of the positions aligned to the vertical meridian (i.e., the positions at 12 and 6 o'clock), all other positions on opposite sides relative to the center of the screen were equally likely to be occupied by the blue and green gapped squares.

Prior to the beginning of the experiment, each participant was informed about the task-relevant color (i.e., either blue or green, counterbalanced across participants) designating cues and targets in the cue and search arrays, respectively. For each participant, the task-relevant color was kept constant for the entire experiment. Each

trial began with the presentation of a white fixation dot (0.4° × 0.4°) at the center of the monitor. Participants were instructed to maintain gaze on the fixation dot, avoiding head and/or eye movements until the end of the trial. Participants started each trial by pressing the spacebar using the thumb of the left or right hand. After the spacebar press, an interval of 500–800 ms (randomly jittered using a rectangular distribution) elapsed before the onset of the cue array, that was exposed for 200 ms. Participants had to memorize the position of the gap(s) of the cue(s) in the task relevant color. Participants had therefore to memorize the gap position of 1 cue (1C trials in Figure 6-1) or the gap positions of 2 cues (2C trials in Figure 6-1). The cues in the cue array could unpredictably and with equal probability be presented on the horizontal meridian (i.e., to the left/right of fixation) or on the vertical meridian (i.e., above/below fixation). The gap position(s) of the cue(s) in the cue array had to be memorized regardless of their spatial arrangement. The cue array was followed by an interval of 1000 ms, followed by the onset of the search array that was exposed for 2000 ms. On half of the trials, the search array contained a target, that is, a gapped square identical to the cue in 1C trials, or to either cues in 2C trials. On the other half of the trials, the target was absent. In the search array, the gap position of the (e.g., blue) cue never matched that of the (green) distractor. Participants were instructed to use the 'L' or 'A' of the computer keyboard (counterbalanced across participants) to indicate whether a target was present or absent, with equal emphasis on response speed and accuracy. Following the detection of the participant's response, the fixation dot disappeared and an inter-trial interval of 1000 ms elapsed before the presentation of the fixation dot indicating the beginning of the next trial. Participants were informed that, during the intertrial interval, they were allowed to make eye blinks.

Participants performed a total of 10 blocks of 96 experimental trials each. Half of the

participants started with 5 blocks of 1C trials, followed by 5 blocks of 2C trials. This order was reversed for the other half of the participants. Each series of 5 blocks was preceded by 18 to 24 1C or 2C practice trials, depending on which trials participants had to perform in the following blocks. Participants were informed they could take a short break between one block and the next.

2.3 EEG recording and pre-processing

EEG activity was recorded continuously from 64 Ag/AgCl electrodes, positioned according to the 10–10 International system (Sharbrough et al., 1991), using a Neuroscan Curry 8 system (Compumedics USA, Charlotte, NC, USA) set in AC mode and using an electrode located between FPz and Fz as ground. Vertical electrooculogram (VEOG) was recorded from two electrodes positioned 1.5 cm above and below the left eye. Horizontal electrooculogram (HEOG) was recorded from two electrodes positioned on the outer canthi of both eyes. EEG, VEOG, and HOEG signals were band-pass filtered between 0.01 and 30 Hz and digitized at a sampling rate of 1000 Hz. EEG activity was referenced online to an electrode located approximately 1.5 cm posterior to Cz and re-referenced offline to the average value of the left and right mastoids. Continuous EEG was then segmented into 1800 ms long epochs, starting 200 ms before the onset of the cue array and ending 400 ms after search array presentation. Independent component analysis (ICA) was applied to correct EEG activity for eye blinks and eye movements (Jung et al., 1997; see Drisdelle, Aubin, & Jolicœur, 2017, for a detailed description of the method and validation for use with lateralized ERP components). EEG epochs were further screened for remaining artefacts (VEOG deflection > 50 µV within a time window of 150 ms; HEOG deflection > 35 µV within a time window of 300 ms; or signal exceeding ±100 µV anywhere in the epoch). On

2323 average, less than 1% of the epochs were excluded as a result of the application of these
2324 exclusion criteria. EEG epochs were baseline corrected by using the average activity in
2325 the time interval -200–0 ms relative to onset of the cue array. After excluding trials
2326 associated with an incorrect response in the visual search task, EEG epochs were then
2327 averaged to generate ERPs for each set of 1C and 2C trials. For laterally displayed cues,
2328 contralateral ERPs were generated by averaging EEG epochs recorded at PO7 on trials
2329 with cues displayed to the right of fixation and EEG epochs recorded at PO8 on trials
2330 with cues displayed to the left of fixation. Ipsilateral ERPs were generated using the
2331 opposite electrode-side pairings. For cues displayed along the vertical midline, a
2332 bilateral ERP was generated by averaging EEG epochs recorded at PO7 and PO8. The
2333 mean amplitude of the N2pc and of the SPCN elicited by lateral cues was computed by
2334 subtracting the ipsilateral activity from the contralateral activity in a 200–300 ms
2335 interval and in a 360–1100 ms interval, respectively. As in Doro et al. (2020), the mean
2336 amplitude of the N2pcb and of the SPCNb elicited by midline cues was computed by
2337 subtracting the ipsilateral activity elicited by lateral cues from the bilateral activity
2338 elicited by midline cues in the same time-windows as those considered for N2pc and
2339 SPCN amplitude estimation.

2340 EEG data in the N2pc/N2pcb and SPCN/SPCNb time-windows were transformed to
2341 scalp current density (SCD) topographic maps using a spherical spline surface
2342 Laplacian (order of the splines = 4, regularization parameter λ = 1e-5, conductivity of
2343 the skin = 0.33 S/m) (Perrin, Pernier, Bertrand, & Echallier, 1989). We opted for SCD
2344 maps because the SCD approach provides a sharper topography compared to spline-
2345 interpolated maps of voltage intensity by reducing blurring effects of volume
2346 conduction on the scalp-recorded EEG voltage signal (Pernier, Perrin, & Bertrand,
2347 1988). In particular, SCD maps provide reference-free mapping of scalp-recorded

electrical activity, thus rendering ERP polarity unambiguous. The SCD approach to scalp topography does not makes any assumptions about the neuroanatomy or about the number, orientation, or independence of the underlying neuronal generators. The sign of these estimates directly reflects the direction of the global radial currents underlying the EEG topography, with positive values representing current flow from the brain towards the scalp, and negative values representing current flow from the scalp into the brain.

All statistical analyses were performed with R (R Development Core Team, 2017), using the ezANOVA function of the 'ez' package (Lawrence, 2011) and the anovaBF/ttestBF function of the 'BayesFactor' package (Rouder & Morey, 2012), which includes the Jeffreys-Zellner-Siow (JZS) default prior on effect sizes (Rouder, Morey, Speckman, & Province, 2012). Greenhouse-Geisser correction for non-sphericity was applied when appropriate (Jennings & Wood, 1976), and all comparisons via t-test were Bonferroni-corrected.

3. Results

3.1 Behavior

Reaction times (RTs) recorded on trials associated with an incorrect response and/or RTs exceeding three standard deviations above/below individual mean RT (1.1%) were excluded from analysis. A summary of the behavioral results in the visual search task is illustrated in Figure 6-2.

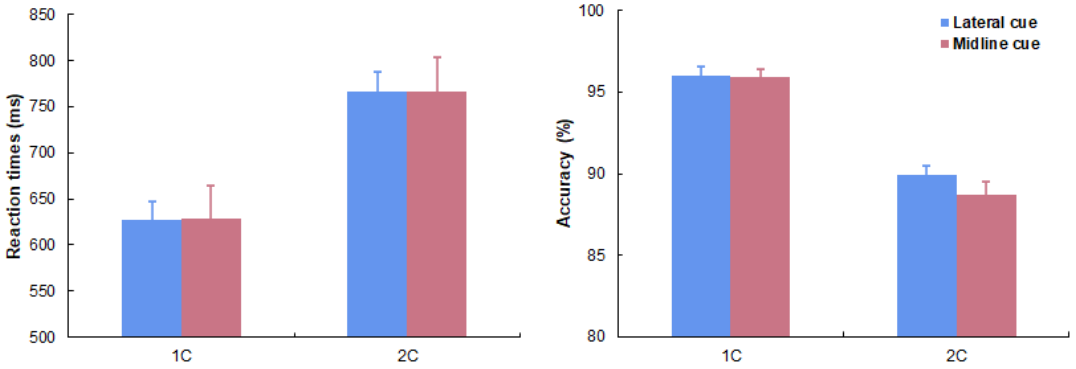

Figure 6-2 Mean RT (left panel) and mean percentage of correct responses (right panel) in the visual search task plotted as a function of memory load (1C vs. 2C) and cue position (lateral vs. midline). Error bars represent standard error of the mean.

Mean RTs and the mean percentage of correct responses were submitted to a 2 × 2 ANOVA considering memory load (1C vs. 2C) and cue position (lateral vs. midline) as within-subject factors. RTs were generally shorter on 1C than 2C trials ($F(1, 20) = 36.8$, $p < .001$, $\eta_p^2 = .648$). RTs were unaffected by cue position, or by the interaction between cue position and memory load (max $F = 0.4$ min $p = 0.5$). Participants were more accurate on 1C than 2C trials ($F(1, 20) = 114.1$, $p < .001$, $\eta_p^2 = .851$), and more accurate with lateral than midline cues ($F(1, 20) = 5.0$, $p = .036$, $\eta_p^2 = .201$). Although the effect of cue position appeared to be confined to 2C trials, the interaction between cue position and memory load fell just short of significance ($F(1, 20) = 3.3$, $p = .086$, $\eta_p^2 = .140$).

3.2 ERPs

3.2.1 SPCN and SPCNb

Figure 6-3 illustrates grand-average contralateral and ipsilateral ERP waveforms recorded at PO7/8 elicited by lateral cues and ERP waveforms elicited by midline cues that was generated by averaging EEG epochs recorded at the same recording sites.

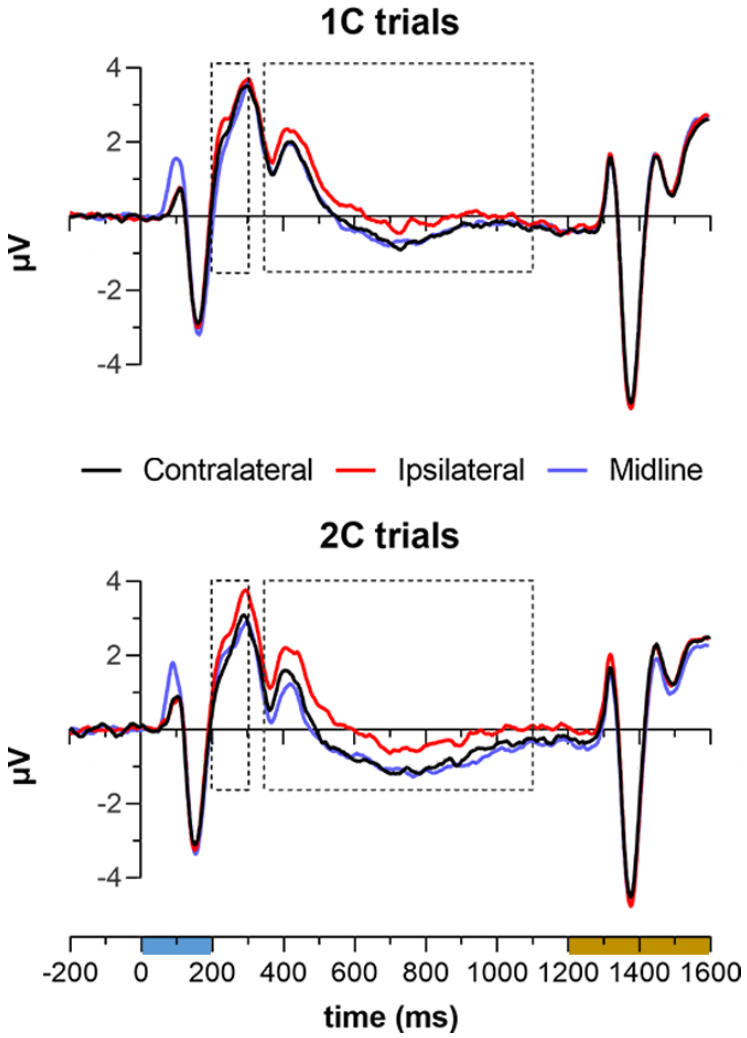

Figure 6-3 ERPs elicited at electrodes PO7/8 on 1C (top) and 2C (bottom) trials. Color bars on the timeline indicate the exposure duration of the cue array (cyan) and of the search array (dark orange). The areas delimited by the dashed-line rectangles in both graphs indicate the time-windows considered for ERP amplitudes estimation. Negative is plotted down in this and following ERP graphs.

Visual inspection of Figure 6-3 makes apparent — in the SPCN/SPCNb time-window (360–1100 ms) — the substantial overlap of ERPs contralateral to lateral cues (black functions in Figure 6-3) and the ERPs to midline cues (blue functions in Figure 6-3) on both 1C and 2C trials. Furthermore, the comparison between both contralateral and midline ERPs and ipsilateral ERPs to lateral cues (red functions in Figure 6-3) suggests that both SPCN and SPCNb increased in amplitude as the number of cues was increased. This is more evident in Figure 6-4, where difference ERPs are plotted. Recall

2400 that the amplitude of SPCN was calculated in the standard way by subtracting ipsilateral
2401 from contralateral ERP activity elicited by lateral cues. The amplitude of SPCNb was
2402 calculated by subtracting ipsilateral ERPs for lateral cues from the average of ERPs at
2403 PO7 and PO8 for midline targets.

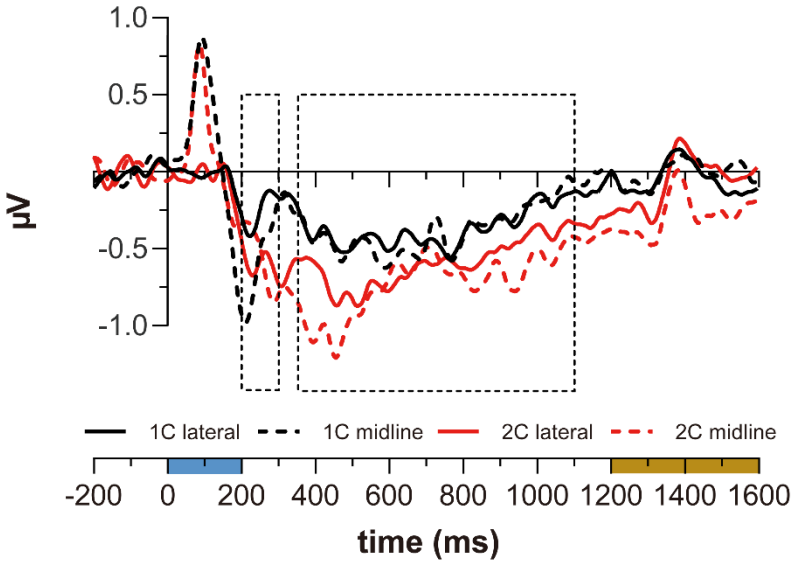

2404

2405 **Figure 6-4** Difference ERPs on 1C and 2C trials. The areas delimited by the dashed-
2406 line rectangles in the graph indicate the time-windows considered for ERP amplitudes
2407 estimation. SPCN activity is represented by solid-line ERP functions and SPCNb by
2408 dashed-line ERP functions. SPCN and SPCNb activity recorded on 1C trials is
2409 represented by black ERP functions and SPCN/SPCNb activity recorded on 2C trials is
2410 represented by red ERP functions. ERP functions were low-pass filtered at 15 Hz for
2411 visualization purposes.

2412 These observations were corroborated by statistical analysis. The amplitude values
2413 recorded in the SPCN/SPCNb time-window were first separately submitted to t-test to
2414 determine whether they differed from 0 μV. SPCN amplitude was significant for both
2415 1C (-0.38 μV; $t(20) = -4.1$, $p < .001$) and 2C trials (-0.60 μV; $t(20) = -5.8$, $p < .001$).
2416 Similarly, SPCNb amplitude was significant for both 1C (-0.39 μV; $t(20) = -4.39$, p
2417 $< .001$) and 2C trials (-0.73 μV; $t(20) = -5.19$ $p < .001$).

2418 These amplitude values were then submitted to a 2 × 2 ANOVA with memory load

(1C vs. 2C) and cue position (lateral vs. midline) as within-subject factors. The analysis detected a main effect of memory load ($F(1, 20) = 7.9$, $p = .011$, $\eta_p^2 = .283$), and no other factor effects (max $F = 0.9$; min $p = 0.4$). Given that the null effects of cue position and of an interaction between cue position and memory load were critical to support our hypothesis of an amplitude equivalence of SPCN and SPCNb, Bayes factors (BF_{01}) were estimated using mixed-effect models in which participants were treated as an additional random factor. A Type 2 approach was adopted to not violate the principle of marginality (Nelder, 1977). The BF_{01} parameter approximates the probability that a given null effect or interaction is truly absent relative to the alternative hypothesis of the presence of such effects. A BF01 value ranging from 1 to 3 is usually taken to imply that the probability of the (possibly undetected) presence of such effects in the statistical comparison between SPCN and SPCNb is minimal/anedoctal. The BF01 was 3.13 for the effect of cue position and 2.83 for the interaction of cue position and memory load. These results provide critical support for the statistical equivalence of SPCN and SPCNb amplitudes on 1C and 2C trials.

3.2.2 N2pc and N2pcb

The present design allowed us to test whether the results of Doro et al. (2020) with reference to the amplitude equivalence of N2pc (lateral targets) and N2pcb (midline targets) could be replicated. The ERP results illustrated in Figures 3 and 4 do suggest that this might be the case. As for SPCN/SPCNb, the amplitude values recorded in the N2pc/N2pcb time-window (see Figure 6-4) were first separately submitted to t-test to inspect whether each of these values differed from 0 µV. N2pc amplitude was only marginally significantly different from 0 µV in 1C trials (-0.27 µV; $t(20) = -1.93$, $p = .07$), but was clearly present in 2C trials (-0.61 µV; $t(20) = -4.29$, $p < .001$). N2pcb

amplitude was significant in both 1C trials (-0.61 μV; $t(20) = -4.23$, $p < .001$) and 2C trials (-0.56 μV; $t(20) = -2.50$, $p = .02$).

These amplitude values were then submitted to a 2 × 2 ANOVA with memory load (1C vs. 2C) and cue position (lateral vs. midline) as within-subject factors. The analysis detected a significant interaction between memory load and cue position ($F(1, 20) = 4.8$, $p = .040$, $\eta_p^2 = .195$), which was most likely driven by the smaller N2pc in 1C trials. Further planned comparisons showed that the amplitude of N2pcb was greater than that of N2pc on 1C trials (-0.61 μV vs. -0.27 μV; $t(20) = 2.3$, $p = .035$), whereas no amplitude difference between N2pc and N2pcb was found in 2C trials (-0.61 μV vs. -0.56 μV; $t(20) = -0.3$, $p = .797$). Although we do not have an explanation for the minimal N2pc activity (vis-a-vis the clear presence of N2pcb activity) on 1C trials, when collectively taken these results support and reinforce Doro's et al. (2020) hypothesis of the existence of N2pcb activity elicited by midline cues. Visual inspection of the results illustrated in Figure 2 by Carlisle et al. (2011; Experiment 1, p. 9317) suggests that even in their case N2pc for one lateral cue was smaller in amplitude than N2pc for two lateral cues. Given it was outside the scope of their work, however, N2pc amplitude was not quantified and/or analyzed by Carlisle et al. (2011), and future work may profitably be addressed to investigate this interesting analogy between the present and Carlisle's et al. results.

3.2.3 N2pcb and SPCNb for upper and lower visual hemifield cues

On the hypothesis of similar sources of N2pcb and SPCNb — and, indirectly, of N2pc and SPCN — one would expect SPCNb to share with N2pcb the property described by Monnier et al. (2020) to be fully-fledged in response to task-relevant information displayed in the lower visual hemifield and absent, or even reversed in

polarity, in response to task-relevant information displayed in the upper visual hemifield.

The difference ERP waveforms, collapsed across 1C and 2C trials, elicited by midline cues displayed in the upper and lower visual hemifields are shown in Figure 6-5.

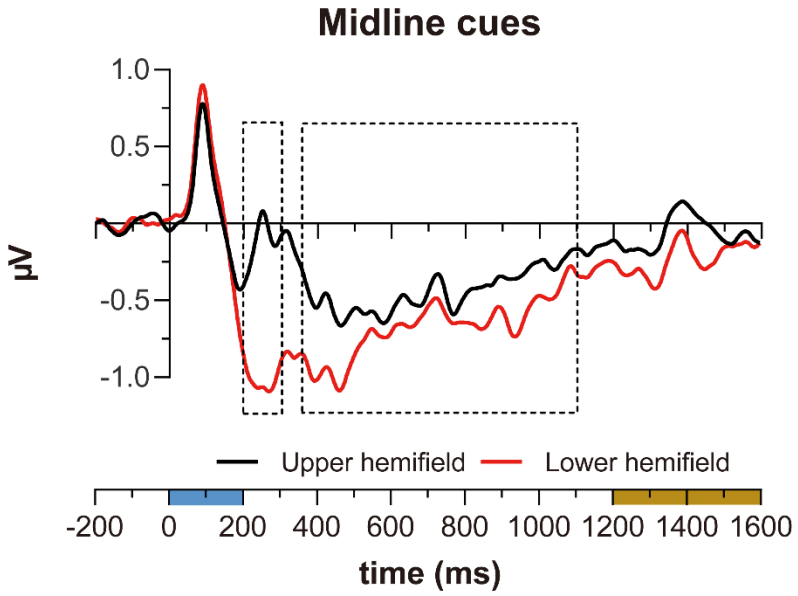

Figure 6-5 N2pcb and SPCNb difference waveforms for midline cues presented in the upper (black function) and lower (red function) hemifields. The area indicated by the dashed-line rectangles in the graph represents the time window considered for ERP amplitude analyses. ERP functions were low-pass filtered at 15 Hz for visualization purposes.

As Figure 6-5 suggests, N2pcb amplitude variations were strongly modulated by cue vertical elevation, as reported by Monnier et al. (2020). N2pcb was clearly larger for cues displayed in the lower visual hemifield and basically absent for cues displayed in the upper visual hemifield. In contrast, SPCNb for cues displayed in the upper visual hemifield, though seemingly reduced in amplitude compared to SPCNb for cues displayed in the lower visual hemifield, was nonetheless clearly evident. The amplitude values of N2pcb and SPCNb were submitted to a 2 × 2 ANOVA with visual hemifield

(upper vs. lower) and component (N2pcb vs. SPCNb) as within-subject factors. The analysis revealed a significantly larger amplitude for SPCNb than N2pcb ($F(1, 20) = 25.9$, $p < .001$, $\eta_p^2 = .564$) and, more importantly, a significant interaction between component and visual hemifield ($F(1, 20) = 56.3$, $p < .001$, $\eta_p^2 = .738$). Planned comparisons confirmed that, for cues displayed in the upper visual hemifield, N2pcb amplitude did not differ from 0 μV (−.12 μV; $t(20) = -.8$, $p = .452$) whereas SPCNb amplitude did (−.44 μV; $t(20) = -3.7$, $p = .001$). In contrast, N2pcb and SPCNb were both significant for lower-hemifield targets (−1.05 and −.67 μV; $t(20) = -5.6$, $p < .001$ and $t(20) = -7.5$, $p < .001$, respectively).

Hints to a possible cause of the different behavior of N2pcb and SPCNb in response to cues displayed in the upper and lower visual hemifields can be inferred from the topographical maps reported in Figure 6-6.

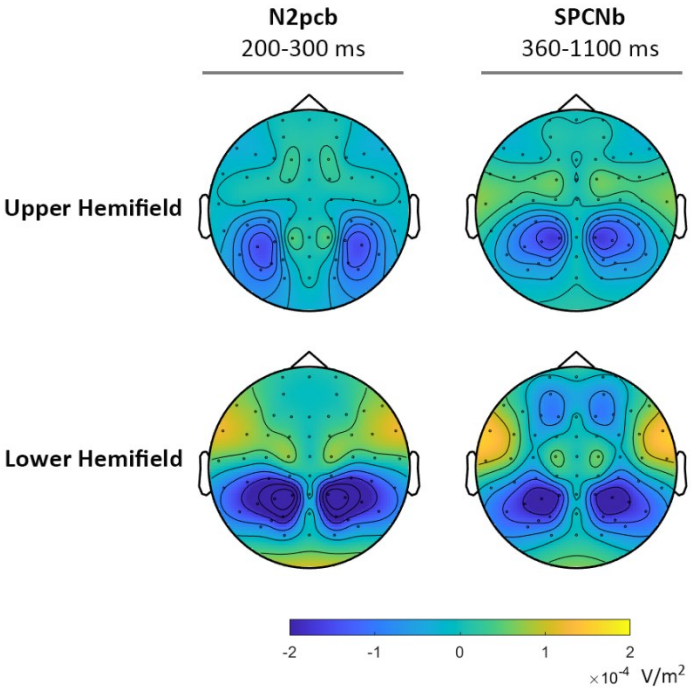

Figure 6-6. Scalp current density (SCD) maps of N2pcb (left) and SPCNb (right) difference waveforms for midline cues presented in the upper and lower hemifields. The components are plotted mirrored in both the hemiscalps.

By comparing the peak of the current densities elicited by cues displayed in the upper visual hemifield, the impression is that the density peak of N2pcb activity is slightly more lateral/ventral in comparison to SPCNb, whose density peak is more dorsal and closer to the mid-scalp. As argued in the Introduction, EEG signals originating from dorsal regions are easier to detect because closer to the scalp, and this may explain why SPCNb activity, though reduced in amplitude, could still be detected whereas N2pc activity was abolished for cues displayed in the upper visual hemifield. Given however the notoriously complex nature of the relationship between the scalp distribution of EEG signal and the brain location of its neural source(s), this explanation must be taken with caution. It is nonetheless worth of mention that the present topographical results dovetail nicely with source localization analyses of MEG signal reported by Becke et al. (2015), Hopf et al. (2000, 2002, 2006), Jolicœur et al. (2011), and Robitaille et al. (2010) that converged to locate the source of SPCN activity in dorso-parietal cortical regions and the source of N2pc activity in ventro-lateral cortical regions.

6.4 Discussion

To summarize, we showed that to-be-memorized visual cues displayed along the vertical midline elicited a bilateral SPCN, or SPCNb, whose amplitude was identical to the SPCN elicited by visual cues displayed laterally relative to the vertical meridian. Confirming a prototypical property of SPCN, both SPCN and SPCNb increased in amplitude as the number of cues was increased from one (on 1C trials) to two (on 2C

trials). This pattern of results suggest that a) SPCNb does exist as a distinguishable ERP component and that b) SPCNb reacts to variations in visual working memory load memory in a similar way to SPCN. Behaviorally, RTs were faster and accuracy was higher when visual search was guided by one cue than two cues, but apart from a slight drop in accuracy when search was guided by two midline cues, search performance was generally unaffected by the spatial arrangement of the cues in the leading cue array. Furthermore, we compared amplitude modulations of SPCNb and N2pcb as a function of the vertical elevation of midline cues, and discovered a dissociation between these two ERP components. Like N2pc, N2pcb was absent when midline cues were displayed in the upper visual hemifield (i.e., above fixation), and was present and particularly pronounced when midline cues were displayed in the lower visual hemifield (i.e., below fixation) (Bacigalupo & Luck, 2019; Doro et al., 2020; Luck et al., 1997; Monnier et al., 2020). In contrast, when midline cues were displayed in the upper visual field, SPCNb was reduced in amplitude — but still clearly present — relative to SPCNb for midline cues displayed in the lower visual field. This finding was complemented by a comparison of N2pcb and SPCNb based on SCD topography, which suggested a more dorsal distribution of SPCNb activity and a more latero-ventral distribution of N2pcb activity. We interpret this pattern of results as consistent with results from MEG explorations of N2pc and SPCN (Becke et al., 2015; Hopf et al., 2000, 2002, 2006; Jolicœur et al., 2011; Robitaille et al., 2010), that pointed to a prominent involvement of the lateral occipital complex (LOC) and infero-temporal (IT) cortex in the generation of N2pc/N2pcb activity and of the intra-parietal sulcus (IPS) in the generation of SPCN/SPCNb activity (see, for fMRI evidence, Brigadoi et al., 2017; Duma et al., 2019; Jolicœur et al., 2011; Naughtin et al., 2016; Robitaille et al., 2010; Todd & Marois, 2004; Xu & Chun, 2006).

Two issues deserve a comment with reference to the present ERP findings. One issue pertains to a possible methodological concern related to the fact that we calculated N2pc and SPCN amplitude for laterally displayed visual cues by subtracting (ipsilateral from contralateral) ERP activity, that is, ERP activity that, though from different electrodes, was recorded on the same trials. N2pcb and SPCNb amplitude for midline cues was calculated using a different approach, by subtracting ERP activity that was recorded on different trials (ipsilateral to lateral cues from bilaterally averaged to midline cues). As we have already claimed in Doro et al. (2020), this choice relies on the assumption that ipsilateral activity for laterally displayed stimuli is relatively invariant to factors' manipulations that exert modulatory effects on N2pc/N2pcb and SPCN/SPCNb amplitude (and latency), implicating that such effects are reflected in modulations of the contralateral portion of these ERP components. As far as N2pc/N2pcb activity is concerned, we provided a comprehensive overview of studies supporting this assumption in Doro et al. (2020), in all of which ipsilateral activity to lateral stimuli in the N2pc time-window remained largely invariant across a number of manipulations affecting the contralateral portion of N2pc. This was the case for manipulations affecting target color (Luck, Fuller, Braun, Robinson, Summerfelt, & Gold, 2006), target vs. nontarget feature selection (Luck & Hillyard, 1994), target position relative to the horizontal midline (Luck et al., 1997; Perron et al., 2009), target numerosity (Benavides-Varela et al., 2018; Mazza & Caramazza, 2011), and target selection difficulty (Luck et al., 1997).

As far as SPCN/SPCNb activity is concerned, we felt even more confident in treating ipsilateral activity as a common baseline for SPCN and SPCNb amplitude calculation based on the flood of work showing that ipsilateral activity is largely unaffected by manipulations of the number of to be memorized visual stimuli in the paradigm used

here (cued visual search paradigms; Carlisle et al., 2011), as well as in other paradigms like change detection (see Luria et al., 2016, for a comprehensive and detailed overview), multiple object tracking (MOT; when no moving objects crossed the vertical midline, see below; Drew, Horowitz, & Vogel, 2013; Drew & Vogel, 2008), and in feature conjunction/grouping paradigms (Luria & Vogel, 2011). To our knowledge, the only exception to the ipsilateral activity invariance in the SPCN/SPCNb time-range is the tendency of ipsilateral activity to become progressively more negative when the retention interval (i.e., the time elapsing from the offset of to-be-memorized visual stimuli to the onset of the event probing visual working memory efficiency) is longer than 1 s (McCollough, Machizawa, & Vogel, 2007). Our retention interval was 1 s, and the ipsilateral ERP activity plotted in Figure 3 in the selected time-window (360–900 ms from the onset of the cue array) did not appear to be deflected towards the negative polarity to such an extent as to determine SPCN/SPCNb amplitude.

Note however that the assumption of invariance of ipsilateral activity is not necessarily in opposition to the hypothesis that such activity reflects some form of suppression/inhibition of ipsilateral stimuli, as originally put forth by Hickey, Di Lollo, and McDonald (2009) for N2pc. An equally plausible stance — which is also in line with current empirical evidence on the role of suppression during visual encoding — is that stimuli falling in the ipsilateral visual hemifield are just suppressed as a single chunk, irrespective of their number and other physical attributes, provided no feature overlap or a particularly pronounced salience disparity is present between target and distractors (Gaspar, Christie, Prime, Jolicœur, & McDonald, 2016; Gaspelin & Luck, 2018, 2019).

In the Introduction, we mentioned that the receptive fields of extrastriate visual

neurons extend into the ipsilateral visual hemifield for as much as 2°. This calls for a clarification concerning the horizontal extension of the area covered by overlapping receptive fields of visual neurons located in each cerebral hemisphere. Certainly, this bilaterally represented area includes the vertical midline, but its lateral extension has been shown to vary considerably based on participants' expectation. One of the most convincing demonstration of this has been provided by Drew, Mance, Horowitz, Wolfe, and Vogel (2014), who instructed participants to first select a static object that was temporarily cued by a color and then to covertly track it when the object started moving. SPCN component, whose amplitude correlates with the number of objects tracked at any one time in the contralateral visual hemifield, was monitored in order to understand how an object moving in a lateral direction and crossing the vertical midline was represented in the posterior cerebral hemispheres. In one of their experiments, one laterally moving object eventually crossed the vertical midline on each trial. The SPCN recorded from the hemisphere contralateral to the starting position of this moving object decreased in amplitude (i.e., stopped tracking the moving object) only after the object was 2° past the vertical midline, whereas SPCN activity recorded from the ipsilateral hemisphere started to increase in amplitude (i.e., started to track the moving object) 1.2° before the object crossed the vertical midline. Interestingly, in another experiment, the event of a lateral object crossing the vertical meridian occurred only on a random 25% of trials. In this condition, the SPCN recorded from the hemisphere contralateral to the starting position of the moving object showed the same response as that in the previous experiment, but signs of SPCN activity in the ipsilateral hemispheres started to be detected when the object was almost 3° past the vertical midline. The interpretation of these results offered by the authors was one according to which the extension of the area of overlapping activity of the cerebral hemispheres is not

structurally determined, but changes dynamically as a function of the participants' attentional set. These results are of clear relevance in the present context. Although in our paradigm midline cue(s) were displayed on a random 50% of trials, they were perfectly aligned to the vertical midline, a segment of the visual field that is structurally bound to be always represented by both cerebral hemispheres. However, it is important to underline that our expectations and/or attentional set can dynamically change the way in which the integration of separate visual hemifields occurs and to what extent, a property that we could not capture in the present study and that certainly warrants further investigation. Incidentally, one neural model that provides an explanation of how dynamic changes in the size of receptive fields may be possible is that of Lamme and Roelfsema (2000), who proposed that one effect of reentrant activity from frontal to more posterior regions is to expand local sensory circuits by coaxing visual neurons that did not contribute to the initial feedforward volley of activation upon stimulus presentation.

In conclusion, we were able to elicit a bilateral SPCN, the SPCNb, analogously to what we did with the bilateral N2pc (N2pcb; Doro et al., 2020; Monnier et al., 2020). We showed that this SPCNb was modulated in the same way as a typical SPCN, namely, showing an increase in amplitude as the number of to-be-memorized objects was increased. Comparisons of ERP modulations induced by the position of the to-be-remembered items (lateral vs. midline, upper vs. lower hemifield), as well as the number of cues to be memorized, allowed us to distinguish the N2pc/N2pcb from the SPCN/SPCNb. Because SPCN/SPCNb amplitude was not reduced to nil nor reversed in polarity when objects to remember were displayed in the upper visual field, contrary to the N2pc/N2pcb, our results are more compatible with models positing these two components have partially overlapping albeit distinct neural sources.

6.5 References

Bacigalupo, F., & Luck, S. J. (2019). Lateralized suppression of alpha-band EEG activity as a mechanism of target processing. *Journal of Neuroscience, 39*(5), 900–917. https://doi.org/10.1523/JNEUROSCI.0183-18.2018

Balaban, H., Fukuda, K., & Luria, R. (2019). What can half a million change detection trials tell us about visual working memory? *Cognition, 191*, 103984. https://doi.org/10.1016/j.cognition.2019.05.021

Becke, A., Müller, N., Vellage, A., Schoenfeld, M. A., & Hopf, J.-M. (2015). Neural sources of visual working memory maintenance in human parietal and ventral extrastriate visual cortex. *NeuroImage, 110*, 78–86. https://doi.org/10.1016/j.neuroimage.2015.01.059

Benavides-Varela, S., Basso Moro, S., Brigadoi, S., Meconi, F., Doro, M., Simion, F., Sessa, P., Cutini, S., & Dell'Acqua, R. (2018). N2pc reflects two modes for coding the number of visual targets. *Psychophysiology, 55*(11), e13219. https://doi.org/10.1111/psyp.13219

Brigadoi, S., Cutini, S., Meconi, F., Castellaro, M., Sessa, P., Marangon, M., Bertoldo, A., Jolicœur, P., & Dell'Acqua, R. (2017). On the role of the inferior intraparietal sulcus in visual working memory for lateralized single-feature objects. *Journal of Cognitive Neuroscience, 29*(2), 337–351. https://doi.org/10.1162/jocn_a_01042

Carlisle, N. B., Arita, J. T., Pardo, D., & Woodman, G. F. (2011). Attentional templates in visual working memory. *Journal of Neuroscience, 31*(25), 9315–

9322. https://doi.org/10.1523/JNEUROSCI.1097-11.2011

Cowan, N. (2001). The magical number 4 in short-term memory: A reconsideration of mental storage capacity. *Behavioral and Brain Sciences, 24*(1), 87–114. https://doi.org/10.1017/S0140525X01003922

Doro, M., Bellini, F., Brigadoi, S., Eimer, M., & Dell'Acqua, R. (2020). A bilateral N2pc (N2pcb) component is elicited by search targets displayed on the vertical midline. *Psychophysiology, 57*(3), e13512. https://doi.org/10.1111/psyp.13512

Eimer, M. (1996). The N2pc component as an indicator of attentional selectivity. *Electroencephalography and Clinical Neurophysiology, 99*(3), 225–234. https://doi.org/10.1016/0013-4694(96)95711-9

Drew, T., & Vogel, E. K. (2008). Neural measures of individual differences in selecting and tracking multiple moving objects. *Journal of Neuroscience, 28*(16), 4183–4191. http://doi.org/10.1523/JNEUROSCI.0556-08.2008

Drew, T., Horowitz, T. S., & Vogel, E. K. (2013). Swapping or dropping? Electrophysiological measures of difficulty during multiple object tracking. *Cognition 126*(2), 213–223. http://doi.org/10.1016/j.cognition.2012.10.003.

Drew, T., Mance, I., Horowitz, T. S., Wolfe, J. M., & Vogel, E. K. (2014). A soft handoff of attention between cerebral hemispheres. *Current Biology, 24*(10), 1133–1137. https://doi.org/10.1016/j.cub.2014.03.054

Drisdelle, B. L., Aubin, S., & Jolicœur, P. (2017). Dealing with ocular artifacts on lateralized ERPs in studies of visual-spatial attention and memory: ICA correction versus epoch rejection. *Psychophysiology, 54*(1), 83–99.

https://doi.org/10.1111/psyp.12675

Duma, G. M., Mento, G., Cutini, S., Sessa, P., Baillet, S., Brigadoi, S., & Dell'Acqua, R. (2019). Functional dissociation of anterior cingulate cortex and intraparietal sulcus in visual working memory. *Cortex, 121*, 277–291. https://doi.org/10.1016/j.cortex.2019.09.009

Eimer, M. (2014). The neural basis of attentional control in visual search. *Trends in Cognitive Sciences, 18*(10), 526–535. https://doi.org/10.1016/j.tics.2014.05.005

Emrich, S. M., Al-Aidroos, N., Pratt, J., & Ferber, S. (2009). Visual search elicits the electrophysiological marker of visual working memory. *PLoS One 4*(11), e8042. http://dx.doi.org/10.1371/journal.pone.0008042

Feldmann-Wüstefeld, T., & Schubö, A. (2015). Target discrimination delays attentional benefit for grouped contexts: An ERP study. *Brain Research, 1629*, 196–209. https://doi.org/10.1016/j.brainres.2015.10.018

Gaspar, J. M., Christie, G. J., Prime, D. J., Jolicœur, P., & McDonald, J. J. (2016). Inability to suppress salient distractors predicts low visual working memory capacity. *Proceedings of the National Academy of Sciences (USA), 113*(13), 3693–3698. https://doi.org/10.1073/pnas.1523471113

Gaspelin, N., & Luck, S. J. (2018). The role of inhibition in avoiding distraction by salient stimuli. *Trends in Cognitive Sciences, 22*(1), 79–92. https://doi.org/10.1016/j.tics.2017.11.001

Gaspelin, N., & Luck, S. J. (2019). Inhibition as a potential resolution to the

attentional capture debate. *Current Opinion in Psychology, 29*, 12–18. https://doi.org/10.1016/j.copsyc.2018.10.013

Henderson, J. M. (2008). Eye movements and visual memory. In S. J. Luck & A. Hollingworth (Eds.), *Visual Memory* (pp. 87–121). New York (NY): Oxford University Press. https://doi.org/ 10.1093/acprof:oso/9780195305487.001.0001

Hickey, C., Di Lollo, V., & McDonald, J. J. (2009). Electrophysiological indices of target and distractor processing in visual search. *Journal of Cognitive Neuroscience, 21*(4), 760–775. https://doi.org/10.1162/jocn.2009.21039

Hillyard, S. A., & Picton, T. W. (1987). Electrophysiology of cognition. In F. Plum (Ed.), *Handbook of Physiology: Sec. 1. The nervous system: Vol. 5. Higher functions of the brain, Part 2* (pp. 519–584). Bethesda (MD): Waverly Press. https://doi.org/10.1001/archneur.1960.03840090124020

Hollingworth, A., Richard, A. M., & Luck, S. J. (2008). Understanding the function of visual short-term memory: Transsaccadic memory, object correspondence, and gaze correction. *Journal of Experimental Psychology: General, 137*(1), 163–181. https://doi.org/10.1037/0096-3445.137.1.163

Hopf, J.-M., Boelmans, K., Schoenfeld, A. M., Heinze, H. J., & Luck, S. J. (2002). How does attention attenuate target-distractor interference in vision? Evidence from magnetoencephalographic recordings. *Cognitive Brain Research, 15*(1), 17–29. https://doi.org/10.1016/S0926-6410(02)00213-6

Hopf, J.-M., Luck, S. J., Boelmans, K., Schoenfeld, M. A., Boehler, C. N., Rieger, J.,

& Heinze, H. (2006). The neural site of attention matches the spatial scale of perception. *Journal of Neuroscience, 26*(13), 3532–3540. https://doi.org/10.1523/ JNEUROSCI.4510-05.2006

Hopf, J.-M., Luck, S. J., Girelli, M., Hagner, T., Mangun, G. R., Scheich, H., & Heinze, H. J. (2000). Neural sources of focused attention in visual search. *Cerebral Cortex, 10*(12), 1233–1241. https://doi.org/10.1093/cercor/10.12.1233

Hubel, D. H., & Wiesel, T. N. (1967). Cortical and callosal connections concerned with the vertical meridian of visual fields in the cat. *Journal of Neurophysiology, 30*(6), 1561–1573. https://doi.org/10.1152/jn.1967.30.6.1561

Jennings, J., & Wood, C. (1976). The e-adjustment procedure for repeated-measures analyses of variance. *Psychophysiology, 13*(3), 277–278. https://doi.org/10.1111/j.1469-8986.1976.tb00116.x

Jolicœur, P., Brisson, B., & Robitaille, N. (2008). Dissociation of the N2pc and sustained posterior contralateral negativity in a choice response task. *Brain Research, 1215*, 160–172. https://doi.org/10.1016/j.brainres.2008.03.059

Jolicœur, P., Dell'Acqua, R., Brisson, B., Robitaille, N., Sauvé, K., Leblanc, É., Prime, D. J., Grimault, S., Marois, R. Sessa, P., Grova, C., Lina, J.-M. & Dubarry, A.-S. (2011). Visual spatial attention and visual short-term memory: Electromagnetic explorations of mind. In V. Coltheart (Ed.), *Tutorials in Visual Cognition* (pp. 143–185). Hove (UK): Psychology Press. https://doi.org/10.4324/9780203847305

Jung, T.-P., Humphries, C., Lee, T. W., Makeig, S., McKeown, M., Iragui, V., & Sejnowski, T. J. (1997). Extended ICA removes artifacts from electroencephalographic recordings. *Advances in neural information processing systems, 10*, 894–900.

Klaver, P., Talsma, D., Wijers, A. A., Heinze, H. J., & Mulder, G. (1999). An event-related brain potential correlate of visual short-term memory. *NeuroReport 10*(10), 2001–2005. https://doi.org/10.1097/00001756-199907130-00002

Lamme, V. A. F., & Roelfsema, P. R. (2000). The distinct modes of vision offered by feedforward and recurrent processing. *Trends in Neurosciences, 23*(11), 571–579. https://doi.org/10.1016/S0166-2236(00)01657-X

Lawrence, M. (2011). *ez: Easy analysis and visualization of factorial experiments*. Computer Software Manual (R Package Version 3.0-0).

Luck, S. J. (2012). Electrophysiological correlates of the focusing of attention within complex visual scenes: N2pc and related ERP components. In Luck S. J. & Kappenman E. S. (Eds.), *The Oxford Handbook of Event-Related Potential Components* (pp. 329–360). New York (NY): Oxford University Press. https://doi.org/10.1093/oxfordhb/9780195374148.001.0001

Luck, S. J., & Hillyard, S. (1994). Electrophysiological correlates of feature analysis during visual search. *Psychophysiology, 31*(3), 291–308. https://doi.org/10.1111/j.1469-8986.1994.tb02218.x

Luck, S. J., & Vogel, E. K. (2013). Visual working memory capacity: From psychophysics and neurobiology to individual differences. *Trends in Cognitive*

Sciences, 17(8), 391–400. http://dx.doi.org/10.1016/j.tics.2013.06.006

Luck, S. J., Fuller, R. L., Braun, E. L., Robinson, B., Summerfelt, A., & Gold, J. M. (2006). The speed of visual attention in schizophrenia: Electrophysiological and behavioral evidence. *Schizophrenia Research, 85*(1-3), 174–195. https://doi.org/10.1016/j.schres.2006.03.040

Luck, S. J., Girelli, M., McDermott, M. T., & Ford, M. A. (1997). Bridging the gap between monkey neurophysiology and human perception: An ambiguity resolution theory of visual selective attention. *Cognitive Psychology, 33*(1), 64–87. https://doi.org/10.1006/cogp.1997.0660

Luria, R., & Vogel, E. K. (2011). Shape and color conjunction stimuli are represented as bound objects in visual working memory. *Neuropsychologia, 49*(6), 1632–1639. http://doi.org/10.1016/j.neuropsychologia.2010.11.031

Luria, R., Balaban, H., Awh, E., & Vogel, E. K. (2016). The contralateral delay activity as a neural measure of visual working memory. *Neuroscience & Biobehavioral Reviews, 62*, 100–108. https://doi.org/10.1016/j.neubiorev.2016.01.003

Mazza, V., & Caramazza, A. (2011). Temporal brain dynamics of multiple object processing: The flexibility of individuation. *PLoS One, 6*(2), e17453. https://doi.org/10.1371/journal.pone.0017453

Mazza, V., Turatto, M., & Caramazza, A. (2009). Attention selection, distractor suppression and N2pc. *Cortex, 45*(7), 879–890. https://doi.org/10.1016/j.cortex.2008.10.009

McCollough, A. W., Machizawa, M. G., & Vogel, E. K. (2007). Electrophysiological measures of maintaining representations in visual working memory. *Cortex, 43*(1), 77–94. https://doi.org/10.1016/S0010-9452(08)70447-7

Monnier, A., Dell'Acqua, R., & Jolicœur, P. (2020). Distilling the distinct contralateral and ipsilateral attentional responses to lateral stimuli and the bilateral response to midline stimuli for upper and lower visual hemifield locations. *Psychophysiology, 57*(11), e13651. https://doi.org/10.1111/psyp.13651

Nakamura, H., Chaumon, M., Klijn, F., & Innocenti, G. M. (2007). Dynamic properties of the representation of the visual field midline in the visual areas 17 and 18 of the ferret (Mustela putorius). *Cerebral Cortex, 18*(8), 1941–1950. https://doi.org/10.1093/cercor/bhm221

Naughtin, C. K., Mattingley, J. B., & Dux, P. E. (2016). Distributed and overlapping neural substrates for object individuation and identification in visual short-term memory. *Cerebral Cortex, 26*(2), 566–575. https://doi.org/10.1093/cercor/bhu212

Nelder, J. A. (1977). A reformulation of linear models. *Journal of the Royal Statistical Society, 140*(1), 48–77. https://doi.org/10.2307/2344517

Pagano, S., & Mazza, V. (2012). Individuation of multiple targets during visual enumeration: New insights from electrophysiology. *Neuropsychologia, 50*(5), 754–761. https://doi.org/10.1016/j.neuropsychologia.2012.01.009

Papaioannou, O., & Luck, S. J. (2020). Effects of eccentricity on the attention-related

N2pc component of the event-related potential waveform. *Psychophysiology, 57*(5), e13532. https://doi.org/10.1111/psyp.13532

Pernier, J., Perrin, F., & Bertrand, O. (1988). Scalp current density fields: Concept and properties. *Electroencephalography and Clinical Neurophysiology, 69*(4), 385–389. https://doi.org/10.1016/0013-4694(88)90009-0

Perrin, F., Pernier, J., Bertrand, O., & Echallier, J. F. (1989). Spherical splines for scalp potential and current density mapping. *Electroencephalography and clinical neurophysiology, 72*(2), 184–187. https://doi.org/10.1016/0013-4694(89)90180-6

Perron, R., Lefebvre, C., Robitaille, N., Brisson, B., Gosselin, F., Arguin, M., & Jolicœur, P. (2009). Attentional and anatomical considerations for the representation of simple stimuli in visual short-term memory: Evidence from human electrophysiology. *Psychological Research, 73*(2), 222–232. https://doi.org/10.1007/s00426-008-0214-y

Pratt, H. (2012). Sensory ERP components. In Luck S. J. & Kappenman E. S. (Eds.), *The Oxford Handbook of Event-Related Potential Components* (pp. 329–360). New York (NY): Oxford University Press. https://doi.org/10.1093/oxfordhb/9780195374148.001.0001

R Development Core Team. (2017). *R: A language and environment for statistical computing*. In Vienna, Austria (p. 1). Foundation for Statistical Computing, Vienna, Austria. ISBN 3-900051-07-0, URL: http://www.R-project.org.

Robitaille, N., Marois, R., Todd, J. J., Grimault, S., Cheyne, D., & Jolicœur, P. (2010).

Distinguishing between lateralized and nonlateralized brain activity associated with visual short-term memory: fMRI, MEG, and EEG evidence from the same observers. *NeuroImage, 53*, 1334–1345. https://doi.org/10.1016/j.neuroimage.2010.07.027

Rouder, J. N., & Morey, R. D. (2012). Default Bayes factors for model selection in regression. *Multivariate Behavioral Research, 47*(6), 877–903. https://doi.org/10.1080/00273171.2012.734737

Rouder, J. N., Morey, R. D., Speckman, P. L., & Province, J. M. (2012). Default Bayes factors for ANOVA designs. *Journal of Mathematical Psychology, 56*(5), 356–374. https://doi.org/10.1016/j.jmp.2012.08.001

Sharbrough, F., Chatrian, G.-E., Lesser, R. P., Lüders, H., Nuwer, M., & Picton T. W. (1991). American electroencephalographic society guidelines for standard electrode position nomenclature. *Journal of Clinical Neurophysiology, 8*(2), 200–202. https://doi.org/10.1097/00004691-199104000-00007

Todd, J. J., & Marois, R. (2004). Capacity limit of visual short-term memory in human posterior parietal cortex. *Nature, 428*(6984), 751–754. https://doi.org/10.1038/nature02466

Vogel, E. K., & Machizawa, M. G. (2004). Neural activity predicts individual differences in visual working memory capacity. *Nature, 428*(6984), 748–751. https://doi.org/10.1038/nature02447

Wandell, B. A., Dumoulin, S. O., & Brewer, A. A. (2007). Visual field maps in human cortex. *Neuron, 56*(2), 366–383. https://doi.org/10.1016/j.neuron.2007.10.012

Xu, Y., & Chun, M. M. (2006). Dissociable neural mechanisms supporting visual short-term memory for objects. *Nature, 440*(7080), 91–95. https://doi.org/10.1038/nature04262

Zeki, S. M. (1993). *A vision of the brain*. Oxford (UK): Blackwell Scientific Publications. https://doi.org/10.3233/BEN-1995-8108

Acknowledgments

Throughout the writing of this thesis, I have received a great deal of support and assistance. I would first like to thank my supervisor, Prof. Roberto Dell'Acqua, whose expertise was invaluable in formulating the research questions and methodology. Your insightful feedback pushed me to sharpen my thinking and brought my work to a higher level. I would particularly like to acknowledge my teammates, Dr. Sabrina Brigadoi and Dr. Arianna Schiano, for their wonderful collaboration and patient support I would also like to thank my Chinese supervisor, Prof. Shimin Fu, for his valuable guidance throughout my studies. You provided me with the tools that I needed to choose the right direction and successfully complete my thesis. In addition, I would like to thank my parents for their wise counsel and sympathetic ear. You are always there for me. Finally, I could not have completed this thesis without the support of my fiancée, Ailouros Leung, who provided stimulating discussions as well as happy distractions to rest my mind outside of my research.